

INFORMATION TO USERS

This was produced from a copy of a document sent to us for microfilming. While the most advanced technological means to photograph and reproduce this document have been used, the quality is heavily dependent upon the quality of the material submitted.

The following explanation of techniques is provided to help you understand markings or notations which may appear on this reproduction.

1. The sign or "target" for pages apparently lacking from the document photographed is "Missing Page(s)". If it was possible to obtain the missing page(s) or section, they are spliced into the film along with adjacent pages. This may have necessitated cutting through an image and duplicating adjacent pages to assure you of complete continuity.
2. When an image on the film is obliterated with a round black mark it is an indication that the film inspector noticed either blurred copy because of movement during exposure, or duplicate copy. Unless we meant to delete copyrighted materials that should not have been filmed, you will find a good image of the page in the adjacent frame. If copyrighted materials were deleted you will find a target note listing the pages in the adjacent frame.
3. When a map, drawing or chart, etc., is part of the material being photographed the photographer has followed a definite method in "sectioning" the material. It is customary to begin filming at the upper left hand corner of a large sheet and to continue from left to right in equal sections with small overlaps. If necessary, sectioning is continued again—beginning below the first row and continuing on until complete.
4. For any illustrations that cannot be reproduced satisfactorily by xerography, photographic prints can be purchased at additional cost and tipped into your xerographic copy. Requests can be made to our Dissertations Customer Services Department.
5. Some pages in any document may have indistinct print. In all cases we have filmed the best available copy.

University
Microfilms
International

300 N. ZEEB RD., ANN ARBOR, MI 48106

8129437

TRAN, LOC BINH

ANALYTICAL DIPOLE MOMENT FUNCTIONS FOR DIATOMIC
MOLECULES: APPLICATION TO CARBON MONOXIDE (CO)

The University of Oklahoma

PH.D. 1981

University
Microfilms
International 300 N. Zeeb Road, Ann Arbor, MI 48106

Copyright 1981

by

Tran, Loc Binh

All Rights Reserved

THE UNIVERSITY OF OKLAHOMA
GRADUATE COLLEGE

ANALYTICAL DIPOLE MOMENT FUNCTIONS FOR DIATOMIC MOLECULES:
APPLICATION TO CARBON MONOXIDE (CO)

A DISSERTATION
SUBMITTED TO THE GRADUATE FACULTY
in partial fulfillment of the requirement for the
degree of
DOCTOR OF PHILOSOPHY

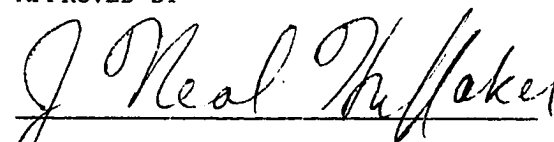
by
LOC BINH TRAN
Norman, Oklahoma
1981

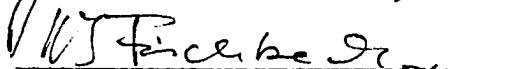
ANALYTICAL DIPOLE MOMENT FUNCTIONS FOR DIATOMIC MOLECULES:
APPLICATION TO CARBON MONOXIDE (CO)

A DISSERTATION

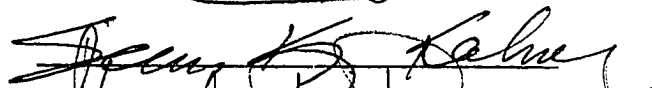
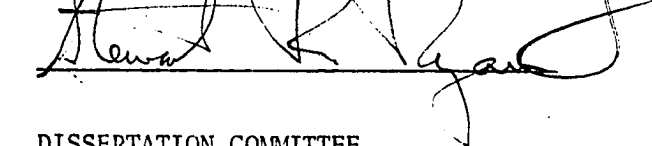
APPROVED FOR THE DEPARTMENT OF PHYSICS AND ASTRONOMY

APPROVED BY







DISSERTATION COMMITTEE

ACKNOWLEDGMENT

I wish to express my deep appreciation and gratitude to Dr. J. N. Huffaker for having suggesting this problem, for his constant help and guidance throughout the completion of this research work, and especially for transferring to me some of his perfect knowledge of computer programming.

I also wish to thank Dr. H. J. Fischbeck, Dr. S. Ryan, Dr. M. A. Morrison, and Dr. S. K. Kahng for reading this thesis, giving many useful suggestions, and for being on my committee.

I feel greatly indebted to Dr. M. L. Coffmann, Dr. B. L. Atkinson, and Dr. M. A. Morrison for their many advices and moral support. Mention should also be made to skillful and generous Jacquine Littel of the Physics Department for typing this thesis and giving me superb technical assistance in the final editing work.

Finally, special mention goes to my son, Eric Anh-Vu, for his long-term good behavior during my writing of this dissertation, and to my wife for her patience and understanding.

TABLE OF CONTENTS

| | |
|---|-----|
| ACKNOWLEDGMENTS | iv |
| LIST OF TABLES | vi |
| LIST OF ILLUSTRATIONS | vii |
| ABSTRACT | ix |
| CHAPTER | |
| I. INTRODUCTION | 1 |
| II. RELATIONS BETWEEN COEFFICIENTS OF VARIOUS EXPANSIONS OF THE ELECTRIC DIPOLE MOMENT | 15 |
| III. MORSE-OSCILLATOR MATRIX ELEMENTS OF u , y , AND z | 25 |
| IV. CUBIC DIPOLE MOMENT FUNCTIONS IN u , y , AND z | 45 |
| V. ANALYTICAL DIPOLE MOMENT FUNCTIONS WITH CORRECT ASYMPTOTIC BEHAVIOR | 64 |
| VI. CALCULATIONS OF ROTATIONLESS TRANSITION MOMENTS | 93 |
| VII. CONCLUSION | 102 |
| APPENDIXES | |
| A. POWER OF A POWER SERIES | 104 |
| B. EXACT MORSE MATRIX ELEMENTS OF y^2 AND y^3 | 107 |
| C. EXPRESSIONS OF SOME INTEGRALS OBTAINED BY IH | 124 |
| REFERENCES | 127 |

LIST OF TABLES

| TABLE | Page |
|--|------|
| 3.1 Morse matrix elements of u for $0 \leq v \leq 9$ and $0 \leq v' \leq 9$. . . | 43 |
| 3.2 Morse matrix elements of y for $0 \leq v \leq 9$ and $0 \leq v' \leq 9$. . . | 44 |
| 4.1 Empirical rotationless vibrational transition moments | 58 |
| 4.2 Values for the Morse parameters and related constants | 59 |
| 4.3 Calculated coefficients of cubic dipole moment functions in u , y , and z | 60 |
| 4.4 Coefficients M_n^* of the y -series expansion equivalent to the cubic dipole moment function in u | 61 |
| 5.1 Values of the parameters C_1 , C_2 , C_3 , β , and B for different generating functions. | 79 |
| 5.2 Values of the parameter M_c in the correction terms $M_c y$ and $M_c y(1-y)$ for different closed-form dipole functions | 81 |
| 6.1 A comparison of rotationless vibrational matrix elements of various dipole moment functions | 97 |
| B.1 Morse matrix elements of y^2 for $0 \leq v \leq 9$ and $0 \leq v' \leq 9$. . . | 120 |
| B.2 Morse matrix elements of y^3 for $0 \leq v \leq 9$ and $0 \leq v' \leq 9$. . . | 121 |
| B.3 Morse matrix elements of u^2 for $0 \leq v \leq 9$ and $0 \leq v' \leq 9$. . . | 122 |
| B.4 Morse matrix elements of u^3 for $0 \leq v \leq 9$ and $0 \leq v' \leq 9$. . . | 123 |

LIST OF ILLUSTRATIONS

| FIGURE | Page |
|---|------|
| 2.1 General shape of the dipole moment function | 24 |
| 4.1 CO cubic dipole moment functions in u, y, and z | 62 |
| 4.2 Plot of coefficients M_n^* of the equivalent y-series versus the index n | 63 |
| 5.1 Plots of various generating functions $F^\alpha(n)$ obtained by fitting 3 known coefficients M_1 , M_2 , and M_3 | 82 |
| 5.2 Graphs of various CO dipole moment functions with correct large-r behavior, obtained by the zero-order approximation. | 83 |
| 5.3 Plots of various generating functions $F^\alpha(n)$ obtained by fitting 3 empirical transition moments. | 84 |
| 5.4 Plots of various generating functions $F^\alpha(n)$ obtained by fitting 6 empirical transition moments. | 85 |
| 5.5 Graphs of several CO dipole moment functions with correct large-r behavior obtained without minimization. | 86 |
| 5.6 Graphs of several CO dipole moment functions with correct large-r behavior obtained with minimization | 87 |
| 5.7 Plots of various generating functions $F^\alpha(n)$ obtained using $M_c y$ correction with minimization. | 88 |
| 5.8 Plots of various generating functions $F^\alpha(n)$ obtained using $M_c y(1-y)$ correction with minimization | 89 |

| Figure | Page |
|---|------|
| 5.9 Graphs of CO dipole moment functions with correct large-r behavior and small-r behavior using $M_c y$ correction with minimization | 90 |
| 5.10 Graphs of CO dipole moment functions with correct large-r behavior and small-r behavior using $M_c y(1-y)$ correction with minimization. | 91 |
| 5.11 A comparison between dipole moment functions $M^A(r)$ obtained using minimization with $M_c y$ and $M_c y(1-y)$ corrections and an <u>ab initio</u> dipole moment function for CO. | 92 |

ANALYTICAL DIPOLE MOMENT FUNCTIONS FOR DIATOMIC MOLECULES:

APPLICATION TO CARBON MONOXIDE (CO)

BY: LOC BINH TRAN

MAJOR PROFESSOR: J. N. HUFFAKER

ABSTRACT

The dipole moment of the ground electronic state ($X^1\Sigma^+$) of CO as a function of the internuclear distance is determined using experimentally deduced rotationless vibrational transition moments. For this purpose, the dipole moment function is expanded in series of powers of the variables u , y , and z , where $u=r-r_e$, $y=1-\exp(-au)$, and $z=\exp(au)-1$, and exact Morse matrix elements of these quantities are used in computation. Using a standard factorization technique, we derive exact matrix elements of y , y^2 , and y^3 . For higher powers of y , we use matrix multiplication. The eigenfunctions of the perturbed Morse oscillator (PMO) are obtained by the method of matrix diagonalization. Morse and PMO cubic dipole moment functions in u , y and z are then determined for CO.

We require the y -series expansion to satisfy the condition that the infinite sum of its coefficients M_n vanishes. Then, expressing M_n as some function of the index n and several parameters, we fit this function to a few known transition moments and obtain an infinite y -series representation with the correct asymptotic behavior for the CO dipole moment. We found three functional forms for M_n that produce infinite series reducible to closed forms. These new forms are adjusted further by a corrective term so that they obtain the correct general behavior at both large r and small r . The various CO dipole moment functions finally are used to predict hot-band transition moments.

ANALYTICAL DIPOLE MOMENT FUNCTIONS FOR DIATOMIC MOLECULES:

APPLICATION TO CARBON MONOXIDE (CO)

CHAPTER I

INTRODUCTION

In the past several years there have been considerable interest in and extensive work on the determination of the electric dipole moments of diatomic molecules as functions of the internuclear distance. The dipole moment function is of great importance since its knowledge is necessary for many physical applications. It may be determined by either of the two general approaches: ab initio (or theoretical) and empirical (or experimental).

In the ab initio calculation of molecular properties, and of the dipole moment in particular, the knowledge of electronic wavefunctions is essential. With advanced computer technology, these wavefunctions are becoming available with high accuracy. They are usually obtained by either the Hartree-Fock (H-F), or configuration interaction (CI), or multi-configuration self-consistent (MCSCF) method, or modifications of these methods. Typical works on theoretical dipole moment functions for diatomic molecules are those by Lie⁽¹⁾ and Kirby-Docken and Liu⁽²⁾ for the ground state ($X^1\Sigma^+$) of the HF and CO molecule respectively.

The electric dipole moment operator for a molecule is defined as the vector sum

$$\underline{M}(\underline{r}_i, \underline{R}_\alpha) = e \left(\sum_\alpha N_\alpha \underline{R}_\alpha - \sum_i \underline{r}_i \right) \quad (1.1)$$

where e is the usual electronic charge, N_α is the atomic number of the α th nucleus, \underline{R}_α the center-of-mass (c.m.) coordinate of the α th nucleus, \underline{r}_i the c.m. coordinate of the i th electron, and the double underlining bar refers to the collectivity of these coordinates. The coordinate system used here is fixed to the molecule at its center of mass and rotates with it. For a diatomic molecule, the z -axis is usually chosen to coincide with its internuclear axis.

In the Born-Oppenheimer approximation, the molecular wavefunction for a diatomic molecule, considered as a rotating oscillator, may be expressed as the product of an electronic, a vibrational, and a rotational factor:

$$\Psi_N(\underline{r}_i, \underline{r}) = \psi_n^{(e)}(\underline{r}_i; \underline{r}) \psi_n^{(v)}(\underline{r}) \psi_J^{(r)}(\theta, \phi) \quad (1.2)$$

where n , v , and J are electronic, vibrational, and rotational quantum numbers respectively, $N = (n, v, J)$, \underline{r} is the internuclear axis vector, and the electronic part depends on \underline{r} parametrically. For clarity and convenience, we have omitted the magnetic quantum number m_J to be associated with the rotational factor $\psi_J^{(r)}$ in the above expression.

In an ab initio calculation, the approximation (1.2) is usually assumed and then the "electric dipole moment" of a diatomic molecule in a particular electronic state n is given by the expectation value of the z -component of the electric dipole moment vector $\underline{M}(\underline{r}_i, \underline{r})$ in this electronic state,

$$M(\mathbf{r}) = e \left[\sum_{\alpha} N_{\alpha} R_{\alpha} - \sum_i \langle \psi_n^{(e)} | z_i | \psi_n^{(e)} \rangle \right] \quad (1.3)$$

where z_i is the z-coordinate of the i th electron and the nuclei are on the z-axis.

On the other hand, the empirical approach takes account of the fact that the probability of transition between two molecular states (n, v, J) and (n', v', J') is proportional to the absolute value squared of the corresponding matrix element $R_{NN'}$, of the electric dipole moment operator \underline{M} :

$$\begin{aligned} |R_{NN'}|^2 &= \left| \int \Psi_N^* \underline{M} \Psi_{N'} d\tau \right|^2, \\ &= \left| \int \psi_N^{(n)*} \psi_{N'}^{(n)} d\underline{\mathbf{r}} \int \psi_n^{(e)*} \underline{M} \psi_n^{(e)} d\underline{\mathbf{r}}_i \right|^2. \end{aligned} \quad (1.4)$$

In Eq. (1.4), the integration over the electronic wavefunctions produces a quantity $\underline{M}_{nn'}^{(e)}(\mathbf{r})$ which depends on \mathbf{r} :

$$\underline{M}_{nn'}^{(e)}(\mathbf{r}) = \int \psi_n^{(e)*}(\underline{\mathbf{r}}_i; \underline{\mathbf{r}}) \underline{M}(\underline{\mathbf{r}}_i, \underline{\mathbf{r}}) \psi_{n'}^{(e)}(\underline{\mathbf{r}}_i; \underline{\mathbf{r}}) d\underline{\mathbf{r}}_i. \quad (1.5)$$

The integration over the rotational functions can be carried out independently, yielding a factor $S_{JJ'}$, called the Hönl-London factor. Hence, Eq. (1.4) can be written as

$$|R_{NN'}|^2 = S_{JJ'} \left| \int \psi_N^{(v)} \underline{M}_{nn'}^{(e)}(\mathbf{r}) \psi_{N'}^{(v)}(\mathbf{r}) d\mathbf{r} \right|^2. \quad (1.6)$$

Assuming that the lower molecular state is labelled by (n, v, J) and the upper state labelled by (n', v', J') , then for the rotating oscillator model, we have

$$S_{JJ'} = J \quad \text{for the P branch,}$$

and

$$S_{JJ'} = J+1 \quad \text{for the R branch.}$$

For electronic transitions, $n \neq n'$, one usually assumes that $\underline{M}_{nn'}^{(e)}$ varies slowly with r according to the Franck-Condon principle, so that it may be replaced by an average value $\overline{M}_{nn'}^{(e)}$. In this case, Eq. (1.6) becomes

$$|\underline{R}_{\underline{NN}'}|^2 = S_{JJ'} |\overline{M}_{nn'}^{(e)}|^2 q_{VV'} \quad (1.7)$$

where $q_{VV'}$, called the Franck-Condon factor, is defined by

$$q_{VV'} = \left| \int \psi_{n'v'J'}^{(v)} \psi_{nvJ}^{(v)} dr \right|^2 \cdot \quad (1.8)$$

For rotation-vibration transitions within the same electronic state, $n = n'$, $\underline{M}_{nn}^{(e)}$ may vary considerably with r , and hence should not be taken out of the integral in Eq. (1.6). In this case, if the z -axis is also the internuclear axis, the magnitude of $\underline{M}_{nn}^{(e)}(r)$ is equal to the dipole moment function $M(r)$ defined in Eq. (1.3):

$$M_{nn}^{(e)}(r) = M(r) \cdot$$

Thus, for convenience we rewrite Eq. (1.6) in the form

$$|\underline{R}_{\underline{VJ}}^{v'J'}|^2 = S_J^{J'} |\langle vJ | M(r) | v'J' \rangle|^2 \quad (1.9)$$

where an electronic state is implied and $|vJ\rangle = \psi_{nvJ}^{(v)}(r)$, the vibrational eigenfunction.

The square of the quantity $\underline{R}_{\underline{VJ}}^{v'J'}$ is commonly known as the line strength and the matrix elements of $M(r)$ are called dipole transition matrix elements or simply transition moments. From the measurements of intensities of rotation-vibration transitions $vJ \rightarrow v'J'$, the squares of matrix elements $\langle vJ | M(r) | v'J' \rangle$ can be deduced, from which

the functional dependence of the electric dipole moment $M(r)$ on r may be determined.

To see how dipole transition matrix elements relate to quantities measured in experiments, we shall discuss the absorption and emission of spectral lines.

1. Absorption of Radiation

The theory of infra-red light absorption by diatomic molecules was treated in full detail by Crawford and Dinsmore.⁽⁴⁾ We reproduce here some important steps and formulas from their work.

When a beam of monochromatic light of frequency ν passes through an absorbing medium of infinitesimal thickness dx , its intensity I_ν decreases according to the following law of light absorption,

$$dI_\nu = -I_\nu \alpha_\nu dx \quad (1.10)$$

where $\alpha_\nu = \alpha(\nu)$, having units of cm^{-1} , is called the absorption coefficient at frequency ν and is proportional to the molecular density of the absorbing material.

Suppose that there are two different energy levels 1 and 2, level 1 being lower than level 2, and that there are degenerate states m and n having these energies respectively. Then a transition between any two states m and n gives a single spectral line of frequency $\nu \equiv \nu_{mn} = \nu_{12} = (E_1 - E_2)/h$, where $m = 1, 2, \dots, g_1$ and $n = 1, 2, \dots, g_2$; g_1 and g_2 being degeneracies of levels 1 and 2 respectively.

According to Einstein's theory, the probability that a transition $m \rightarrow n$ will take place is given by

$$P_{mn} = \rho_\nu B_{mn}$$

where ρ_ν , having units of $\text{erg}\cdot\text{cm}^{-3}$, is the energy density of the incident beam and is related to the energy flux I_ν (in units of $\text{erg}\cdot\text{cm}^{-2}\cdot\text{sec}^{-1}$) by

$$I_\nu = \rho_\nu c ,$$

and B_{mn} is the Einstein transition probability of absorption.

If there are N_m molecules in the state m at the lower energy level, then the rate of energy absorption, that is the energy absorbed from the incident beam of 1 cm^2 cross section for the transition $m \rightarrow n$, is

$$(dI_\nu)_{mn} = -I_\nu \frac{h\nu}{c} N_m B_{mn} dx . \quad (1.11a)$$

Therefore, if the lower level 1 has population N_1 and degeneracy g_1 , then the total intensity of absorption I_{12} due to all transitions $1 \rightarrow 2$ is

$$\begin{aligned} dI_\nu &= \sum_{m,n} (dI_\nu)_{mn} , \\ dI_\nu &= -I_\nu \frac{h\nu}{c} N_1 B_{12} dx \end{aligned} \quad (1.11b)$$

where

$$B_{12} = \frac{1}{g_1} \sum_{m,n} B_{mn}$$

is the total probability coefficient of absorption.

Comparing Eqs. (1.10) and (1.11b), we get

$$\alpha_\nu = \frac{h\nu}{c} N_1 B_{12} . \quad (1.12)$$

While spontaneous emission, being isotropic, can be neglected, induced emission cannot because it is in the direction of the

inducing radiation. Therefore, if this effect is included, the net α_ν should be less than that in Eq. (1.12):

$$\alpha_\nu = \frac{h\nu}{c} N_1 B_{12} (1 - e^{-h\nu/kT}) \quad (1.13)$$

The Einstein coefficient B_{mn} is related to the line strength T_{mn} (i.e., the square of matrix element of the dipole moment \underline{M}) by⁽⁵⁾

$$B_{mn} = \frac{8\pi^3}{3h^2} T_{mn} \quad (1.14a)$$

hence,

$$B_{12} = \frac{1}{g_1} \sum_{m,n} B_{mn} = \frac{8\pi^3}{3h^2 g_1} T_{12} \quad (1.14b)$$

where

$$T_{12} = \sum_{m,n} T_{mn} \quad (1.14c)$$

and

$$T_{mn} = |\langle m | \underline{M} | n \rangle|^2 \quad (1.14d)$$

Substituting Eq. (1.14b) into Eq. (1.13) yields

$$\alpha_\nu = \frac{8\pi^3 \nu_{mn}}{3hc} \frac{N_1}{g_1} T_{12} (1 - e^{-h\nu_{mn}/kT}) \quad (1.15)$$

For rotation-vibration transitions $\nu, J \rightarrow \nu', J'$ in diatomic molecules, application of Eq. (1.15) gives

$$\alpha_{\nu J}^{\nu' J'} = \left(\frac{8\pi^3}{3hc} \right) \nu_{\nu J}^{\nu' J'} \frac{N_{\nu J}}{g_J} T_{\nu J}^{\nu' J'} (1 - e^{-h\nu_{\nu J}^{\nu' J'}/kT}) \quad (1.16)$$

where

$$g_J = 2J + 1 \quad ,$$

and

$$T_{\nu J}^{\nu' J'} = \sum_{m, m'} T_{\nu J m}^{\nu' J' m'} = \sum_{m, m'} \langle \nu J m | M(r) | \nu' J' m' \rangle$$

is the total line strength.

The quantity measured in experiments is the integrated absorption coefficient or total intensity, $A_V^{v'}$, which theoretically is equal to

$$A_V^{v'} = \sum_{J, J'} \alpha_{vJ}^{v'J'} ,$$

$$A_V^{v'} = \left(\frac{8\pi^3}{3hc} \frac{N_V}{Z_R} \right) \sum_{J, J'} \nu_{vJ}^{v'J'} g_J e^{-E_J/kT} T_{vJ}^{v'J'} (1 - e^{-h\nu_{vJ}^{v'J'}/kT}) \quad (1.17)$$

where

$$Z_R = \sum_{J=0} g_J e^{-E_J/kT}$$

is the rotational partition function and is dependent on v and N_V is the total number density of absorbing vibrating molecules present at pressure P and temperature T and is related to the concentration N_{vJ} of molecules at a state (v, J) by

$$N_{vJ} = N_V \frac{g_J e^{-E_J/kT}}{Z_R} .$$

In practice, Eq. (1.17) may be replaced by an integral:

$$A_V^{v'} = \int \alpha(v) dv .$$

Another measured quantity is the total intensity of the n th harmonic vibrational band observed at ν_0^n approximately; it is obtained by summing the intensities A_V^{v+n} over all values of v :

$$A^{(n)} = \sum_{v=0} A_V^{v+n} = \left(\frac{8\pi^3}{3hc} \frac{N}{Z_V} \right) \sum_{v=0} \nu_v^{v+n} T_n^{v+n} e^{-E_v/kT} (1 - e^{-h\nu_v^{v+n}/kT}) \quad (1.18)$$

where N is the total molecular concentration and Z_V is the vibrational

partition function,

$$Z_v = \sum_{v=0} e^{-E_v/kT}.$$

2. Emission of Radiation

If there are N_n molecules in the state n , then the intensity of a spectral line in emission by the transition $n \rightarrow m$ is defined by the energy emitted by the source per second⁽³⁾ and given by

$$I_{nm} = \frac{h\nu}{c} N_n A_{nm} \quad (1.19a)$$

where A_{nm} is the Einstein transition probability of spontaneous emission and is related to the matrix element of the electric dipole moment by

$$A_{nm} = \frac{64\pi^4 \nu_{nm}^3}{3hc^2} T_{nm}, \quad (1.19b)$$

T_{nm} being equal to T_{mn} defined by Eq. (1.14d).

Thus, if the upper level 2 has population N_2 and degeneracy g_2 , then the total intensity of emission I_{21} for the transition $2 \rightarrow 1$ is

$$I_{21} = \frac{h\nu}{c} N_2 A_{21} \quad (1.19c)$$

where the total Einstein coefficient A_{21} is given by

$$A_{21} = \frac{1}{g_2} \sum_{m,n} A_{nm} = \frac{64\pi^4 \nu_{21}^3}{3hc^2 g_2} T_{21} \quad (1.19d)$$

with $T_{21} = T_{12}$ in Eq. (1.14c).

Comparison between Eqs. (1.14b) and (1.19d) gives the relation between the Einstein coefficients A_{21} and B_{12} ,

$$B_{12} = \left(\frac{c^3}{8\pi h c^3} \right) \frac{g_2}{g_1} A_{21} . \quad (1.20)$$

Thus we have seen that the absolute values squared of the matrix elements of the dipole moment $M(r)$ can be deduced from certain experimentally measured quantities. Molecular beam resonance experiments and microwave experiments yield the matrix elements of $M(r)$ which are diagonal in v , while infrared absorption experiments give matrix elements which are off-diagonal in v .

In our present work, we are concerned with two problems: first determining the dipole moment $M(r)$ as a function of the internuclear distance r for diatomic molecules from experimental data on vibrational dipole matrix elements, and second using an extrapolation technique to obtain the correct asymptotic behaviors of $M(r)$. Our formalism is then applied to carbon monoxide (CO).

The empirical approach requires that some assumption about the form of $M(r)$ must be made. This assumption may be valid over a small range of r . When n independent dipole matrix elements are known, the usual procedure is to choose a function $M(r; c_i)$ depending on a set of n parameters c_i , $i = 1, \dots, n$, which then may be determined by solving a system of linear or non-linear equations:

$$\langle v | M(r; c_i) | v' \rangle = \mu_{vv'} .$$

Usually a limited amount of experimental data is available, and this is insufficient to determine a unique dipole moment function since there would be an infinite number of functions which agree with the experiments.

So far only three choices for the functional form of $M(r)$ are found in the literature, namely:

i) Expansion of $M(r)$ in a Taylor series about the equilibrium internuclear distance r_e . In practice, the series must be truncated giving the polynomial approximation. This approach has been the most commonly used, and there have been a great deal of works ⁽⁶⁻¹⁴⁾ based on it.

ii) Expansion of the product $M(r)\psi_v(r)$ in terms of a number of orthonormal vibrational eigenfunctions $\psi_{v'}(r)$ so that $M(r)$ can be written in the form

$$M(r) = \frac{1}{\psi_v(r)} \sum_{v'=0}^N C_{vv'} \psi_{v'}(r) = C_{vv} + \sum_{v' \neq v}^N C_{vv'} \frac{\psi_{v'}(r)}{\psi_v(r)} .$$

For $v = 0$, this equation determines $M(r)$; but for $v > 0$, because of the zeros of ψ_v , it is subject to certain restrictions. This method was first proposed by Trischka and Salwen⁽¹⁵⁾ who called it the "wavefunction approximation". It has been applied to HCl and DCl molecules by Herman and Rubin,⁽¹⁶⁾ and to OH, HCl, and CO by Cashion.⁽¹⁷⁾

iii) Linear combination of exponential functions $e^{-a_i r}$:

$$M(r) = \sum_{i=1}^N C_i e^{-a_i r}$$

where the parameters C_i and a_i are to be determined through $2N$ empirical dipole matrix elements. This form was suggested by Chakraborty, Pan and Chang,⁽¹⁸⁾ but they and Learner⁽¹⁹⁾ retained only one term of the expansion in their works related to electronic band strengths.

Although the Taylor series method is the simplest and most obvious way to analyze transition intensities, it has the serious drawback of being convergent over a small region about r_e (at most,

$0 < r < 2r_e$). The effect of its divergence for larger limits its use to low vibrational levels with v less than about 10 for CO.

The "wavefunction approximation" seems to be more powerful than the Taylor expansion because in principle, if the complete set of wavefunctions is included, it is valid over the whole range $0 \leq r < \infty$. Trischka and Salwen⁽¹⁵⁾ showed that the dipole moment function $M(r)$ can be completely determined if all the matrix elements $\langle v | M(r) | v' \rangle$ in a given column or row are given. Their method, however, has not been widely applied because it also requires a sufficient amount of experimental data. Besides, the convergence of the wavefunction expansion and the effect of neglecting the continuum have not been investigated yet.

Since there are only a few works applying what we call the "exponential approximation", one can conclude little about its usefulness. However, from a mathematical point of view, some remarks can be made. If all the parameters C_i and a_i have non-zero values, then $M(r) = 0$ at $r = \infty$ and $M(r)$ at $r = 0$ is the sum of all coefficients C_i . If one parameter, say a_i , vanishes then $M(r) = C_i$ at $r = \infty$. Thus, this exponential combination has a finite value at $r = \infty$ while the Taylor expansion blows up. This approach, however, does have some disadvantages. Because the parameters a_i are unknowns, the system of equations to be solved is non-linear. In addition, matrix elements involving $e^{-a_i r}$ are generally difficult to evaluate.

In the present work, in addition to considering u as the variable for the Taylor expansion of $M(r)$, we introduce two new variables $y = 1 - \exp(-au)$ and $z = \exp(au) - 1$, where $u = r - r_e$ and

a is a characteristic of the Morse potential function [Eq. (3.1a)], in order to obtain an expansion of $M(r)$ in powers of y and an expansion in powers of z . The choice of z is suitable and convenient because the calculation of matrix elements of any power of z can be made easily by application of a recursion relation obtained by Huffaker and Dwivedi.⁽²⁰⁾ The choice of y for expanding $M(r)$ may be justified by the fact that the perturbed-Morse-oscillator (PMO) potential⁽²¹⁾ which is a power series of y has been proven to be an extremely accurate model for the effective vibrational potential for diatomic molecules and much superior than the Dunham potential which is an expansion in powers of u .

Mathematically, the y -expansion is a particular case of the "exponential expansion" in which all parameters a_i are integral multiples of the Morse parameter a . Therefore, the y -series has the property that its value at $r = \infty$ is the sum of all expansion coefficients. By requiring this sum to vanish at $r = \infty$ we can force the dipole moment function to have a correct asymptotic behavior. Besides, the y -expansion involves a linear system of equations and the matrix elements of y can be easily calculated using exact formulas.

The relationships between coefficients of the three expansions of $M(r)$ in powers of u , y and z are given in Chapter II. In Chapter III we present formulas for matrix elements of these variables and derive the exact expression for the off-diagonal elements of y .

The cubic dipole moment functions in u , y , and z are obtained for CO in Chapter IV, using Morse-oscillator wavefunctions and perturbed-Morse-oscillator (PMO) wavefunctions.

Chapter V presents a technique of generating all coefficients in the y -expansion of $M(r)$, using two additional parameters which are to be determined by iterations so that the dipole moment function $M(r)$ will display the correct asymptotic behavior at both large r and small r . The most interesting feature of this technique is that it permits one to reduce the various infinite series expansions of $M(r)$ into compact analytical forms. Chapter VI lists dipole matrix elements calculated from these various y -expansions of $M(r)$.

Appendix A gives formulas to calculate coefficients of a power series resulting from raising another power series to any power. In Appendix B, exact expressions for matrix elements of y^2 and y^3 are derived by the factorization technique. This makes use of several results that have been obtained by Infeld and Hull⁽²²⁾ and are listed in Appendix C.

CHAPTER II
RELATIONS BETWEEN COEFFICIENTS OF VARIOUS EXPANSIONS
OF THE ELECTRIC DIPOLE MOMENT

For covalently-bonded diatomic molecules, there are two general types of dipole moment functions $M(r)$ as shown in Fig. 2.1.^(17,23) The upper curve (a) shows the general behavior of the dipole moment of a class of diatomic molecules that have unique polarity like HCl. The lower curve (b) is typical of a molecule such as CO which undergoes a reversal of polarity at certain value of r . In both cases, the dipole moment approaches zero as the molecule dissociates into neutral atoms.

In case of CO, if the positive direction points from O to C, then by definition positive values of $M(r)$ indicate the polarity C^+O^- while negative values refer to the polarity C^-O^+ . Discussions on the reversal of sign of the CO dipole moment can be found in papers by Mulliken⁽²³⁾ and Huo.⁽²⁴⁾ For small r , the polarity may be expected, since the triple bond $C\equiv O^+$ is then the strongest. As r becomes larger, the polarity should be reversed, since C^+O^- then has considerably lower energy than C^-O^+ .

At the present, most theoretical and experimental treatments of the dipole moment can give information about it only over a limited range of r about the equilibrium r_e , and none provides a detailed picture of the dipole moment over the whole range of r . Theoretically, the general behavior of $M(r)$ is expected to be

$$M(r) \rightarrow 0 \text{ for } r \rightarrow 0 \text{ and } r \rightarrow \infty.$$

Although the behavior of $M(r)$ at very small values of r has never been fully understood, we assume that the above general asymptotic behavior is correct and try to find functions satisfying these conditions to represent the dipole moments of diatomic molecules.

As mentioned in Chapter I, $M(r)$ is commonly expanded in a Taylor series as

$$M(r) = M(u) = m_0 + \sum_{n=1}^{\infty} m_n u^n \quad (2.1)$$

where $u = r - r_e$, and

$$m_n = \frac{1}{n!} \left[\frac{d^n M(r)}{dr^n} \right]_{r=r_e}$$

If r is expressed in units of cm and electric charge in units of esu, then $M(r)$ has units of esu·cm. For molecules, $M(r)$ is usually expressed in units of Debye (abbreviated D), where $1D = 10^{-18}$ esu·cm. Thus, if r is in units of Å ($1\text{Å} = 10^{-8}$ cm) then the Taylor coefficient m_n has units of $D \cdot \text{Å}^{-n}$.

The Taylor series (2.1) is valid only for $|u| < r_e$, that is, over a small range of r : $0 < r < 2r_e$. In practice, only a finite number of coefficients m_n can be determined through empirical dipole matrix elements. Even if a large number of these coefficients can be calculated, the Taylor expansion does not provide any information on the dipole moment beyond the distance $2r_e$ because the series diverges there. Although there is no theoretical justification for using the Taylor expansion of $M(r)$, this choice is convenient and sometimes can predict transitions probabilities in quite good agreement⁽²⁵⁾ with

experiments. However, this requires extremely accurate intensity data. Up to the present, for CO there are only three reliable measured vibrational absorption intensities: those for the fundamental and the first two overtone bands. Therefore, the cubic dipole moment function in u for CO is usually determined. This is satisfactory for many practical purposes but inadequate for detailed analysis of fine structure of intensity bands.

As alternative approaches, the dipole moment function can be expanded in an infinite series of powers of the variable y or z introduced earlier:

$$M(y) = M_0 + \sum_{n=1} M_n y^n, \quad (2.2)$$

or

$$M(z) = T_0 + \sum_{n=1} T_n z^n, \quad (2.3)$$

where M_n and T_n have units of Debye (D).

The expansion $M(y)$ is valid only for $|y| < 1$, or

$$-1 < 1 - e^{-au} < 1$$

from which we get

$$r_e - \frac{1}{a} \ln 2 < r < \infty. \quad (2.4a)$$

In particular, for CO the range for y -expansion is

$$0.84 \text{ \AA} < r < \infty. \quad (2.4b)$$

Similarly, the expansion range for $M(z)$ is determined by

$$|z| < 1,$$

or

$$-1 < e^{au} - 1 < 1,$$

thus by

$$-\infty < r < r_e + \frac{1}{a} \ln 2 . \quad (2.5a)$$

For CO, this gives

$$0 < r < 1.42 \text{ \AA} . \quad (2.5b)$$

Mathematically, the y-expansion and z-expansion of any function of r, and of M(r) in particular, are analytical continuations of its u-expansion from the limited range $2r_e$ over an infinite range toward the positive side and an infinite range toward the negative side of r respectively. Of course, all three expansions represent the same function within the "overlap range", which is

$$r_e - \frac{1}{a} \ln 2 < r < r_e + \frac{1}{a} \ln 2 ,$$

and for CO,

$$0.84 \text{ \AA} < r < 1.42 \text{ \AA} .$$

The y-series, which has the longest positive expansion range, seems to be the most useful of all. In fact, it has one advantage that, at $r=\infty$, since $y=1$, it becomes

$$M(y=\infty) = M_0 + \sum_{n=1}^{\infty} M_n . \quad (2.6)$$

Therefore, one may force the function M(y) to satisfy the large-r asymptotic behavior by imposing the condition

$$M(y=\infty) = \sum_{n=0}^{\infty} M_n = 0 . \quad (2.7)$$

This is done in Chapter V.

The z-model, despite its smallest positive portion of expansion range, offers more convenience because the matrix elements $\langle v | z^n | v' \rangle$ can be evaluated very easily by a recurrence formula as stated in Chapter I.

We shall now derive the relations between coefficients m_n , M_n , and T_n . Huffaker⁽²¹⁾ has obtained these relations for the case of the Dunham potential and PMO potential. In the light of his general approach,⁽²⁶⁾ we find an alternative way to obtain these relationships.

1. Relations between m_n and M_n

Defining $t = e^{-au}$ and using the binomial expansion, we write

$$y^n = (1-t)^n = 1 + \sum_{k=1}^n (-1)^k \binom{n}{k} t^k. \quad (2.8)$$

Substituting the series representation of t ,

$$t^k = e^{-kau} = 1 + \sum_{m=1}^{\infty} (-1)^m \frac{k^m}{m!} (au)^m, \quad (2.9)$$

into Eq. (2.8), one gets

$$y^n = 1 + \sum_{k=1}^n (-1)^k \binom{n}{k} + \sum_{m=1}^{\infty} \sum_{k=1}^n (-1)^{k+m} \binom{n}{k} \frac{k^m}{m!} (au)^m.$$

The sum of the first two terms in the right-hand-side of this equation is the value of y^n given by Eq. (2.8) for $t=0$, thus is equal to zero, yielding

$$y^n = \sum_{m=n}^{\infty} A_m^n (au)^m \quad (2.10)$$

where A_m^n are two-dimensional coefficients given by

$$A_m^n = \sum_{k=1}^n (-1)^{m+k} \binom{n}{k} \frac{k^m}{m!} \quad (2.11a)$$

where $\binom{n}{k}$ is the binomial coefficient,

$$\binom{n}{k} = \frac{n!}{(n-k)! k!}, \quad (2.11b)$$

$$0! = 1 .$$

We note that the lowest power in the expansion [Eq. (2.10)] of y^n is n and

$$A_n^n = 1 ; \quad (2.11c)$$

hence,

$$\sum_{k=1}^n (-1)^{k+n} \frac{k^n}{(n-k)! k!} = 1 . \quad (2.11d)$$

Putting Eq. (2.10) into Eq. (2.2) and changing the order of summations, then comparing to Eq. (2.1) we finally get

$$\bar{m}_m = \frac{m_m}{a^m} = \sum_{n=1}^m A_m^n M_n . \quad (2.12)$$

Alternatively, we can write y^n as a series in power n ,

$$y^n = \left[\sum_{m=1}^{\infty} \frac{(-1)^{m-1}}{m!} (au)^m \right]^n ,$$

and use Eq. (A.9) in the Appendix A to obtain an induction relation for A_m^n :

$$A_m^n = \frac{1}{m-n} \sum_{k=n}^{m-1} (-1)^{m-k+1} \left[\frac{n(m-k+1) - k}{(m-k+1)!} \right] A_k^n \quad (2.13)$$

for $m > n$, and starting with $A_n^n = 1$.

Coefficients M_n can also be calculated inductively in terms of coefficients \bar{m}_m by

$$M_n = \bar{m}_m - \sum_{m=1}^{n-1} A_n^m M_m , \quad (2.14a)$$

or directly by

$$M_n = \sum_{m=1}^n B_n^m \bar{m}_m . \quad (2.14b)$$

The coefficients B_n^m can be obtained either by inversion of the matrix of coefficients A_m^n or by an inductive relation similar to

Eq. (2.13):

$$B_n^m = \frac{1}{n-m} \sum_{k=m}^{n-1} \left[\frac{m(n-k+1) - k}{n-k+1} \right] B_k^m \quad (2.14c)$$

where $n > m$ and $B_m^m = 1$.

2. Relations between m_n and T_n

Using the same technique as before, we write

$$v^k = (e^{au})^k = 1 + \sum_{m=1}^{\infty} \frac{k^m}{m!} (au)^m,$$

and

$$\begin{aligned} z^n &= (v-1)^n = (-1)^n (1-v)^n, \\ z^n &= (-1)^n \sum_{m=1}^{n-1} \sum_{k=1}^n [(-1)^k \binom{n}{k} \frac{k^m}{m!}] (au)^m \\ &\quad + \sum_{m=n}^{\infty} \sum_{k=1}^n [(-1)^{n+k} \binom{n}{k} \frac{k^m}{m!}] (au)^m. \end{aligned}$$

The coefficient in the first bracket in the above equation vanishes, reducing it to

$$z^n = \sum_{m=n}^{\infty} C_m^n (au)^m \quad (2.15)$$

where C_m^n is given by

$$C_m^n = \sum_{k=1}^n (-1)^{n+k} \binom{n}{k} \frac{k^m}{m!} \quad (2.16)$$

which can be related to the coefficient A_m^n in Eq. (2.11a):

$$C_m^n = (-1)^{m+n} A_m^n.$$

Substituting Eq. (2.15) into Eq. (2.3), then comparing the resulting equation to Eq. (2.1), we finally obtain

$$\bar{m}_m = \frac{m}{a^m} = \sum_{n=1}^m C_m^n T_n. \quad (2.17)$$

Inversely, T_n can be written in terms of \bar{m}_m by

$$T_n = \sum_{m=1}^n D_n^m \bar{m}_m \quad (2.18a)$$

where coefficients D_n^m can also be calculated by inversion of the matrix of coefficients C_m^n or by an inductive formula similar to Eq. (2.14c),

$$D_n^m = \frac{1}{n-m} \sum_{k=m}^{n-1} (-1)^{n+k} \left[\frac{m(n-k+1) - k}{n-k+1} \right] D_k^m. \quad (2.18b)$$

Note that a relation similar to Eq. (2.14b) also can be obtained from Eq. (2.17).

3. Relations between M_n and T_n

First we express the relations between y and z : from $y = 1 - e^{-au}$ and $z = e^{au} - 1$, one has

$$y = z(1+z)^{-1}, \quad (2.19a)$$

and

$$z = y(1-y)^{-1}. \quad (2.19b)$$

Then using the binomial formula, we can write,

$$y^n = \sum_{n=1}^{\infty} (-1)^k \binom{n+k-1}{k} z^{n+k}, \quad (2.20a)$$

or

$$y^n = \sum_{m=n}^{\infty} (-1)^{m-n} \binom{m-1}{m-n} z^m. \quad (2.20b)$$

Substitution of this expression into Eq. (2.2) gives

$$M(r) = \sum_{n=0}^{\infty} \sum_{m=n}^{\infty} (-1)^{m-n} \binom{m-1}{m-n} z^m M_n$$

which can be rearranged into

$$M(x) = \sum_{m=0}^{\infty} \left\{ \sum_{n=0}^m [(-1)^{m-n} \binom{m-1}{m-n} M_n] \right\} z^m = \sum_{m=0}^{\infty} T_m z^m$$

Thus we obtain

$$T_m = \sum_{n=0}^m G_m^n M_n \quad (2.21a)$$

where

$$G_m^n = (-1)^{m-n} \binom{m-1}{m-n} = (-1)^{m-n} \frac{(m-1)!}{(n-1)!(m-n)!} \quad (2.21b)$$

which can be cast into an inductive form:

$$G_m^n = \left[\frac{m-1-n}{n-1} \right] G_m^{n-1} \quad (2.21c)$$

We note that T_m can be expressed equivalently as

$$T_m = \sum_{k=0}^m (-1)^k \binom{m-1}{k} M_{m-k} \quad (2.22)$$

To obtain the expression of M_n in terms of T_m , we write

$$z^m = y^m (1-y)^{-m} = \sum_{n=m}^{\infty} \binom{n-1}{n-m} y^n$$

and substitute it into Eq. (2.3); then rearranging and comparing to Eq. (2.2), we get

$$M_n = \sum_{m=0}^n H_n^m T_m \quad (2.23a)$$

where

$$H_n^m = \binom{n-1}{n-m} = \frac{(n-1)!}{(m-1)!(n-m)!}, \quad (2.23b)$$

or

$$H_n^m = \left[\frac{n-m+1}{m-1} \right] H_n^{m-1} \quad (2.23c)$$

Also note that $G_m^m = H_n^n = 1$.

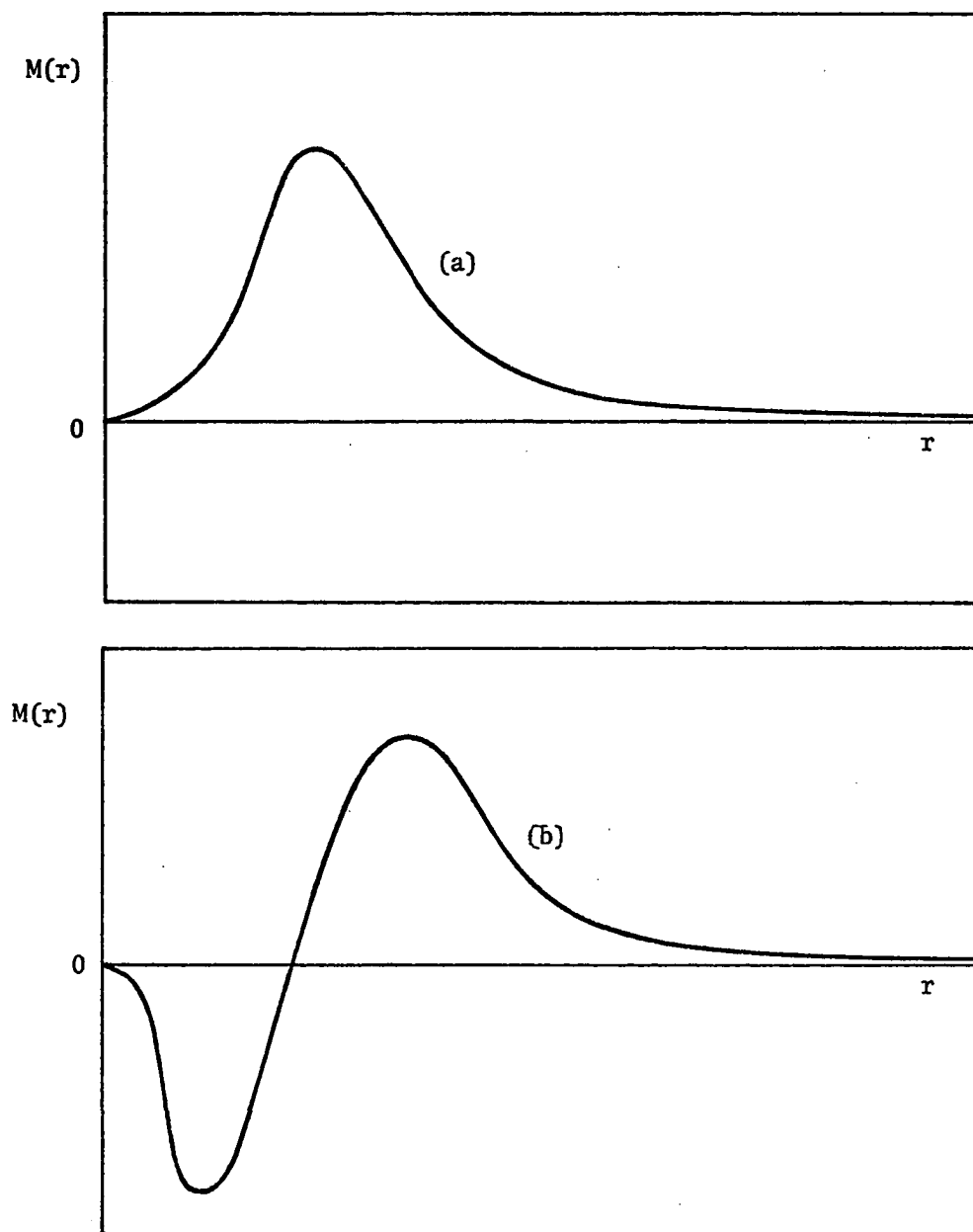


Fig. 2.1. General shape of the dipole moment function. Curve (a) for a molecule with unique polarity, HCl, for example. Curve (b) for a molecule with reversal of polarity, CO, for example.

CHAPTER III

MORSE-OSCILLATOR MATRIX ELEMENTS OF u , y , AND z

1. Factorization Treatment of The Morse Oscillator

The Morse function⁽²⁷⁾

$$V_M(r) = D[\exp(-2au) - 2\exp(-au)] \quad (3.1a)$$

where $u = r - r_e$, r is the internuclear distance, r_e is the point of minimum potential, and D the well depth, is frequently used to describe the internuclear potential energy for diatomic molecules because of its many advantages:

First, considering that it has only three parameters, the Morse function fits the empirical potential curves for diatomic molecules like CO quite well at fairly low vibrational levels. Second, it supports a finite number of bound states, allowing us in some cases to use matrix representations in solving many problems. Third, the Morse function has correct behavior at very large r :

$$V_M(r) \rightarrow 0 \quad \text{as} \quad r \rightarrow \infty .$$

At $r = 0$, where the potential should have a positive pole,

$$V_M(0) = D[\exp(2ar_e) - 2\exp(ar_e)]$$

which is between $100D$ and $10,000D$ for many molecules; in particular, for CO, $V_M(0) = 190D$. These values are large enough that they produce

nearly the same effect as infinity on the energy levels and wavefunctions.

Another important advantage is that the Schroedinger equation representing the vibrational motion of the nuclei in a diatomic molecule with the Morse potential,

$$\frac{d^2\psi}{du^2} + \frac{2\mu D}{\hbar^2} [-\exp(-2au) + 2\exp(-au)]\psi + \frac{2\mu}{\hbar^2} E\psi = 0, \quad (3.1b)$$

$$(-\infty < u < \infty)$$

is exactly solvable by two approaches: the confluent hypergeometric method⁽²⁷⁾ and the factorization method.^(20,22)

Although Morse eigensolutions of the above equation are defined over the whole range of r (or u), they may be considered to vanish over the negative range of r because of very large value of $V_M(0)$, so that their normalization may be considered as the "physical" normalization, i.e.,

$$\int_{-\infty}^{\infty} \psi_v \psi_{v'} du \approx \int_0^{\infty} \psi_v \psi_{v'} dr = \delta_{vv'}.$$

For the same reason, matrix elements using Morse wavefunctions may be evaluated over the whole range of r instead over the physical positive range for many diatomic molecules.

Using a variation of the factorization method, Huffaker and Dwivedi⁽²⁰⁾ obtained two useful recursion relations, one of which permits very easy calculation of some matrix elements. Since their technique of evaluating matrix elements can be extended to other matrix elements we shall require, we recall in the following some important results from their work.

Infeld and Hull⁽²²⁾ (hereinafter referred to as IH) showed

that the substitutions

$$s + \frac{1}{2} = (2\mu D)^{\frac{1}{2}}/a\hbar , \quad (3.2a)$$

$$m_{\ell}^2 = -2\mu E/(a\hbar)^2 , \quad (3.2b)$$

$$x = -au + \ell n(2s + 1) \quad (3.2c)$$

allow one to transform Eq. (3.1b) into the form

$$\frac{d^2 R(x)}{dx^2} + [-\frac{1}{4}e^{2x} + (s + \frac{1}{2})e^x]R(x) - m_{\ell}^2 R(x) = 0 . \quad (3.3)$$

According to IH,⁽²²⁾ the above equation is of Type B factorization with characteristic functions

$$k(x, s) = \frac{1}{2}\exp(x) - s ,$$

and

$$L(s) = -s^2 .$$

$L(s)$ being a decreasing function of s , Eq. (3.3) is a class II problem for which IH⁽²²⁾ obtained the following results:

The eigenvalue:

$$-m_{\ell}^2 = L(\ell) = -(\ell)^2 \quad (3.4)$$

which gives $\ell = m_{\ell}$.

The normalized key solution:

$$R_m^m(x) = \Gamma^{-\frac{1}{2}}(2m)\exp(mx - \frac{1}{2}e^x) \quad (3.5a)$$

which satisfies the first-order differential equation

$$\left[\frac{e^x}{2} - m + \frac{d}{dx}\right]R_m^m(x) = 0 . \quad (3.5b)$$

The normalized s-changing operators:

$$\mathcal{H}_m^{\pm}(s) = [(s-m)(s+m)]^{-\frac{1}{2}}\left\{\frac{1}{2}e^x - s \pm \frac{d}{dx}\right\} \quad (3.6a)$$

which act on s according to

$$R_m^s = \mathcal{H}_m^-(s) R_m^{s-1}, \quad (3.6b)$$

$$R_m^{s-1} = \mathcal{H}_m^+(s) R_m^s. \quad (3.6c)$$

Since $s \geq m$, the quantity $v = s - m$ must be a positive integral number which can be identified as the vibrational quantum number. Substituting $m = s - v$ into Eq. (3.2b), we get the expression for vibrational eigenenergies:

$$E_v = -D + (s + \frac{1}{2})\gamma(v + \frac{1}{2}) - \frac{1}{2}\gamma(v + \frac{1}{2})^2 \quad (3.7)$$

where

$$\gamma = (\hbar a^2)/\mu.$$

The recursion relation:

Eliminating d/dx in Eqs. (3.6b) and (3.6c), one obtains the recursion relation

$$e^x R_m^s = A^s R_m^s + B_m^s R_m^{s-1} + B_m^{s+1} R_m^{s+1} \quad (3.8a)$$

where

$$A^s = 2s + 1, \quad (3.8b)$$

$$B_m^s = [(s-m)(s+m)]^{\frac{1}{2}}. \quad (3.8c)$$

The orthonormality condition:

A solution R_m^s and its corresponding eigenfunction ψ_v can be obtained via the key solution R_m^m by applying Eq. (3.6b) repeatedly a total number of $(s-m) = v$ times. Solutions R_m^s are orthonormal according to

$$\int_{-\infty}^{\infty} R_{m'}^s R_m^s dx = \delta_{m',m} \quad (3.9a)$$

corresponding to the "physical" orthonormality condition:

$$\int_0^{\infty} \psi_{v'} \psi_v dr = \delta_{v',v}. \quad (3.9b)$$

To relate R_m^s and ψ_v we write

$$\begin{aligned} R_m^s &= C_v \psi_v, \\ dx &= -adu, \end{aligned} \quad (3.10a)$$

and substituting these relations into Eq. (3.9a), we get for $v' = v$

$$aC_v^2 = 1$$

from which

$$C_v = a^{-\frac{1}{2}};$$

hence,

$$R_m^s = a^{-\frac{1}{2}} \psi_v. \quad (3.10b)$$

Huffaker and Dwivedi⁽²⁰⁾ showed that the substitutions

$$R(x) = \exp(y/2) W(y), \quad (3.11a)$$

$$x = \ln[y(s + \frac{1}{2})] \quad (3.11b)$$

transform Eq. (3.3) into

$$\frac{d^2W}{dy^2} + \left[\frac{1}{y} - \frac{(m - \frac{1}{2})(m + \frac{1}{2})}{y^2} \right] W - \frac{1}{4}(s + \frac{1}{2})^{-2} W = 0 \quad (3.12)$$

which can be recognized as a type F equation with characteristic functions

$$k(y, m - \frac{1}{2}) = \frac{m - \frac{1}{2}}{y} - \frac{1}{2(m - \frac{1}{2})},$$

$$L(m - \frac{1}{2}) = -\frac{1}{4}(m - \frac{1}{2})^{-2}.$$

Since $L(m - \frac{1}{2})$ is an increasing function of m , Eq. (3.12) is classified as a Class I problem for which Huffaker and Dwivedi⁽²⁰⁾ obtained the following results:

The eigenvalues:

$$\lambda_\ell = L(\ell + 1) = -\frac{1}{4}(\ell + 1)^{-2} = -\frac{1}{4}(s + \frac{1}{2})^{-2} \quad (3.13)$$

from which we see that $\ell = s - \frac{1}{2}$.

The normalized key solution:

$$W_s^s = (s + \frac{1}{2})^{-(s+1)} \Gamma^{-\frac{1}{2}} 2(s + \frac{1}{2}) y^{s+\frac{1}{2}} \exp[-\frac{y}{2(s + \frac{1}{2})}] \quad (3.14a)$$

which satisfies the equation

$$[\frac{(s - \frac{1}{2})}{y} - \frac{1}{2s - 1} - \frac{d}{dy}] W_s^s = 0 . \quad (3.14b)$$

The normalized m-changing operators:

$$\mathcal{K}_s^{\pm(m)} = \frac{2(m - \frac{1}{2})(s + \frac{1}{2})}{[(s + m)(s - m + 1)]^{\frac{1}{2}}} \left\{ \frac{m - \frac{1}{2}}{y} - \frac{1}{2m - 1} \pm \frac{d}{dy} \right\} \quad (3.15a)$$

which generates W-functions with different m according to

$$W_s^{m-1} = \mathcal{K}_s^{+(m)} W_s^m , \quad (3.15b)$$

$$W_s^m = \mathcal{K}_s^{-(m)} W_s^{m-1} . \quad (3.15c)$$

The orthonormality condition:

$$\int_{-\infty}^{\infty} W_{s'}^m W_s^m dy = \delta_{s',s} \quad (3.16)$$

The relationship between W_s^m and R_m^s is given by

$$W_s^m(y) = [4m(s + \frac{1}{2})^2]^{-\frac{1}{2}} \exp(\frac{x}{2}) R_m^s(x) . \quad (3.17)$$

The normalized m-changing operators acting on R_m^s :

Substituting the relation (3.17) and

$$dy = (s + \frac{1}{2}) e^x dx$$

into Eqs. (3.15a, b, c), we obtain

$$R_m^s = \mathcal{L}_s^{-(m)} R_{m-1}^s , \quad (3.18a)$$

$$R_{m-1}^s = \mathcal{L}_s^{+(m)} R_m^s \quad (3.18b)$$

where

$$\mathcal{L}_m^{+(m)} = \left[\frac{4(m-1)(m-\frac{1}{2})^2}{m(s+m)(s-m+1)} \right]^{\frac{1}{2}} \left\{ m e^{-x} - \frac{s+\frac{1}{2}}{2m-1} + e^{-x} \frac{d}{dx} \right\}, \quad (3.18c)$$

$$\begin{aligned} \mathcal{L}_s^{-(m)} = & \left[\frac{4m(m-\frac{1}{2})^2}{(m-1)(s+m)(s-m+1)} \right]^{\frac{1}{2}} \left\{ (m-1)e^{-x} - \frac{s+\frac{1}{2}}{2m-1} \right. \\ & \left. - e^{-x} \frac{d}{dx} \right\}. \end{aligned} \quad (3.18d)$$

The recursion relation:

Eliminating $e^{-x}(d/dx)$ in Eqs. (3.18c, d), one obtains a second recursion relation connecting solutions R_m^s with different m ,

$$e^{-x} R_m^s = \alpha_m^s R_m^s + \beta_m^s R_{m-1}^s + \beta_{m+1}^s R_{m+1}^s \quad (3.19a)$$

$$\alpha_m^s = \frac{s+\frac{1}{2}}{2(m-\frac{1}{2})(m+\frac{1}{2})},$$

$$\beta_m^s = \frac{1}{4(m-\frac{1}{2})} \left[\frac{(s+m)(s-m+1)}{m(m-1)} \right]^{\frac{1}{2}}. \quad (3.19b)$$

Eqs. (3.19a, b, c) can be rewritten in terms of the Morse eigenfunctions, using Eqs. (3.2c) and (3.10b):

$$(e^{au} - 1)\psi_v = A_v \psi_v + B_v \psi_{v-1} + B_{v+1} \psi_{v+1} \quad (3.20a)$$

where

$$A_v = \frac{2(s+\frac{1}{2})(v+\frac{1}{2}) - v(v+1)}{(s+\frac{1}{2}-v)(s-\frac{1}{2}-v)}, \quad (3.20b)$$

$$B_v = \left[\frac{s+\frac{1}{2}}{s+\frac{1}{2}-v} \right] \left[\frac{v(2s+1-v)}{(s-v)(s+1-v)} \right]^{\frac{1}{2}}. \quad (3.20c)$$

Eq. (3.20a) is a very important result because it permits easy calculation of the matrix elements $\langle v' | z^n | v \rangle$ for any power n . It served as a basis for a treatment of the perturbed-Morse oscillator. (21)

2. Signs of the Morse Eigenfunctions

Eq. (3.4) for the eigenvalues and the condition that $s-m$ must be an integer show that a Morse oscillator has a finite number of bound states, which is approximately equal to the quantity s defined in Eq. (3.2a). For CO, this number is about 77.

If the Morse radial equation [Eq. (3.1b)] is solved by the usual confluent hypergeometric method, the relative phases of the various eigenfunctions are completely arbitrary. When one uses the factorization method, however, this arbitrariness is removed, since one generates all eigensolutions by repeated application of either a class I operator or a class II operator on the corresponding key solution.

First, in the class I problem, if the key solution W_s^S is given as in Eq. (3.14a) then the corresponding function R_s^S is

$$R_s^S(x) = (\text{positive const.}) e^{sx} \exp(-\frac{1}{2}e^x), \quad (3.21a)$$

and the corresponding Morse function is

$$\psi_0(r) = (\text{positive const.}) e^{-sau} \exp[-(s+\frac{1}{2})e^{-au}]. \quad (3.21b)$$

We see that both these functions approach zero positively as r tends to 0 or $+\infty$:

$$R_s^S \text{ and } \psi_0 \text{ } \underbrace{\hspace{2cm}}_{\substack{r \rightarrow 0 \\ \text{or} \\ r \rightarrow +\infty}} 0^+ \quad (3.22)$$

Other solutions R_m^S and ψ_v with different m and v can be obtained from R_s^S and ψ by using either Eq. (3.18b) or the class I recursion relations (3.19a) and (3.20a). The last equation can be

rewritten in the form

$$\psi_v = \left[\frac{e^{au} - 1 - A_{v-1}}{B_v} \right] \psi_{v-1} - \left[\frac{B_{v-1}}{B_v} \right] \psi_{v-2} . \quad (3.23)$$

As $r \rightarrow \infty$, so that the term in e^{au} is predominant, we have

$$\psi_v \underset{r \rightarrow +\infty}{\sim} \left[\frac{e^{au}}{B_v} \right] \psi_{v-1} ,$$

which by induction, leads to

$$\psi_v(r) \underset{r \rightarrow +\infty}{\sim} \left[\frac{e^{vau}}{B_v B_{v-1} \dots B_1} \right] \psi_0 ,$$

and hence,

$$\psi_v(r) \underset{r \rightarrow +\infty}{\sim} 0^+ . \quad (3.24a)$$

This means that all class I Morse eigenfunctions are positive for very large r . Since ψ_v has v nodes, its sign at $r = 0$ is given by $(-1)^v$, that is,

$$\psi_v(r) \underset{r \rightarrow 0}{\sim} (-1)^v 0^+ . \quad (3.24b)$$

Now in the class II treatment, the key function R_m^m and the corresponding Morse function ψ_0^{s-v} (which is the ground state wavefunction of another Morse oscillator described by $s' = s-v$) are

$$R_m^m(x) = (\text{positive const.}) \exp(mx - \frac{1}{2}e^x) , \quad (3.25a)$$

and

$$\psi_0^{s-v}(r) = (\text{positive const.}) \exp[(s-v)au - (s+\frac{1}{2})e^{-au}] , \quad (3.25b)$$

which clearly have the same asymptotic behaviors as R_s^s and ψ_0 ,

$$R_m^m \text{ and } \psi_0^{s-v} \underset{r \rightarrow 0 \text{ or } +\infty}{\sim} 0^+ . \quad (3.26)$$

Then, in a similar manner, the $r = \infty$ behavior of other solutions, R_m^s and ψ_v^{s-v} with different s , can be seen by rewriting the class II recursion relation as

$$R_m^s = \left[\frac{e^x - A^{s-1}}{B_m^s} \right] R_m^{s-1} - \left[\frac{B_m^{s-1}}{B_m^s} \right] R_m^{s-1}$$

from which one sees that

$$R_m^s(x) \underset{x \rightarrow +\infty}{\sim} \left[\frac{e^{(s-m)x}}{B_m^s B_m^{s-1} \dots B_m^{m+1}} \right] R_m^m,$$

hence,

$$\psi_v^{s-v}(r) \underset{r \rightarrow 0}{\sim} 0^+, \quad (3.27a)$$

and

$$\psi_v^{s-v}(r) \underset{r \rightarrow +\infty}{\sim} (-1)^v 0^+. \quad (3.27b)$$

Thus, all class II Morse eigenfunctions begin with positive values at very small r and from the above results we obtain the relation between class I and class II Morse wavefunctions:

$$\psi_v^{(I)} = (-1)^v \psi_v^{(II)}. \quad (3.28)$$

This means that eigenfunctions of the two classes are the same for even values of v and have opposite sign for odd values of v .

The difference in sign between class I and class II Morse wavefunctions, of course, results in the difference in sign between Morse matrix elements of any function $f(r)$. Using the relation (3.28), one obtains immediately

$$\langle \psi_v^{(I)} | f(r) | \psi_{v'}^{(I)} \rangle = (-1)^{v+v'} \langle \psi_v^{(II)} | f(r) | \psi_{v'}^{(II)} \rangle. \quad (3.29)$$

3. Matrix Elements of u

In Chapter I we have mentioned that in the analysis of intensities of rotation-vibration or rotationless vibration transitions of diatomic molecules the dipole moment is usually expanded in a Taylor series of the variable $u = r - r_e$. Thus, in the Morse oscillator model, the vibrational matrix elements of powers of u are important quantities. Morse matrix elements of u and u^2 have been analytically evaluated by several authors⁽²⁸⁻³⁰⁾ by the usual integration method. The formula for u is in a rather simple closed form, but that for u^2 is quite complicated. Herman and Rubin⁽³¹⁾ were able to obtain a general formula from which it is possible to extract matrix elements of higher power of u for the rotating Morse oscillator (Morse-Pekeris). However, even their expression for matrix elements of u is very complicated. Herman, Rothery and Rubin⁽³²⁾ succeeded in reducing it to a considerably simplified form, only after a great deal of algebra. Up to the present, formulas obtained by integration for powers of u higher than the quadratic are not suitable for numerical calculation.

The factorization method⁽²²⁾ provides a more powerful and more elegant technique than the integration method for the evaluation of matrix elements in many eigenvalue problems. Using this procedure, IH⁽²²⁾ worked out the exact expression for the off-diagonal Morse matrix elements of x , the variable related to u by Eq. (3.2c). Huffer and Dwivedi⁽²⁰⁾ then obtained the diagonal Morse matrix elements of x , thus completing the evaluation of the full x -matrix in the Morse basis of bound state eigenfunctions. From these, the matrix elements of u are easily obtained, as shown by the following:

3a. Diagonal matrix elements of u

Huffaker and Dwivedi⁽²⁰⁾ showed that

$$\langle m|x|m\rangle = \psi(2m) - \sum_{k=1}^{s-m} \left[\frac{1}{2m+k} \right], \quad (3.30a)$$

or

$$\langle m|x|m\rangle = 2\psi(2m) - \psi(s+m+1) + \frac{1}{2m} \quad (3.30b)$$

where ψ is the digamma function defined by

$$\psi(z) = \frac{\Gamma'(z)}{\Gamma(z)} = \frac{1}{\Gamma(z)} \cdot \frac{d\Gamma(z)}{dz} \quad (3.31a)$$

with the properties:

$$\psi(z+1) = \psi(z) + \frac{1}{z}, \quad (3.31b)$$

and

$$\psi(z+n) = \psi(z) + \sum_{k=1}^n \left[\frac{1}{z+n-k} \right], \quad (3.31c)$$

or

$$= \psi(z) + \sum_{k=0}^{n-1} \left[\frac{1}{z+k} \right]. \quad (3.31d)$$

Using the relation (3.2c) between x and u and the relation (3.10b) between R_m^s and ψ_v , we get from Eq. (3.30) the non-diagonal matrix elements of u

$$\langle v|u|v\rangle = \frac{1}{a} [\ln(2s+1) - \psi(2s-2v) - \sum_{k=1}^v \frac{1}{2(s-v)+k}], \quad (3.32a)$$

or

$$\langle v|u|v\rangle = \frac{1}{a} [\ln(2s+1) - 2\psi(2s-2v) + \psi(2s-v+1) + \frac{1}{2(s-v)}]. \quad (3.32b)$$

According to Dunham,⁽²⁸⁾ the digamma function $\psi(z)$ can be approximately with very high accuracy for $z \gtrsim 50$ by

$$\psi(z) \approx \ln(z - \frac{1}{2}). \quad (3.33)$$

Therefore, if this approximation is applied to the gamma function $\psi(2s-2v)$ in Eqs. (3.32a, b), the required condition should be

$$v \lesssim s - 25 ,$$

and for CO,

$$v \lesssim 51 . \quad (3.34a)$$

For the digamma function $\psi(2s-v+1)$ in Eq. (3.32b), we should have

$$v \lesssim 2s + 1 ,$$

hence for CO,

$$v \lesssim 154 . \quad (3.34b)$$

Thus, the digamma function $\psi(2s-v+1)$ may be approximated by Eq. (3.33) for all bound states of CO, while values obtained by this approximation for $\psi(2s-2v)$ become increasingly less accurate when v exceeds the value of about 51. Since levels have been measured only up through $v=37$, the approximation should be satisfactory.

3b. Non-diagonal matrix elements of u

Off-diagonal matrix elements of x were obtained by IH⁽²²⁾ in the form

$$\langle m|x|m' \rangle = \frac{2}{(m-m')(m+m')} \left[\frac{(s-m')!}{(s-m)!} \frac{\Gamma(s+m'+1)}{\Gamma(s+m+1)} m'm \right]^{\frac{1}{2}} \quad (3.35)$$

where it is assumed that $m > m'$ or $v < v'$.

From this, non-diagonal matrix elements of u follow,

$$\langle v|u|v' \rangle = - \frac{2}{a(v'-v)(2s-v'-v)} \left[\frac{v'!}{v!} \frac{\Gamma(2s-v'+1)}{\Gamma(2s-v+1)} (s-v')(s-v) \right]^{\frac{1}{2}} . \quad (3.36)$$

We note that all diagonal matrix elements of u are positive while all off-diagonal elements are negative as shown by Eqs. (3.32b)

and (3.36). These values are also listed in Table 3.1 for $0 \leq v \leq 9$ and $0 \leq v' \leq 9$.

4. Matrix Elements of y

4a. Diagonal matrix elements of y

Huffaker and Dwivedi⁽²⁰⁾ also obtained diagonal elements of e^x in a very simple form,

$$\langle m | e^x | m \rangle = 2m \quad (3.37)$$

from which diagonal matrix elements of e^{-au} and y are obtained:

$$\langle v | e^{-au} | v \rangle = \frac{s - v}{s + \frac{1}{2}}, \quad (3.38)$$

$$\langle v | y | v \rangle = \frac{v + \frac{1}{2}}{s + \frac{1}{2}}. \quad (3.39)$$

4b. Integral $\langle R_m^{s+1} | R_{m'}^s \rangle$

Evaluation of the off-diagonal matrix elements of y requires the knowledge of this integral. Let us denote the overlap integral of two functions R_m^s and $R_{m'}^{s'}$ by $K_{m,m'}^{s,s'}$. Then, using the s -raising and lowering operators and their mutual adjointness, we can write

$$\begin{aligned} K_{m,m'}^{s+1,s} &= \int_{-\infty}^{\infty} \mathcal{H}_m^-(s+1) R_m^s R_{m'}^s dx, \\ &= \int_{-\infty}^{\infty} R_m^s \mathcal{H}_m^+(s+1) R_{m'}^s dx, \\ &= (B_m^{s+1})^{-1} \int_{-\infty}^{\infty} R_m^s \left\{ e^x - (s+1) + \frac{d}{dx} \right\} R_{m'}^s dx, \\ &= (B_{m'}^s / B_m^{s+1}) \int_{-\infty}^{\infty} R_m^s R_{m'}^{s-1} dx, \\ K_{m,m'}^{s+1,s} &= (B_{m'}^s / B_m^{s+1}) K_{m,m'}^{s,s-1}. \end{aligned}$$

Thus, by induction, this equation gives

$$K_{m,m'}^{s+1,s} = \left[\frac{B_{m'}^s B_{m'}^{s-1} \dots B_{m'}^m}{B_m^{s+1} B_m^s \dots B_m^{m+1}} \right] K_{m,m'}^{m,m-1} \quad (3.40a)$$

Recalling that $B_m^s = [(s-m)(s+m)]^{\frac{1}{2}}$ as defined by Eq. (3.8c), the constant (denoted by C) in the square brackets in Eq. (3.40a) can be expressed as

$$C = \left[\frac{(s-m)! \Gamma(s+m'+1) \Gamma(2m+1)}{(m-m'-1)! (s-m+1)! \Gamma(s+m+2) \Gamma(m+m')} \right]^{\frac{1}{2}} .$$

The integral $K_{m,m'}^{s,s-1}$ is given by Eq. (C.8a) in Appendix C. Thus, substituting the value of C and the expression of this integral into Eq. (3.40), then after some reduction we obtain

$$\langle R_m^{s+1} | R_{m'}^s \rangle = \left[\frac{(s-m)! \Gamma(s+m'+1)}{(s-m+1)! \Gamma(s+m+2)} 4m'm \right]^{\frac{1}{2}} . \quad (3.41)$$

4c. Non-diagonal matrix elements of y

Multiplying both sides of the class II recursion relation (3.8a) by $R_{m'}^s$, integrating with respect to x and using the orthonormality of R-functions, one gets

$$\langle R_m^s | e^x | R_{m'}^s \rangle = B_m^{s+1} \langle R_m^{s+1} | R_{m'}^s \rangle .$$

The B-factor and the integral in the right-hand side of this equation can be replaced by their expressions to yield

$$\langle m | e^x | m' \rangle = \left[\frac{(s-m')! \Gamma(s+m'+1)}{(s-m)! \Gamma(s+m+1)} 4m'm \right]^{\frac{1}{2}} \quad (3.42)$$

which then leads to the matrix elements of e^{-au} and y:

$$\langle v | e^{-au} | v' \rangle = -\langle v | y | v' \rangle , \quad (3.43)$$

$$\langle v|y|v'\rangle = -\frac{1}{s + \frac{1}{2}} \left[\frac{v'!}{v!} \frac{\Gamma(2s-v'+1)}{\Gamma(2s-v+1)} (s-v')(s-v) \right]^{\frac{1}{2}} . \quad (3.44)$$

Comparison between matrix elements of y and u shows that they are related to each other by

$$\langle v|y|v'\rangle = \frac{a(v'-v)(2s-v'-v)}{2s+1} \langle v|u|v'\rangle . \quad (3.45)$$

Also, as for the u -matrix, all diagonal matrix elements of y are positive while all off-diagonal elements are negative. To give some idea of the magnitude of the y -matrix elements, we list these in Table 3.2 for CO and for $0 \leq v \leq 9$ and $0 \leq v' \leq 9$.

5. Numerical Calculation of Matrix Elements of Any Power of u , y , and z

The set of bound state and continuum state Morse wavefunctions forms a complete set in terms of which a function of r can be expanded. In practical calculations, this complete set, however, has to be truncated so that one has finite and discrete matrix representations. Therefore, for diatomic molecules with many bound states, one may retain only a reasonably large number of bound states in the Morse basis. For CO which has about 77 bound states, Huffaker^(21e) found that, for a given v , the basis size M is at least $v + 14$ so that the effect of truncation is insignificant. For $M = 48$, the matrix diagonalization yields highly accurate perturbed-Morse-oscillator (PMO) eigenfunctions up to $v = 30$. Thus, for CO at least, it is reasonable to neglect all continuum states and make the approximation

$$\sum_{v=0}^N |v\rangle\langle v| = I \quad (3.46)$$

where I is the unit operator and $N \geq 48$.

As seen before, a matrix representation of z can be easily obtained from the class I recursion relation (3.20a) and thus has a simple tridiagonal form:

$$Z = \begin{bmatrix} A_0 & B_1 & & & \\ B_1 & A_1 & B_2 & & \\ & B_2 & A_2 & B_3 & \\ & & & \ddots & \ddots \\ & & & & \ddots & \ddots \end{bmatrix} .$$

Noting that

$$y = 1 - (z + 1)^{-1} ,$$

matrix representation of y can be produced numerically from that of z by taking the matrix representation of the above equation, ⁽²¹⁾ i.e., by inverting the matrix representing $(z + 1)$.

For CO, matrix size 50x50 is adequate to give highly accurate values for y -matrix by inversion method. If the full size 76x76 is used, values obtained are nearly the same as those by exact formulas. Also, note that, since the inversion method involves class I wavefunctions while the exact calculation makes use of class II functions, values of y -matrix elements obtained by the two methods differ in sign according to Eq. (3.29):

$$Y_{vv'}^{(I)} = (-1)^{v+v'} Y_{vv'}^{(II)} .$$

Exact formulas for matrix elements of y^2 and y^3 are derived in Appendix B. Formulas for higher powers of y can be obtained by the same technique, but are increasingly lengthy and complicated. Therefore, matrix multiplication appears to be more appropriate and conve-

nient. In this method, the approximation (3.46) permits one to write

$$\langle v | f^n(r) | v' \rangle = \sum_{\lambda=0}^N \langle v | f^p | \lambda \rangle \langle \lambda | f^q | v' \rangle$$

where $p + q = n$, and $f(r)$ is u , or y , or z , or any function of r .

To maintain good accuracy, one can use exact expressions for matrix elements of the first three powers of y , from which one can obtain matrix elements for higher powers using matrix multiplication.

TABLE 3.1. Morse matrix elements of u for $0 \leq v$ and $v' \leq 9$. The entry $.408287 -2$ means $.408287 \cdot 10^{-2}$.

| $v' \backslash v$ | 0 | 1 | 2 | 3 | 4 |
|-------------------|-------------|-------------|-------------|-------------|-------------|
| 0 | .408287 -2 | -.337712 -1 | -.193399 -2 | -.181451 -3 | -.221872 -4 |
| 1 | -.337712 -1 | .123346 -1 | -.479160 -1 | -.337182 -2 | -.366500 -3 |
| 2 | -.193399 -2 | -.479160 -1 | .207130 -1 | -.588783 -1 | -.480001 -2 |
| 3 | -.181451 -3 | -.337182 -2 | -.588783 -1 | .292238 -1 | -.682123 -1 |
| 4 | -.221872 -4 | -.366500 -3 | -.480001 -2 | -.682124 -1 | .378702 -1 |
| 5 | -.324605 -5 | -.502711 -4 | -.585272 -3 | -.623816 -2 | -.765184 -1 |
| 6 | -.543705 -6 | -.808384 -5 | -.882366 -4 | -.836017 -3 | -.769143 -2 |
| 7 | -.101513 -6 | -.146745 -5 | -.153775 -4 | -.136598 -3 | -.111713 -2 |
| 8 | -.207533 -7 | -.293896 -6 | -.299435 -5 | -.255361 -4 | -.195798 -3 |
| 9 | -.458702 -8 | -.639467 -7 | -.638254 -6 | -.529214 -5 | -.389563 -4 |
| $v' \backslash v$ | 5 | 6 | 7 | 8 | 9 |
| 0 | -.324605 -5 | -.543705 -6 | -.101513 -6 | -.207533 -7 | -.458702 -8 |
| 1 | -.520711 -4 | -.808384 -5 | -.146745 -5 | -.293896 -6 | -.639467 -7 |
| 2 | -.585272 -3 | -.882365 -4 | -.153775 -4 | -.299435 -5 | -.638254 -6 |
| 3 | -.623816 -2 | -.836017 -3 | -.136598 -3 | -.255361 -4 | -.529214 -5 |
| 4 | -.765184 -1 | -.769143 -2 | -.111713 -2 | -.195796 -3 | -.389563 -4 |
| 5 | .466562 -1 | -.841036 -1 | -.916211 -2 | -.142747 -2 | -.266275 -3 |
| 6 | -.841036 -1 | .555861 -1 | -.911497 -1 | -.106515 -1 | -.176621 -2 |
| 7 | -.916211 -2 | -.911497 -1 | .646417 -1 | -.977752 -1 | -.121603 -1 |
| 8 | -.142747 -2 | -.106515 -1 | -.977752 -1 | .738950 -1 | -.104062 +0 |
| 9 | -.266275 -3 | -.176621 -2 | -.121603 -1 | -.104062 +0 | .832834 -1 |

TABLE 3.2. Morse matrix elements of y for $0 \leq v$ and $v' \leq 0$.

| $v \backslash v'$ | 0 | 1 | 2 | 3 | 4 |
|-------------------|-------------|-------------|-------------|-------------|-------------|
| 0 | .647508 -2 | -.796825 -1 | -.906659 -2 | -.126754 -2 | -.205280 -3 |
| 1 | -.796825 -1 | .194252 -1 | -.111574 +0 | -.155984 -1 | -.252618 -2 |
| 2 | -.906659 -2 | -.111574 +0 | .323754 -1 | -.135277 +0 | -.219083 -1 |
| 3 | -.126754 -2 | -.155984 -1 | -.135277 +0 | .453256 -1 | -.154611 +0 |
| 4 | -.205280 -3 | -.252618 -2 | -.219083 -1 | -.154611 +0 | .582757 -1 |
| 5 | -.372901 -4 | -.458893 -3 | -.397976 -2 | -.280859 -1 | -.171069 +0 |
| 6 | -.744470 -5 | -.916147 -4 | -.794530 -3 | -.560714 -2 | -.341527 -1 |
| 7 | -.161046 -5 | -.198206 -4 | -.171894 -3 | -.121309 -2 | -.738884 -2 |
| 8 | -.373748 -6 | -.459936 -5 | -.398880 -4 | -.281497 -3 | -.171458 -2 |
| 9 | -.922950 -7 | -.113578 -5 | -.985011 -5 | -.695140 -4 | -.423405 -3 |
| $v \backslash v'$ | 5 | 6 | 7 | 8 | 9 |
| 0 | -.372901 -4 | -.744470 -5 | -.161064 -5 | -.373748 -6 | -.922950 -7 |
| 1 | -.458893 -3 | -.916147 -4 | -.198206 -4 | -.459936 -5 | -.113578 -5 |
| 2 | -.397976 -2 | -.794530 -3 | -.171894 -3 | -.398880 -4 | -.985011 -5 |
| 3 | -.280859 -1 | -.560714 -2 | -.121309 -2 | -.281497 -3 | -.695140 -4 |
| 4 | -.171069 +0 | -.341527 -1 | -.738884 -2 | -.171458 -2 | -.423405 -3 |
| 5 | .712259 -1 | -.185423 +0 | -.401158 -1 | -.930885 -2 | -.229877 -2 |
| 6 | -.185423 +0 | .841761 -1 | -.198136 +0 | -.459774 -1 | -.113538 -1 |
| 7 | -.401158 -1 | -.198136 +0 | .971262 -1 | -.209511 +0 | -.517376 -1 |
| 8 | -.930885 -2 | -.459774 -1 | -.209511 +0 | .110076 +0 | -.219761 +0 |
| 9 | -.229877 -2 | -.113538 -1 | -.517376 -1 | -.219761 +0 | .123027 +0 |

CHAPTER IV

CUBIC DIPOLE MOMENT FUNCTIONS IN u , y , AND z

Although there have been numerous determinations of dipole moments of diatomic molecules as functions of the internuclear separation using intensity data, this problem is still of considerable importance and interest. In this empirical approach, the correctness of the results depends on three factors:

- i) Reliability and sufficiency of the experimental data;
- ii) Accuracy of the internuclear potential used, whether analytical or numerical;
- iii) Reasonable form chosen for the dipole moment.

The first condition appears to be a major concern. The very small number of experimental data points per molecule usually limits the choice of form for the dipole moment to a Taylor series expansion which, in turn, requires the measurements to be highly accurate. Infrared absorption experiments are frequently performed to provide absolute intensities of individual lines^(9,13,14,25) or integrated intensities⁽³³⁻³⁵⁾ of the lines in a given vibrational transition, as well as in electronic transitions. This measurement technique is not accurate when the population of the lower level is so low that emission transition is possible. In this case, emission experiments^(36,37) are more preferable.

Two techniques have been developed for determining the coefficients of the dipole moment expansion. The first procedure⁽⁸⁾ makes direct use of the integrated absorption intensities at low temperature for various vibration bands and requires the evaluation of rotation-vibration matrix elements. The second⁽⁹⁾ extracts the squares of rotationless dipole matrix elements from individual line intensities using least-squares fit and thus involves only purely vibrational eigenfunctions in the calculation of the expansion coefficients. In the latter approach, it is usually assumed that the square of the rotation-vibration matrix element $\langle vJ|M(r)|v'J'\rangle$ may be factorized in the form

$$|\langle vJ|M(r)|v'J'\rangle|^2 \equiv |\mu_{vJ,v'J'}|^2 = |\mu_{vJ,v'}|^2 F_{vJ,v'J'}(m)$$

where

$$\mu_{vJ,v'} = \langle vJ|M(r)|v'J'\rangle$$

is the rotationless dipole matrix element and $F_{vJ,v'J'}(m)$ is called the Herman-Wallis factor representing the rotation-vibration interaction, and

$$m = J + 1 \quad \text{for R branch,}$$

$$m = -J \quad \text{for P branch.}$$

A great deal of effort^(9,13,14,25,34-38) combined with modern equipment and techniques has been made to obtain highly accurate intensity data for the fundamental (0-1) band and the first two overtone (0-2 and 0-3) bands of CO ($X^1\Sigma$), from which reliable absolute values of the corresponding rotationless transition moments have been deduced. Three sets of these empirical quantities for CO are listed in Table

4.1 together with less accurate values for some low hot bands. Also shown are the values averaged over the three sets of values for μ_{01} , μ_{02} , and μ_{03} , and uncertainties reported by Toth, Hunt, and Plyler⁽⁹⁾ on their values for these quantities. These averaged values shall be used in all our calculations.

In Chapter III we showed how the eigenfunctions and some matrix elements for the Morse oscillator can be easily obtained. Since this model is good only for low vibrational levels, $v \lesssim 10$ for CO, we shall also use the perturbed-Morse-oscillator (PMO) potential energy which is expressed by

$$V_{\text{PMO}}(r) = Dy + D \sum_{n=4}^N b_n y^n \quad (4.1)$$

where $y = 1 - e^{-au}$, $u = r - r_e$, and the first term represents the unperturbed Morse oscillator.

The PMO potential function was shown by Huffaker⁽²¹⁾ to be a useful model for describing diatomic molecules (within the framework of the Born-Oppenheimer approximation) as accurately as the potential obtained via the RKR method. Using the WKB method, Huffaker⁽⁴⁴⁾ was able to extract from the spectral data the coefficients b_n from b_4 up to b_{62} for the ground electronic of CO, together with the three parameters that he used to characterize the equivalent (unperturbed) Morse oscillator:

$$\rho = ar_e, \quad (4.2a)$$

$$\sigma = s + \frac{1}{2} = \frac{(2\mu D)^{\frac{1}{2}}}{ah}, \quad (4.2b)$$

$$\tau = \frac{D}{hc}. \quad (4.2c)$$

In Huffaker's energy-related works, these quantities are more convenient than the usual Morse parameters, a , r_e , and D ; but in our study we shall use the latter set of characteristics. Therefore, we list in Table 4.2 empirical values obtained by Huffaker^(44,45) for the first set of parameters and corresponding values for the second set.

Next we shall describe a technique employed by Huffaker to produce eigenfunctions of the perturbed Morse oscillator.

1. PMO Eigenfunctions for CO

These eigenfunctions have been obtained analytically by perturbation-method calculations,^(21c) which included the effects of PMO coefficients from b_4 to b_7 only. If a larger number of these coefficients is to be included, finite perturbation theory is impracticable as the complexity of the perturbation formulas increases geometrically with increasing order of terms.

Therefore, in order to obtain more accurate eigenfunctions, matrix diagonalization was used by Huffaker.^(21e) In this technique, it is necessary to neglect the continuum of unbound states of the Morse oscillator and retain a certain number M of bound states in order to have a finite and discrete matrix representation. For CO where the total number of bound states is about 77, we choose $M=48$ which is adequately large to yield very accurate eigenfunctions and not too large for numerical calculations.

The Hamiltonian of the perturbed Morse oscillator can be written as

$$H = H^0 + H^1 \quad (4.3a)$$

where

$$H^0 = \frac{\hbar^2}{2\mu} \frac{d^2}{dr^2} + Dy^2 \quad (4.3b)$$

is the unperturbed Hamiltonian of the equivalent Morse oscillator, and

$$H' = D \sum_{n=4}^N b_n y^n \quad (4.3c)$$

is the perturbation Hamiltonian consisting of a finite sum of terms.

The unperturbed Hamiltonian H^0 has eigenfunctions ϕ_v and eigenvalues E_v^0 satisfying the Schroedinger equation

$$H^0 \phi_v = E_v^0 \phi_v$$

The eigenvalue E_v^0 , which is the pure Morse matrix element, can be obtained from Eq. (3.7) and written in the form

$$E_v^0 = H_{vv}^0 = D \left[\frac{2(v + \frac{1}{2})}{\sigma} - \frac{(v + \frac{1}{2})^2}{\sigma^2} \right] \delta_{vv} \quad (4.4)$$

The eigenfunctions and eigenvalues of the unperturbed system are related by

$$H \Psi_v = E_v \Psi_v$$

From Eq. (4.3a), the perturbed Hamiltonian matrix element $H_{vv'}$, in the basis of the equivalent Morse oscillator can be written

$$H_{vv'} = H_{vv'}^0 + H'_{vv'} \quad (4.5)$$

where $H'_{vv'}$, may be called the "perturbation" matrix element:

$$H'_{vv'} = D \sum_{n=4}^N b_n \langle v | y^n | v' \rangle \quad (4.6)$$

The finite matrix representation of the PMO Hamiltonian is then diagonalized to produce eigenvectors, expressing PMO eigenfunctions as linear combinations of Morse eigenfunctions. Since the perturbed Hamiltonian matrix is nearly diagonal and its eigenvalues are known experimentally, eigenvectors can be produced by a simple procedure. Calling $\bar{\Psi}_V$ the unnormalized eigenfunction corresponding to eigenvector D_{-V} and eigenvalue E_V , we can write

$$\bar{\Psi}_V = \sum_{V'} D_{VV'} \phi_{V'}$$

Then choosing $D_{VV} = 1$, one obtains the other components of D_{-V} by solving the set of $(M - 1)$ inhomogeneous linear equations

$$\sum_{V' \neq V} (H_{VV'} - E_V \delta_{VV'}) D_{VV'} = -H_{VV''} \quad (4.7)$$

by matrix inversion.

Consistency can be checked by comparing

$$\bar{E}_V = \sum_{V'} H_{VV'} D_{VV'}$$

to the eigenvalue E_V . If the difference between \bar{E}_V and E_V is more than the desired accuracy, one replaces E_V in Eq. (4.7) by \bar{E}_V and repeat the process until the desired accuracy degree is reached. Finally, the normalized eigenfunctions are obtained in the form

$$\Psi_V = \sum_{V'} C_{VV'} \phi_{V'} \quad (4.8)$$

where

$$C_V = \frac{D_V}{\left[\sum_{V'} (D_{VV'})^2 \right]^{1/2}}$$

A computer code has been written by Huffaker to solve this problem for PMO eigenfunctions for CO. The results were found to be good for $v \leq 28$ and $J \leq 160$. We use his program to obtain rotationless ($J = 0$) PMO eigenfunctions for all calculations in this work.

2. Various Cubic Dipole Moment Functions for CO

With a few reliable experimental data, and with accurate PMO eigenfunctions available, our next task is to solve for the coefficients of the cubic dipole moment functions in u , y , and z for CO:

$$M(u) = m_0 + m_1u + m_2u^2 + m_3u^3 , \quad (4.9a)$$

$$M(y) = M_0 + M_1y + M_2y^2 + M_3y^3 , \quad (4.9b)$$

$$M(z) = T_0 + T_1z + T_2z^2 + T_3z^3 . \quad (4.9c)$$

Since at $r = r_e$, $u = y = z = 0$, we have

$$M(r_e) = m_0 = M_0 = T_0 ,$$

which is called the permanent dipole moment of the molecule.

For convenience, let us denote all three variables of u , y , and z by a single letter q and write

$$M(q) = M_0 + P_1q + P_2q^2 + P_3q^3 . \quad (4.10)$$

Then the coefficients P_1 , P_2 , and P_3 can be determined simply by solving an inhomogeneous set of three linear equations which can be written in the matrix form:

$$\begin{bmatrix} q_{01} & q_{01}^2 & q_{01}^3 \\ q_{02} & q_{02}^2 & q_{02}^3 \\ q_{03} & q_{03}^2 & q_{03}^3 \end{bmatrix} \begin{bmatrix} P_1 \\ P_2 \\ P_3 \end{bmatrix} = \begin{bmatrix} \mu_{01} \\ \mu_{02} \\ \mu_{03} \end{bmatrix} \quad (4.11)$$

where

$$q_{0v}^n = \langle 0 | q^n | v \rangle, \quad n = 1, 2, 3, \dots,$$

is the Morse or PMO matrix element of q^n .

Now, another problem one usually faces is an ambiguity in the dipole moment function $M(q)$ which arises from the fact that spectral intensity measurements determine only the absolute magnitudes and not the algebraic signs of the matrix elements. Consequently, one has 2^3 possible cubic dipole moment functions $M(q)$ for each variable q . In general, if K coefficients in the expansion of $M(q)$ are to be determined, and if the sign of M has been fixed, then the number of solutions will be 2^K .

In most experiments, only the absolute magnitude of the permanent dipole moment M_0 may be determined. By observing the Stark effect on microwave transitions, Burrus⁽⁴⁶⁾ obtained the value of $0.112 \pm 0.005D$ for M_0 . Other measurements⁽⁴⁷⁾ gave the value $0.114 D$. In the past few years, molecular beam electric resonance spectroscopy^(48,49) has been used to provide data from which Muentner⁽⁵⁰⁾ could extract a more accurate value and also determine the sign for M_0 :

$$M_0 = -0.1222 D \quad (4.12)$$

with the negative sign indicating the C^{-0+} orientation.

Further, the negative sign of M_0 has been confirmed by an ab initio calculation of Billingsley and Krauss⁽⁵¹⁾ using the optimized valence configurations multiconfiguration self-consistent-field method (OVC MCSCF), and by Toth et al.⁽⁹⁾ who found that the negative value of M_0 gave the best agreement between the calculated and observed values of the Herman-Wallis factors.

To remove the ambiguity on the dipole moment function, one usually fixes the sign of the coefficient P_1 and selects signs of μ_{01} , μ_{02} , and μ_{03} for which the corresponding dipole moment function is the most physically reasonable. We shall assume that the CO dipole moment function has the behavior about r_e as shown in Fig. 2.1, curve (b), so that P_1 has positive value, i.e., the curve has positive slope at r . Since at low vibrational levels the contribution to the dipole matrix element $\mu_{v'v}$, comes mainly from values of $M(r)$ over a small region about r_e , we have found a way to fix the signs of μ_{01} , μ_{02} , and μ_{03} by approximating $M(q)$ as a linear function in q ,

$$M(q) \approx M_0 + P_1 q ,$$

so that

$$\mu_{0v} \approx \langle 0 | M(q) | v \rangle^{\text{Morse}} \approx P_1 \langle 0 | q | v \rangle^{\text{Morse}} < 0 \quad (4.13)$$

because all off-diagonal Morse matrix elements of u and y have been shown to be negative in Chapter III, Eqs. (3.36) and (3.45). Also, the condition (4.13) implies that Class II Morse eigenfunctions are used.

Thus, we shall give negative signs to the empirical dipole transition moments μ_{01} , μ_{02} , and μ_{03} , and also to μ_{13} , μ_{24} , and μ_{35} for hot bands.

2a. Results Using Morse Eigenfunctions

$$M(u) = -0.1222 + 3.0908u - 0.1986u^2 - 2.3781u^3 , \quad (4.14)$$

$$M(y) = -0.1222 + 1.2930y + 0.6127y^2 + 0.2171y^3 , \quad (4.15)$$

$$M(z) = -0.1222 + 1.2933z - 0.6837z^2 + 0.2709z^3 . \quad (4.16)$$

Using the above dipole moment functions, we calculated μ_{00} , the vibrationally averaged dipole moment at $v = 0$, and found that it is negative for CO. Therefore, the empirical value for μ_{00} as listed in Table 4.1 should be given negative sign: $\mu_{00} = -0.1098$ D. Then, from this value, we can recalculate the permanent dipole moment by

$$P_0 = \mu_{00} - \sum_{n=1}^3 P_n \langle 0 | q^n | 0 \rangle \quad (4.17)$$

where P_0 denotes the new calculated value. Values of P_0 , P_1 , P_2 , and P_3 for different Morse cubic dipole moment functions are recorded in Table 4.3. Values of P_0 differ only at the fourth decimal digit, so for all three models we may take $P_0 = -0.1212$ D.

2b. Results Using PMO Eigenfunctions

$$M(u) = -0.1222 + 3.0925 u - 0.2046 u^2 - 2.5203 u^3, \quad (4.18)$$

$$M(y) = -0.1222 + 1.2937 y + 0.6113 y^2 + 0.2041 y^3, \quad (4.19)$$

$$M(z) = -0.1222 + 1.2940 z - 0.6847 z^2 + 0.2636 z^3. \quad (4.20)$$

The permanent dipole moment is also recalculated using these PMO cubic functions. Values obtained are listed in Table 4.3, and they differ very little from those obtained previously. Graphs of the various PMO cubic dipole moment functions are shown in Fig. 4.1.

3. Discussions

Comparison between Morse and PMO for P_0 , P_1 , P_2 , and P_3 of the same cubic expansion $M(q)$ shows that the effect of the PMO eigenfunctions increases with increasing order of the coefficients. Indeed, this effect appears on the fifth, third, second, and first decimal

digit of P_0 , P_1 , P_2 , and P_3 respectively. It can be explained by the fact that the difference between corresponding Morse and PMO eigenfunctions increases with the vibrational quantum number v .

If we use the dipole matrix elements deduced by Young and Euchus,⁽⁸⁾ we obtain the following PMO cubic dipole moment function $M(u)$ for CO:

$$M(u) = -0.1222 + 3.0912 u - 0.1221 u^2 - 2.4680 u^3 \quad (4.21)$$

which agrees fairly well with their result obtained using the RKR potential and numerical techniques:

$$M(u)^{YE} = -0.112 + 3.11 u - 0.15 u^2 - 2.36 u^3 . \quad (4.22)$$

Comparing Eq. (4.21) to the PMO dipole function (4.18) obtained by using the set of averaged dipole matrix elements, we see that the second terms differ very little but the third and the fourth terms show significant differences. This is because in the two sets of data, μ_{00} is the same and μ_{01} and μ_{02} are changed. Therefore, as Cahion⁽¹⁷⁾ indicated, if the overtone matrix elements are not known accurately then the cubic dipole moment function may not be more useful than the linear approximation. Fortunately, averaged values of the three dipole transition moments used in our work come from reliable sources.

The effect of truncating the series expansion to the cubic power also can be examined. Suppose that the cubic polynomial

$$M(u) = m_0 + m_1 u + m_2 u^2 + m_3 u^3$$

were an exact expression of the dipole moment; then its equivalent

expansion in powers of y is

$$M^*(y) = M_0 + \sum_{i=1}^{\infty} M_i^* y^i \quad (4.23a)$$

where M_i is given by Eq. (2.14b),

$$M_i^* = \sum_{j=1}^N B_i^j \bar{m}_j \quad (4.23b)$$

where $N = j$ for $i \leq 3$ and $N = 3$ for $i > 3$, and $\bar{m}_j = m_j/a^j$.

For the cubic dipole function (4.18) with

$$m_1 = 3.0925, \quad m_2 = -0.2046, \quad m_3 = -2.5203,$$

the coefficients M_i^* of its equivalent infinite power series in y are listed in Table 4.4. We see that the three coefficients

$$M_1^* = 1.2937, \quad M_2^* = 0.6110, \quad M_3^* = 0.2109$$

are very closed to the corresponding coefficients of the PMO cubic dipole moment function $M(y)$, Eq. (4.19):

$$M_1 = 1.2937, \quad M_2 = 0.6113, \quad M_3 = 0.2041.$$

Clearly, this shows that the truncation of the power expansion of $M(y)$ at the cubic term does not have a serious effect on calculated values of the retained coefficients and that the effect is most pronounced on the last coefficient M_3 .

In the same manner, we can obtain the equivalent infinite z -series for the cubic function $M(u)$, the equivalent u -series with coefficients shown in Table 4.4 for the PMO cubic function $M(y)$, and so on. In any case, the first three coefficients after the zero-

order term of the equivalent infinite series do not deviate considerably from those of the corresponding cubic approximation.

The y -expansion representing the cubic dipole moment function in Eq. (4.19) shows an interesting feature. As shown in Table 4.4, the first three coefficients after M_0 are positive and all others from M_5^* are negative while those in the last column alternate in signs from m_5^* . If we graph the coefficients M_n^* versus the ordinal number n , we get a curve as shown in Fig. 4.2. There is a minimum at $n = 14$, and as $n \rightarrow \infty$ M_n^* does not vanish. Therefore,

$$M_0 + \sum_{n=1}^{\infty} M_n^* = -\infty ,$$

that is, the coefficients M_n^* form a diverging series.

This result may be explained by the fact that, due to the truncation of the Taylor series, coefficients of higher order than \bar{m}_3 are excluded from the expression of M_n^* in Eq. (4.23b). Therefore, from a theoretical consideration, we may infer that, had all Taylor coefficients m_n been exactly known, then all coefficients M_n^* would be also exactly known and they would satisfy the condition that their infinite sum including M_0 should vanish. This condition constitutes a basis for an extrapolation technique we shall use later to generate all coefficients M_n^* from the first few ones.

A final point to be made is that at $r = 0$ the Morse and PMO cubic dipole moment functions have values -0.456 and -0.251 respectively, suggesting that the PMO eigenfunctions give better dipole functions than the Morse eigenfunctions and the behavior $M(r = 0) = 0$ should be expected for CO.

TABLE 4.1. Experimentally deduced purely vibrational dipole matrix elements μ_{VV} , in absolute values (units of Debye).

| Ref. | μ_{00} | μ_{01} | μ_{02} | μ_{03} |
|-------|------------|----------------------|--|--|
| (8) | | 0.104 | 0.625×10^{-2} | 0.383×10^{-3} |
| (9) | | 0.104 ± 0.002 | 0.653×10^{-2} $\pm 0.010 \times 10^{-2}$ | 0.424×10^{-3} $\pm 0.060 \times 10^{-3}$ |
| (10) | 0.1098 | 0.104 | 0.638×10^{-2} | 0.384×10^{-3} |
| Aver. | 0.1098 | 0.104 | 0.639×10^{-2} | 0.397×10^{-3} |

| Ref. | μ_{13} | μ_{24} | μ_{35} |
|------|------------------------|------------------------|------------------------|
| (10) | 0.114×10^{-1} | 0.164×10^{-1} | 0.214×10^{-1} |

TABLE 4.2. Two sets of Morse parameters and an additional set of related constants.

| | |
|---|--|
| $\rho = 2.6971864555362350$ $\sigma = 77.2191124730286411$ $\tau = 83774.5923674853693 \text{ cm}^{-1}$ | |
| $a = 2.3904392015124602 \text{ \AA}$ $r_e = 0.1128322550027498 \text{ \AA}$ $D = 83774.5923674853693 \text{ cm}^{-1}$ | |
| Reduced mass for CO: | $\mu = 6.8562087141 \text{ amu}$ |
| Speed of light: | $c = 2.99792458 \times 10^8 \text{ m/s}$ |
| Planck's constant: | $h = 6.626176 \times 10^{-34} \text{ J/s}$ |
| Atomic unit mass | $1 \text{ amu} = 1.6605655 \times 10^{-27} \text{ kg}$ |

TABLE 4.3. Empirically calculated coefficients of cubic dipole moment functions in u , y , and z , using Morse and PMO eigenfunctions respectively.

| Expansion ↓ | | P_0 | P_1 | P_2 | P_3 |
|----------------|-------|---------|--------|--------|---------|
| M(u) | Morse | -.12125 | 3.0908 | -.1986 | -2.3781 |
| | PMO | -.12124 | 3.0925 | -.2046 | -2.5203 |
| M(y) | Morse | -.12125 | 1.2930 | .6127 | .2171 |
| | PMO | -.12124 | 1.2937 | .6113 | .2041 |
| M(z) | Morse | -.12124 | 1.2933 | -.6837 | .2709 |
| | PMO | -.12123 | 1.2940 | -.6847 | .2636 |

TABLE 4.4. Coefficients M_n^* of the infinite power series in y equivalent to the PMO cubic dipole moment function $M(u)$, and coefficients m_n^* of the infinite power series in u equivalent to the PMO dipole moment function $M(y)$.

| n | m_n (Truncated) | M_n^* (Infinite) | M_n (Truncated) | m_n^* (Infinite) |
|----|----------------------|-----------------------|----------------------|-----------------------|
| 1 | 3.09254 | 1.29368 | 1.29375 | 3.09262 |
| 2 | -0.20462 | 0.61103 | 0.61134 | -0.20302 |
| 3 | -2.52029 | 0.21091 | 0.20413 | -2.61700 |
| 4 | | 0.13831-1 | | -0.11380 |
| 5 | | -0.93996-1 | | 8.82847 |
| 6 | | -0.15760 | | -19.08000 |
| 7 | | -0.19697 | | 25.92200 |
| 8 | | -0.22206 | | -27.21335 |
| 9 | | -0.23825 | | 23.84022 |
| 10 | | -0.24865 | | -18.13796 |
| 11 | | -0.25517 | | 12.27972 |
| 12 | | -0.25901 | | -7.52017 |
| 13 | | -0.26098 | | 4.21533 |
| 14 | | -0.26161 | | -2.18211 |
| 15 | | -0.26127 | | 1.05053 |
| 16 | | -0.26024 | | -0.47303 |
| 17 | | -0.25870 | | 0.20016 |
| 18 | | -0.25679 | | -0.79907-1 |
| 19 | | -0.25462 | | 0.30201-1 |
| 20 | | -0.25226 | | -0.10839-1 |

The last negative digit refers to the power of 10.

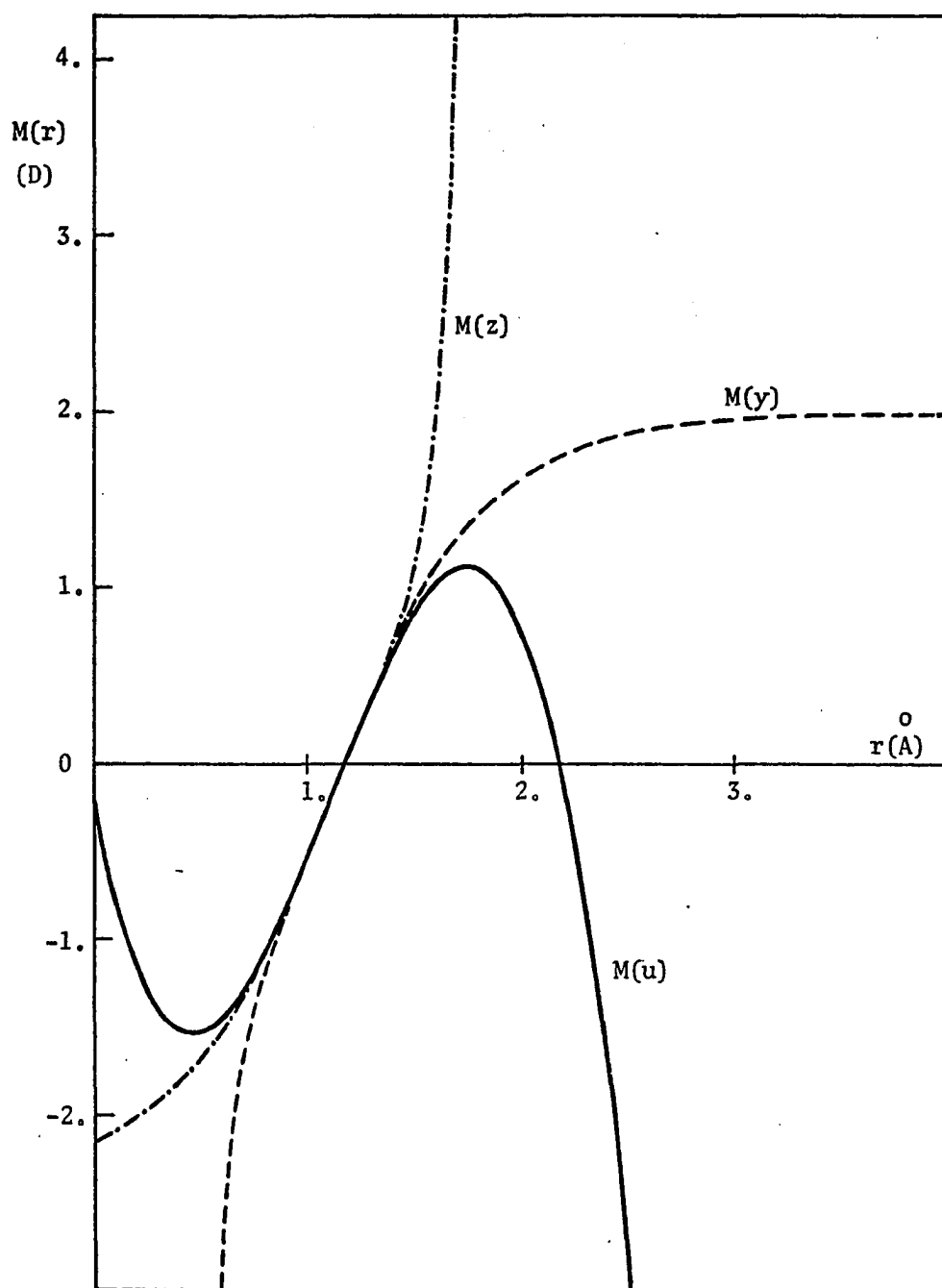


Fig. 4.1. Solid, dashed, and dash-dotted curves represent the PMO cubic dipole moment functions $M(u)$, $M(y)$, and $M(z)$ respectively.

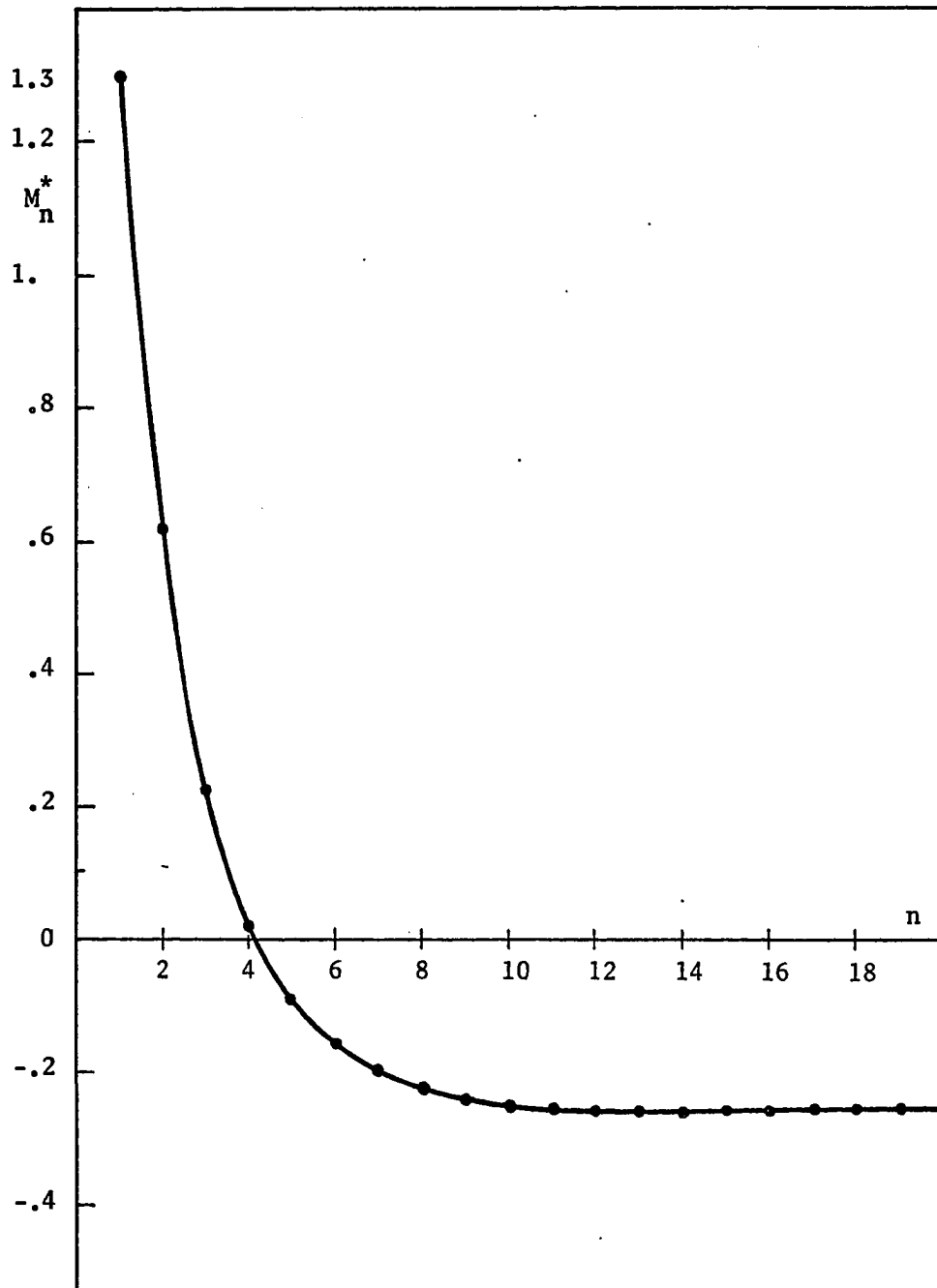


Fig. 4.2. Graph of coefficients M_n^* of the equivalent y -series versus the number n .

CHAPTER V

ANALYTICAL DIPOLE MOMENT FUNCTIONS WITH CORRECT ASYMPTOTIC BEHAVIOR

1. Introduction

The main objective of the present work is to produce approximate values for unknown coefficients of the y -series expansion of the dipole moment $M(r)$ from a few known coefficients or given intensity data, in such a way that the infinite sum of coefficients M_n vanishes:

$$M_0 + \sum_{n=1}^{\infty} M_n = 0, \quad (5.1)$$

so that the dipole moment function exhibits the correct asymptotic behavior as r becomes very large (i.e. the molecule approaches dissociation).

The behavior of equivalent y -expansion coefficients M_n^* with respect to the index n as shown in Fig. 4.2 or Table 4.3, Chapter III, suggests that the coefficients M_n also have the same general behavior for small values of n , but as $n \rightarrow \infty$, M_n must tend to zero in such a way that the asymptotic condition (5.1) is satisfied.

Therefore, in order to generate values for unknown coefficients M_n , $n \geq 4$ for CO, we assume a functional form for M_n , i.e., we express

$$M_n = F(n, C_1, C_2, \dots, C_M, \beta) \quad (5.2)$$

where F is a function of the index n and the parameters C_1, C_2, \dots, C_M , and β . The function F is subject to the asymptotic condition

$$M_0 + \sum_{n=1}^{\infty} F(n, C_m, \beta) = 0 \quad (5.3a)$$

where C_m stands for the set of M parameters $\{C_1, C_2, \dots, C_M\}$. Thus, the series generated by the function F is convergent and must satisfy a necessary condition

$$\lim_{n \rightarrow \infty} F(n, C_m, \beta) = 0. \quad (5.3b)$$

The parameter β will be determined by the asymptotic condition (5.3b), and M parameters C_m are to be determined from N empirical dipole matrix elements $\mu_{VV'}$, or N given y -expansion coefficients M_n . Therefore, this problem can be solved by either of the following two approaches:

i) Indirect method: One first determines the first N coefficients M_n other than M_0 using N known values of $\mu_{VV'}$, by solving a system of inhomogeneous linear equations of the form

$$\sum_{n=1}^N \langle v | y^n | v' \rangle M_n = \mu_{VV'}, \quad (5.4)$$

as has been done in Chapter IV.

The parameters $\{C_M\}$ are then obtained by fitting the function $F(n, C_M, \beta)$ to N coefficients M_n , subject to the asymptotic condition (5.3a) which will determine β . In cases where $F(n, C_m, \beta)$ is linear in C_m and non-linear in β , and $M = N$, one has a system of linear equations

$$F(n, C_1, C_2, \dots, C_m, \beta) = M_n, \quad n = 1, \dots, N. \quad (5.5)$$

which one solves for the C-parameters for each trial value of β . This iteration will continue until the asymptotic condition (5.3a) is satisfied within a desired accuracy degree. One then obtains a new dipole-moment expansion in powers of y ,

$$M^*(y) = M_0 + \sum_{n=1}^N M_n y^n + \sum_{i=N+1}^L M_i^* y^i \quad (5.6)$$

which has been truncated so that a sufficiently large number of newly produced coefficients M_i^* is retained.

In the second step, the new coefficients M_i^* are included in Eqs. (5.4) which now become

$$\sum_{n=1}^N \langle v | y^n | v' \rangle M_n = \mu_{vv'} - \sum_{i=N+1}^L M_i \langle v | y^i | v' \rangle . \quad (5.7)$$

The above procedure is then repeated over and over until the difference between the old set and the new set of parameters $\{C_m, \beta\}$ or coefficients M_i^* falls within a desired degree of accuracy.

ii) Direct method: In this approach, we express matrix elements of $M(r)$ directly in terms of the parameters C_1, \dots, C_M , and β :

$$\langle v | M(r) | v' \rangle = M_0 \delta_{vv'} + \sum_{n=1}^L F(n, C_1, C_2, \dots, C_M, \beta) \langle v | y^n | v' \rangle \quad (5.8)$$

Then, using N experimental data $\mu_{vv'}$, we determine the set of parameters $\{C_m, \beta\}$ by the least-squares method for the case $M < N$, being always subject to the asymptotic condition (5.3a). If $M = N$ and $F(n, C_m, \beta)$ is linear in C_m but non-linear in β , we determine these parameters by iterating β and solving a system of linear equations.

2. Functional Forms For Coefficients M_n

In principle, it is possible to find an infinite number of functions of the variable n which fit known coefficients M_n or transition moments μ_{vv} , and simultaneously satisfy the asymptotic behavior (5.3a). We, however, are interested in those functions that are simple enough and contain a few parameters so that our problem can be handled easily by analytical or numerical methods.

We have found various simple generating functions for M_n with $n > 0$ as follows:

$$M_n^1 \equiv F^1(n, C_1, C_2, C_3, \beta) = (C_1 + nC_2 + n^2C_3) e^{-\beta n}, \quad (5.9A)$$

$$M_n^2 \equiv F^2(n, C_1, C_2, C_3, \beta) = (C_1 + \frac{C_2}{n} + \frac{C_3}{n^2}) e^{-\beta n}, \quad (5.9B)$$

$$M_n^3 \equiv F^3(n, C_1, C_2, C_3, \beta) = (C_1 + \frac{C_2}{n} + nC_3) e^{-\beta n}, \quad (5.9C)$$

$$M_n^4 \equiv F^4(n, C_1, C_2, C_3, \beta) = (C_1 + \frac{C_2}{n} + \frac{C_3}{n(n+1)}) e^{-\beta n}, \quad (5.9D)$$

$$M_n^5 \equiv F^5(n, C_1, C_2, C_3, \beta) = \begin{cases} (C_1 + C_2) e^{-\beta} & , \quad n = 1, \\ (C_1 + \frac{C_2}{n} + \frac{C_3}{n(n-1)}) e^{-\beta n} & , \quad n \geq 2, \end{cases} \quad (5.9E)$$

where β is now a positive parameter and the superscript refers to different models of function or coefficient.

All five above generating functions produce convergent series, i.e.,

$$M_0 + \sum_{n=1}^{\infty} M_n^{\alpha} = S, \quad \alpha = 1, 2, \dots, 5, \quad (5.10)$$

where S is a finite value. This can be easily shown: for a finite

number k positive or negative, we see that

$$\lim_{n \rightarrow \infty} \left[\frac{(n+1)^k e^{-\beta(n+1)}}{n^k e^{-\beta n}} \right] = \lim_{n \rightarrow \infty} \left[\left(1 + \frac{1}{n}\right)^k e^{-\beta n} \right] < 1$$

which leads to

$$\lim_{n \rightarrow \infty} \left[\frac{M_{n+1}^\alpha}{M_n^\alpha} \right] < 1$$

which is a sufficient condition for convergence of the series M_n^α .

In order to produce a dipole moment function with correct asymptotic behavior, the model series M_n^α must also fulfill the condition (5.3a), that is, we must have $S = 0$ in Eq. (5.10). Although the first model function F^1 gives a dipole moment function in a closed form which is simpler than those resulted from other models, this model is not suitable for CO because we cannot find values of the parameters C_1 , C_2 , C_3 , and β for which $S = 0$ so that the corresponding dipole moment function vanishes at infinite r . The other model functions work well for CO.

We shall show that the proposed generating functions produce closed-form dipole moment functions. First, for convenience, we express all five model functions in a general form:

$$M_n^\alpha = (g_n^1 C_1 + g_n^2 C_2 + g_n^3 C_3) B \quad (5.11a)$$

where

$$B = e^{-\beta}, \quad 0 < B < 1, \quad (5.11b)$$

$$g_n^1 = 1, \quad (5.11c)$$

$$g_n^2 = n, \quad 1/n, \quad (5.11d)$$

$$g_n^3 = n^2, \frac{1}{n^2}, \frac{1}{n(n+1)}, \frac{1}{n(n-1)}. \quad (5.11e)$$

Substituting Eq. (5.11a) into the y -expansion of $M(r)$, we obtain

$$M^\alpha(y) = M_0 + C_1 \sum_{n=1}^{\infty} (By)^n + C_2 \sum_{n=1}^{\infty} g_n^2 (By)^n + C_3 \sum_{\substack{n=1 \\ \text{or} \\ n=2}}^{\infty} g_n^3 (By)^n. \quad (5.12)$$

Defining $Y = By$, the first sum in the above equation can be reduced to a single term:

$$\sum_{n=1}^{\infty} Y^n = \frac{Y}{1-Y}. \quad (5.13a)$$

The second sum in Eq. (5.12) can also be reduced to one term:

For $g_n^2 = n$, we have

$$\sum_{n=1}^{\infty} nY^n = Y \sum_{n=1}^{\infty} nY^{n-1} = B \frac{d}{dB} \left(\sum_{n=1}^{\infty} Y^n \right) = \frac{Y}{(1-Y)^2}. \quad (5.13b)$$

For $g_n^2 = 1/n$, we have

$$\sum_{n=1}^{\infty} \frac{Y^n}{n} = -\ln(1-Y). \quad (5.13c)$$

Except for $g_n^3 = n^{-2}$, the third sum in Eq. (5.12) can also be compressed into a compact term for other models:

$$\sum_{n=1}^{\infty} n^2 Y^n = \frac{Y(1+Y)}{(1-Y)^3}. \quad (5.13d)$$

$$\begin{aligned} \sum_{n=1}^{\infty} \frac{Y^2}{n^2} &= \int_0^B \frac{1}{B} \left(\sum_{n=1}^{\infty} \frac{Y^n}{n} \right) dY = -\int_0^B \frac{\ln(1-Y)}{Y} dY \\ &= \text{Li}_2(Y) = Y\zeta(2,1,Y), \end{aligned} \quad (5.13e)$$

where $\text{Li}_2(Y)$ is called the dilogarithm⁽⁵²⁾ and $\zeta(2,1,Y)$ is the Lerch

zeta function. (52) General forms of these functions are

$$\text{Li}_n(x) = \int_0^x x^{-1} \text{Li}_{n-1}(x) dx : \text{ polylogarithm of order } n ;$$

or

$$\text{Li}_n(x) = \sum_{k=1}^{\infty} \frac{x^k}{k^n} ;$$

and

$$\zeta(s, 1, x) = \frac{1}{x} \sum_{k=1}^{\infty} \frac{x^k}{k^s} ;$$

$$\zeta(x, a, x) = \sum_{k=0}^{\infty} \frac{x^k}{(k+a)^s} .$$

For $g_n^3 = 1/n(n+1)$ and $g_n^3 = 1/n(n-1)$, we obtain

$$\sum_{n=1}^{\infty} \frac{Y^n}{n(n+1)} = \left(\frac{1-B}{B}\right) \ln(1-B) - 1 , \quad (5.13f)$$

$$\sum_{n=2}^{\infty} \frac{Y^n}{n(n-1)} = (1-B) \ln(1-B) . \quad (5.13g)$$

Using these expressions (5.13a-g), the series expansions (5.12) of the dipole moment, except for model F^2 , can be reduced to analytical closed forms:

$$M^1(y) = M_0 + C_1 \frac{By}{1-By} + C_2 \frac{By}{(1-By)^2} + C_3 \frac{By(1+By)}{(1-By)^3} , \quad (5.14A)$$

$$M^2(y) = M_0 + C_1 \frac{By}{1-By} - C_2 \ln(1-By) + C_3 \text{Li}_2(By) , \quad (5.14B)$$

$$M^3(y) = M_0 + C_1 \frac{By}{1-By} - C_2 \ln(1-By) + C_3 \frac{By}{(1-By)^2} , \quad (5.14C)$$

$$M^4(y) = M_0 + C_1 \frac{By}{1-By} - C_2 \ln(1-By) + C_3 \left[1 + \left(\frac{1-By}{By}\right) \ln(1-By)\right] , \quad (5.14D)$$

$$M^5(y) = M_0 + C_1 \frac{By}{1-By} - C_2 \ln(1-By) + C_3 [By + (1-By) \ln(1-By)] . \quad (5.14E)$$

The asymptotic condition (5.3a) now also can be written in the same compact forms by letting $y = 1$ in the above expressions for

$M^\alpha(y)$. We note that the first dipole moment function in Eq. (5.14A) is simpler than the other ones.

Since all the above functions are linear in C_1 , C_2 , and C_3 , but non-linear in B or β , analytical and numerical determinations of these parameters are not very complicated using the procedure described in the Introduction of this chapter. We choose to use the direct approach by fitting these functions directly to the experimental transition moments. However, to find the zero-order approximation values for the parameters C_m and β , we fit the model functions to the known coefficients M_1 , M_2 , and M_3 of the PMO cubic dipole moment function in y .

In cases where there are more intensity data than parameters C_m , the method of least-squares fit as described below should be used.

3. Minimization of Errors

Denoting the pair of vibrational quantum numbers (v, v') by v , then using the general forms (5.11a) and (5.12), the matrix elements of the dipole moment function can be expressed as

$$\mathcal{M}_{vv'} = \langle v | M(r) | v' \rangle = \sum_{m=1}^M Q_{vm} C_m, \quad v \neq v', \quad (5.15a)$$

where $M = 3$ in our case, and

$$Q_{vm} = \sum_{n=1}^L [\langle v | y^n | v' \rangle B^n g_n^m] \quad (5.15b)$$

where L is the number of terms retained in the expansion.

Calling N the number of empirical transition moments $\mu_{vv'}$ available, then if $N = M$, the parameters C_m are obtained by solving a system of inhomogeneous linear equations:

$$\sum_{m=1}^M Q_{\nu m} C_m = \mu_{\nu}, \quad \nu = 1, 2, \dots, N. \quad (5.16)$$

The parameter β is determined by iteration until the asymptotic condition (5.3) is satisfied.

If $N > M$, one forms the quantity

$$E = \sum_{\nu=1}^N [w_{\nu}(\mathcal{N}\sigma_{\nu} - \mu_{\nu})]^2 \quad (5.17)$$

where the weighting factor w_{ν} is the inverse of the standard deviation σ_{ν} describing the uncertainty associated with the corresponding μ_{ν} .

Substituting the expression (5.15a) of $\mathcal{N}\sigma_{\nu}$ into Eq. (5.17), we obtain

$$E = \sum_{\nu=1}^N \left[\sum_{m=1}^M w_{\nu} Q_{\nu m} C_m - w_{\nu} \mu_{\nu} \right]^2. \quad (5.18)$$

This quantity can be minimized with respect to the C_m by establishing

$$\frac{\partial E}{\partial C_m} = 0, \quad m = 1, 2, \dots, M,$$

from which one obtains M linear equations in the form

$$\sum_{m=1}^M T_{pm} C_m = R_p, \quad p = 1, 2, \dots, M, \quad (5.19a)$$

where

$$T_{pm} = \sum_{\nu=1}^N w_{\nu}^2 Q_{\nu p} Q_{\nu m} \quad (5.19b)$$

which is symmetric, and

$$R_p = \sum_{\nu=1}^N w_{\nu}^2 \mu_{\nu} Q_{\nu p}, \quad \nu = 1, 2, \dots, N. \quad (5.19c)$$

If the quantity E defined by Eq. (5.17) does not depend linearly on C_m , then the problem should be solved numerically. For this purpose, a general computer code has been written by Huffaker⁽⁴⁵⁾ to handle a minimization problem involving more than 3 parameters.

4. Numerical Results for CO ($X^1\Sigma^+$)

4a. Dipole moment function with correct large-r behavior

We first carry out the zero-order approximation by fitting the various generating functions M_n^α [Eqs. (5.9A) - (5.9D)] to the calculated coefficients M_1 , M_2 , and M_3 of the PMO cubic dipole moment function in y given by Eq. (4.19). Then for each value of β or B , we solve the following inhomogeneous linear equations for C_1 , C_2 , and C_3 :

$$\begin{bmatrix} 1 & g_1^2 & g_1^3 \\ 1 & g_2^2 & g_2^3 \\ 1 & g_3^2 & g_3^3 \end{bmatrix} \begin{bmatrix} C_1 \\ C_2 \\ C_3 \end{bmatrix} = \begin{bmatrix} M_1 B^{-1} \\ M_2 B^{-2} \\ M_3 B^{-3} \end{bmatrix} \quad (5.20)$$

where the general expression (5.11a) has been used.

The parameter β is iterated until the asymptotic condition (5.1) is satisfied within the desired accuracy. Final values obtained for the set of parameters $\{C_1, C_2, C_3, \beta\}$ for different models F^2 , F^3 , F^4 , and F^5 are listed in Table 5.1 together with values given by other calculations. From these parameters, coefficients M_n are calculated and plotted against the index number n in Fig. 5.1, and graphs of various corresponding dipole moment functions in reduced forms are shown in Fig. 5.2.

To take account of the effect of higher order terms in the y -expansion, we next fit the generating functions directly to the empirical transition moments μ_{01} , μ_{02} , μ_{03} , μ_{13} , μ_{24} , and μ_{35} , whose values are given in Table 4.1. In this case, if all six matrix elements are used, the minimization method as described in the previous Section should be employed. If only three matrix elements μ_{01} , μ_{02} , and μ_{03} are used, then the parameter C_m can be evaluated also by solving a system of three homogeneous linear equations:

$$\begin{bmatrix} Q_{11} & Q_{12} & Q_{13} \\ Q_{21} & Q_{22} & Q_{23} \\ Q_{31} & Q_{32} & Q_{33} \end{bmatrix} \begin{bmatrix} C_1 \\ C_2 \\ C_3 \end{bmatrix} = \begin{bmatrix} \mu_{01} \\ \mu_{02} \\ \mu_{03} \end{bmatrix} \quad (5.21)$$

where

$$Q_{vm} = \sum_{n=1}^L \langle 0 | y^n | v' \rangle B^n g_n^v, \quad v = v' = 1, 2, 3.$$

The parameter β is obtained by iteration as usual.

Using both ways of calculations, without and with minimization, values of parameters C_1 , C_2 , C_3 , and β are obtained and listed in Table 5.1 for different generating functions. Coefficients M_n are then calculated and plotted versus n in Fig. 5.3 and Fig. 5.4 for the two cases respectively. Various dipole moment functions in reduced forms $M^2(y)$, $M^3(y)$, $M^4(y)$, and $M^5(y)$ are also plotted in Fig. 5.5 for the case without minimization and in Fig. 5.6 for the case with minimization.

4b. Dipole moment functions with correct large- r and small- r behaviors

Since the dipole moment function as an infinite expansion in powers of y is not convergent for $r < 0.84 \text{ \AA}$ in case of CO, this series

displays wrong behavior at small r , having very large negative values as depicted in Figs. 5.2, 5.5, and 5.6 for the function $M^2(r)$ given by Eq. (5.14B). However, it is interesting to see that the other dipole moment functions $M^3(r)$, $M^4(r)$, and $M^5(r)$ in closed forms given by Eqs. (5.14C-5.14E) have much less exaggerated values at small r . This suggests that by some adjustment one can force their representative curves to pass through the origin. We found that this can be done by adding to the closed-form dipole moment function one extra term which is either

$$M_c y , \quad (5.22a)$$

or

$$M_c y(1 - y) , \quad (5.22b)$$

where M_c is an additional adjusting parameter to be determined by iteration.

Then, in each iteration of M_c , the whole calculation procedure used in the preceding Section is carried out to obtain the correct large- r behavior of the dipole moment function. This iteration is repeated until its value at $r = 0$ is as close to zero as desired. Since the dipole moment function $M^2(y)$ [Eq. (5.14B)] cannot be reduced to a completely closed form, the above technique of small- r behavior correction is not applicable to this function as it is to $M^3(r)$, $M^4(r)$, and $M^5(r)$. The two modes of small- r behavior correction as expressed by (5.22a) and (5.22b) are performed for the cases of non-minimization and minimization. Values obtained for M_c for different closed-form functions are recorded in Table 5.2. From the set of parameters $\{C_1, C_2, C_3, \beta, M_c\}$ obtained using minimization, coefficients

M_n are evaluated and plotted in Fig. 5.7 for the $M_c y$ correction and in Fig. 5.8 for the $M_c y(1-y)$ correction. Graphs of corresponding closed-form dipole moment functions having correct large- r and small- r behaviors are shown in Figs. 5.9 and 5.10. For comparison, the plot of coefficients M_n^* [Fig. 4.2] of the y -series equivalent to the PMO cubic dipole moment function in u and graph of this function are reproduced in related Figures. In addition, the dipole moment function for CO obtained numerically by Kirby-Docken and Liu⁽²⁾ using an ab initio calculation is plotted in Fig. 5.11 for comparison with results obtained for the "best" function $M^4(y)$ using the least-squares fit with $M_c y$ and $M_c y(1-y)$ corrections respectively.

It should be mentioned that the PMO vibrational eigenfunctions obtained by the diagonalization technique (Chapter IV) have been used in all calculations in this Chapter.

5. Analysis of Numerical Results

We have now obtained several analytical functions representing the dipole moment for CO in the ground electronic state ($X^1\Sigma^+$). As shown in various graphs, all these functions agree quite well with each other within a small range of r about r_e , $0.85 \text{ \AA} < r < 1.5 \text{ \AA}$. For smaller r and larger r , they reveal significant discrepancies whose effect will be discussed in Chapter VI. Thus, the question now is: which functional form will best represent the CO dipole moment? Before trying to answer this question, let us analyze the numerical values as depicted by plotted curves for different calculations. Starting with Fig. 5.1 for the zero-order approximation, one sees considerable differences between corresponding coefficients M_n given

by various generating functions for $4 \leq n \leq 14$. Since the first few coefficients M_n^* after M_3^* may differ slightly from the true values, one may expect that a good generated- M_n curve should be close to the "equivalent M_n^* " curve for $n \lesssim 6$. Clearly, the F^2 and F^4 curves, which are closest to the M_n^* curve at small n , would most likely produce the best representations of the dipole moment for CO. Indeed, as shown in Fig. 5.2, the $M^4(r)$ curve has small- r behavior much closer to that of the cubic $M(u)$ curve than $M^3(r)$ and $M^5(r)$ curves, and the last function shows largest deviation at both small r and large r . Since the function $M^2(r)$ cannot be reduced to a closed form, its graph displays a wrong behavior at small r ; but its large- r behavior is quite good, being very close to that of $M^4(r)$. Noting that the $M^2(r)$ curve lies above the $M^4(r)$ at large r , one can infer that, if the closed form of $M^2(r)$ was known, then its representative curve would also lie above the $M^4(r)$ curve at small r and hence would have even better small- r behavior than $M^4(r)$. However, since $M^2(r)$ is irreducible to a closed form, it is useful only for the large- r behavior analysis, and the functional form $M^4(r)$ becomes the most appropriate for describing the dipole moment over the whole range of r . We also note that the minima of M_n curves in Fig. 5.1 and the minima and maxima of $M^\alpha(r)$ curves are shifted increasingly to the right in the order $F^3(n)$, $F^4(n)$, $F^2(n)$, and $F^5(n)$, and the order $M^3(y)$, $M^4(y)$, and $M^5(y)$, respectively.

The effect of including a large number of higher order terms in y is shown to be small in Fig. 5.2 by the fact that the various zero-order approximation dipole moment functions deviate slightly

about r_e from the PMO cubic function $M(u)$. Further, little improvement is made on results by calculation using three and six-data point fittings as shown by Figs. 5.3-5.6 where the curves are almost the same as those obtained by the zero-order approximation. The new results, of course, give better dipole moment values at r about r_e . In both cases of data fitting, the small- r behavior of the dipole moment curves change very little as compared to the zero-approximation results.

The two modes of small- r correction bring about significant improvement on the CO dipole moment functions. In general, the $M_c y$ correction yields better results than the $M_c y(1-y)$ correction, since the curves plotted in Figs. 5.7 and 5.9 for the former case are closer to each other than the curves shown in Figs. 5.8 and 5.10 for the latter case. We also see that the dipole moment function $M^5(r)$ corrected by the $M_c y(1-y)$ term changes sign a second time near $r=0$, which we do not expect. Finally, agreement is excellent between our "best" analytical dipole moment functions $M^4(r)$ obtained using $M_c y$ and $M_c y(1-y)$ corrections with minimization and the numerical dipole moment function determined by Kirby-Docken and Liu⁽²⁾ using an ab initio method, as can be seen in Fig. 5.11. We note that the curves obtained by the two methods do not coincide but have nearly the same slope at r about r_e .

From the above analysis, one may conclude that the functional form $M^4(r)$ is better than the other alternative models in representing the CO dipole moment in the sense that it gives better small- r behavior and is also quite simple to use conveniently.

TABLE 5.1. Values of the parameters C_1 , C_2 , C_3 , β and B for different generating functions. For each parameter and each model function, the seven numbers correspond respectively to: a) the zero-order approximation, b) the large-r behavior correction without minimization, c) the large-r behavior correction with minimization, d) the large-r and small-r behavior correction using $M_c y$ without minimization, e) the large-r and small-r behavior correction using $M_c y$ with minimization, f) the large-r and small-r behavior correction using $M_c y(1-y)$ without minimization, g) the large-r and small-r behavior correction using $M_c y(1-y)$ with minimization.

| Param. | F^α | F^2 | F^3 | F^4 | F^5 |
|---------|------------|---------|---------|---------|-----------|
| β | (a) | .145964 | .307664 | .169765 | .847423-1 |
| | (b) | .141476 | .297095 | .163783 | .842746-1 |
| | (c) | .142172 | .297828 | .164488 | .849194-1 |
| | (d) | (*) | .244844 | .144613 | .123565 |
| | (e) | (*) | .245993 | .145509 | .124320 |
| | (f) | (*) | .285370 | .158605 | .885459-1 |
| | (g) | (*) | .286182 | .159360 | .892025-1 |
| B | (a) | .864118 | .735163 | .843863 | .918749 |
| | (b) | .868076 | .742973 | .848926 | .919179 |
| | (c) | .867472 | .742429 | .848328 | .918586 |
| | (d) | (*) | .782827 | .865357 | .883764 |
| | (e) | (*) | .781927 | .864582 | .883097 |
| | (f) | (*) | .751739 | .853333 | .915261 |
| | (g) | (*) | .751129 | .852689 | .914660 |

TABLE 5.1 (continued)

| Param. | F^α | F^2 | F^3 | F^4 | F^5 |
|--------|------------|-----------|-----------|------------|----------|
| C_1 | (a) | -1.102545 | 2.337736 | -1.579703 | -.425785 |
| | (b) | -1.054344 | 2.162822 | -1.493841 | -.422965 |
| | (c) | -1.060839 | 2.171860 | -1.502591 | -.426184 |
| | (d) | (*) | .753355 | -1.143460 | -.796463 |
| | (e) | (*) | .764099 | -1.153872 | -.802462 |
| | (f) | (*) | 1.867305 | -1.403022 | -.443644 |
| | (g) | (*) | 1.876751 | -1.412200 | -.446967 |
| C_2 | (a) | 5.084945 | .338275-1 | 8.403582 | 1.833947 |
| | (b) | 4.915706 | .140312 | 8.017195 | 1.830492 |
| | (c) | 4.935633 | .135526 | 8.052700 | 1.834672 |
| | (d) | (*) | 1.628770 | 5.849976 | 3.434898 |
| | (e) | (*) | 1.623208 | 5.894921 | 3.451069 |
| | (f) | (*) | .366308 | 7.523692 | 1.797786 |
| | (g) | (*) | .361325 | 7.561464 | 1.801646 |
| C_3 | (a) | -2.485333 | -.611751 | -10.581506 | .466134 |
| | (b) | -2.371062 | -.561987 | -9.998919 | .458113 |
| | (c) | -2.383407 | -.564916 | -10.050183 | .460622 |
| | (d) | (*) | -.285138 | -5.794522 | -.278459 |
| | (e) | (*) | -.288409 | -5.863409 | -.281748 |
| | (f) | (*) | -.495403 | -9.188876 | .675131 |
| | (g) | (*) | -.498431 | -9.243763 | .679329 |

(*) The functional form (5.14B) is not completely closed, so the small- r correction cannot be carried out.

Last negative digits refer to powers of 10.

TABLE 5.2. Values of the parameter M_c in small-r behavior correction terms $M_c y$ and $M_c y(1-y)$ for different closed-form dipole moment functions.

| M_c \ M^α | $M^3(r)$ | $M^4(r)$ | $M^5(r)$ |
|--------------------------------------|------------|------------|-----------|
| $M_c y$ without minimization | -.347906 | -.271955 | -1.038042 |
| $M_c y$ with minimization | -.347476 | -.270699 | -1.045216 |
| $M_c y(1-y)$ without minimization | -.130409-1 | -.870230-2 | .543606-1 |
| $M_c y(1-y)$ with minimization | -.130206-1 | -.865950-2 | .547315-1 |

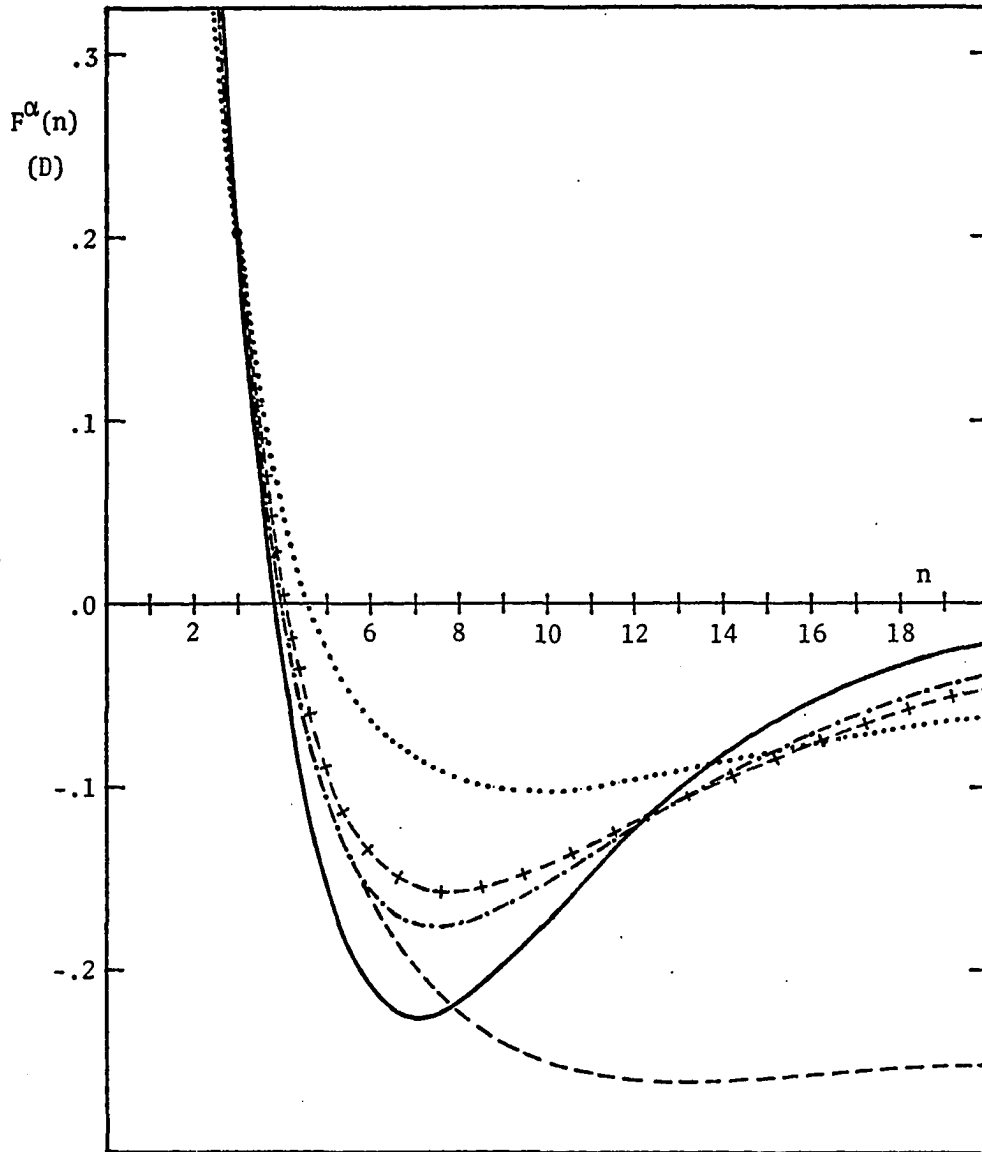


Fig. 5.1. Plots of various generating functions $F^\alpha(n)$ for CO obtained fitting 3 known coefficients M_1 , M_2 , and M_3 . Dash-crossed, solid, dash-dotted, and dotted curves represent $F^2(n)$, $F^3(n)$, $F^4(n)$, and $F^5(n)$ respectively. The dashed curve shows coefficients M_n^* of the y-series equivalent to the PMO cubic dipole moment function in u for CO.

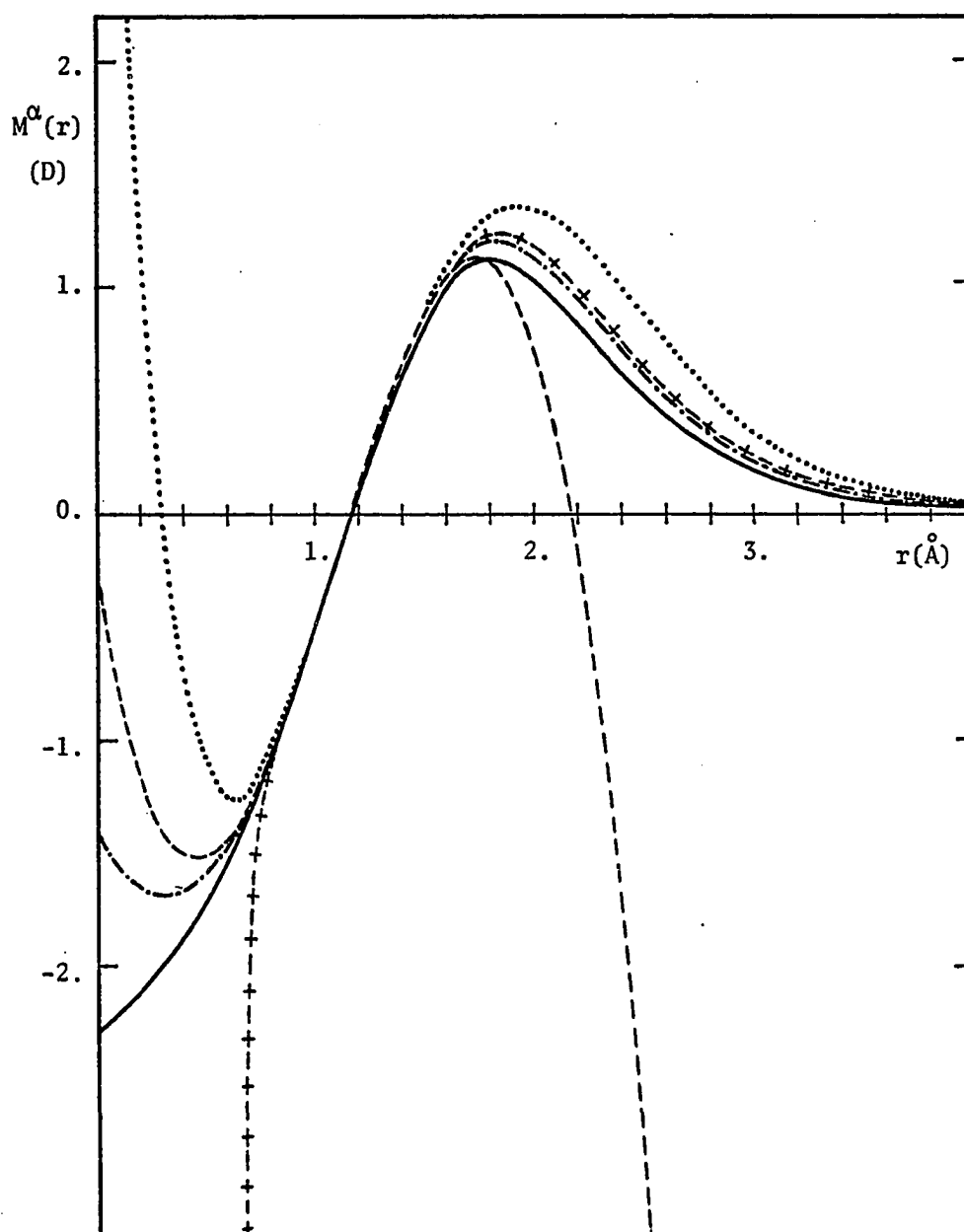


Fig. 5.2. Graphs of CO dipole moment functions with correct large- r behavior, obtained by the zero-order approximation. Dash-crossed, solid, dash-dotted, and dotted curves are $M^2(r)$, $M^3(r)$, $M^4(r)$, and $M^5(r)$ respectively. The dashed curve represents the PMO cubic dipole moment function in u for CO.

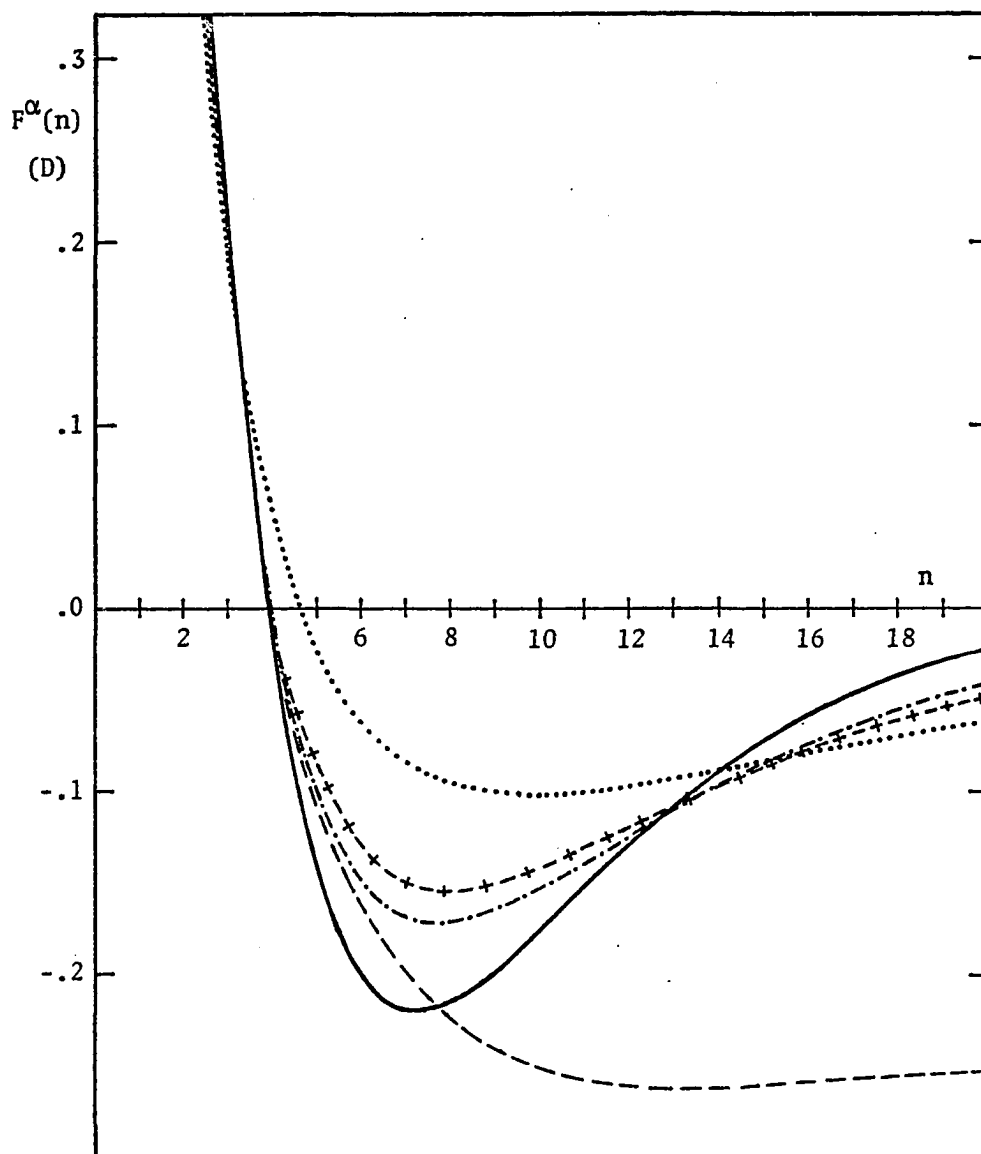


Fig. 5.3. Plots of various generating functions $F^\alpha(n)$ for CO obtained for correct large- r behavior using 3 dipole matrix elements. Dash-crossed, solid, dash-dotted, and dotted curves show $F^2(n)$, $F^3(n)$, $F^4(n)$, and $F^5(n)$ respectively. The dashed curve represents coefficients M_n^* of the y -series equivalent to the PMO cubic dipole moment function in u for CO.

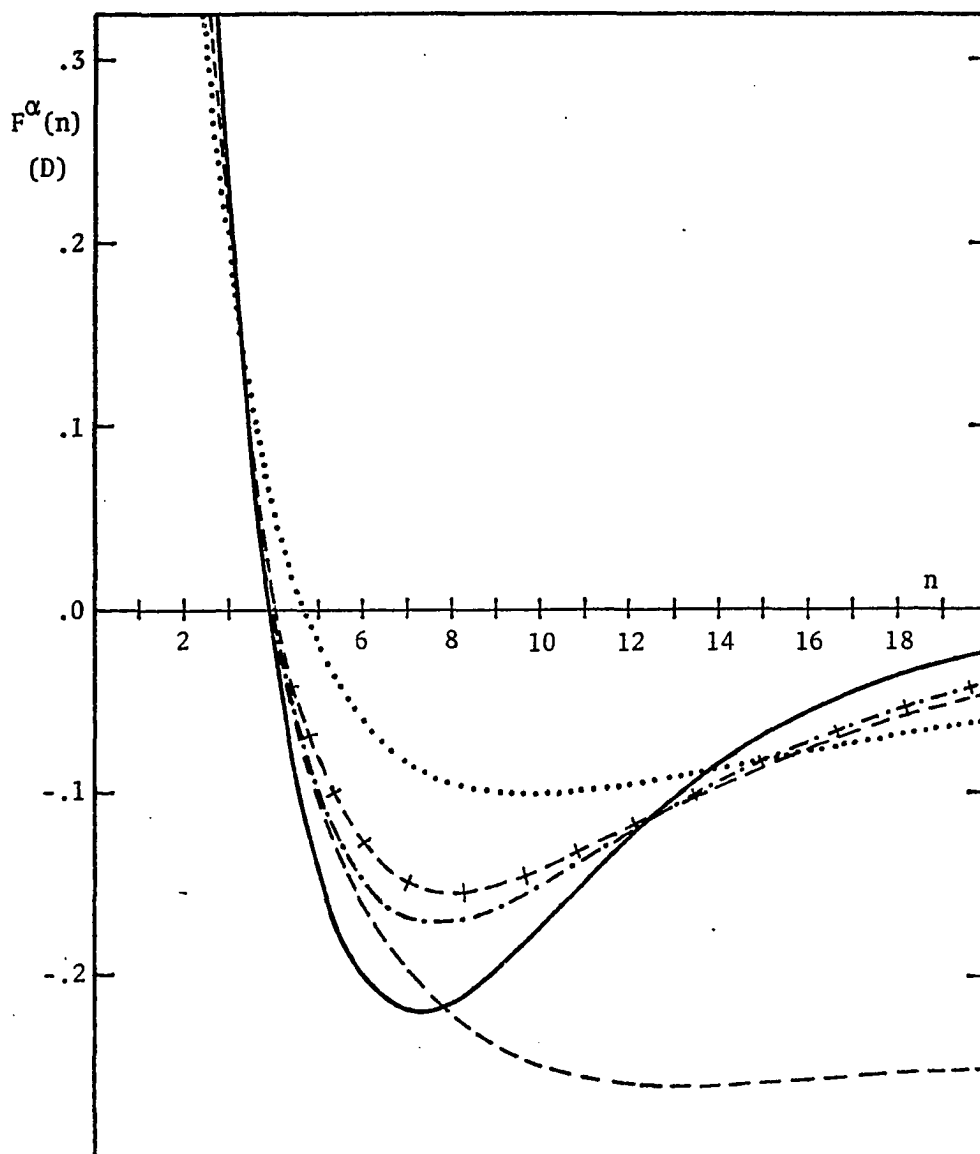


Fig. 5.4. Plots of various generating function $F^\alpha(n)$ for CO obtained for correct large- r behavior fitting 6 dipole matrix elements. Dash-crossed, solid, dash-dotted, and dotted curves show $F^2(n)$, $F^3(n)$, $F^4(n)$, and $F^5(n)$ respectively. The dashed curve represents coefficients M_n^* of the y -series equivalent to the PMO cubic dipole moment function in u for CO.

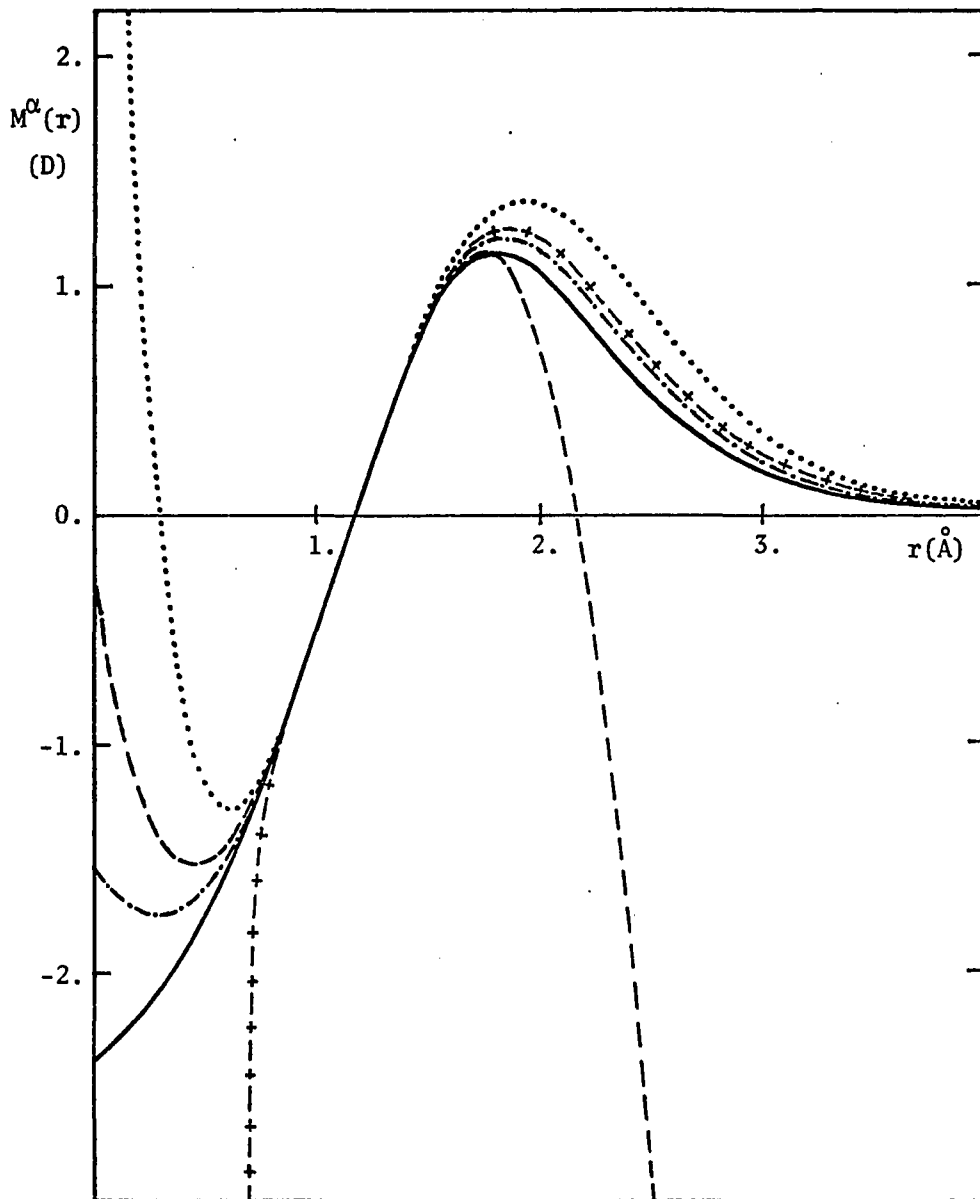


Fig. 5.5. CO dipole moment functions with correct large- r behavior obtained without minimization. Dash-crossed, solid, dash-dotted, and dotted curves represent $M^2(r)$, $M^3(r)$, $M^4(r)$, and $M^5(r)$ respectively. The dashed curve is the PMO cubic dipole moment function in u for CO.

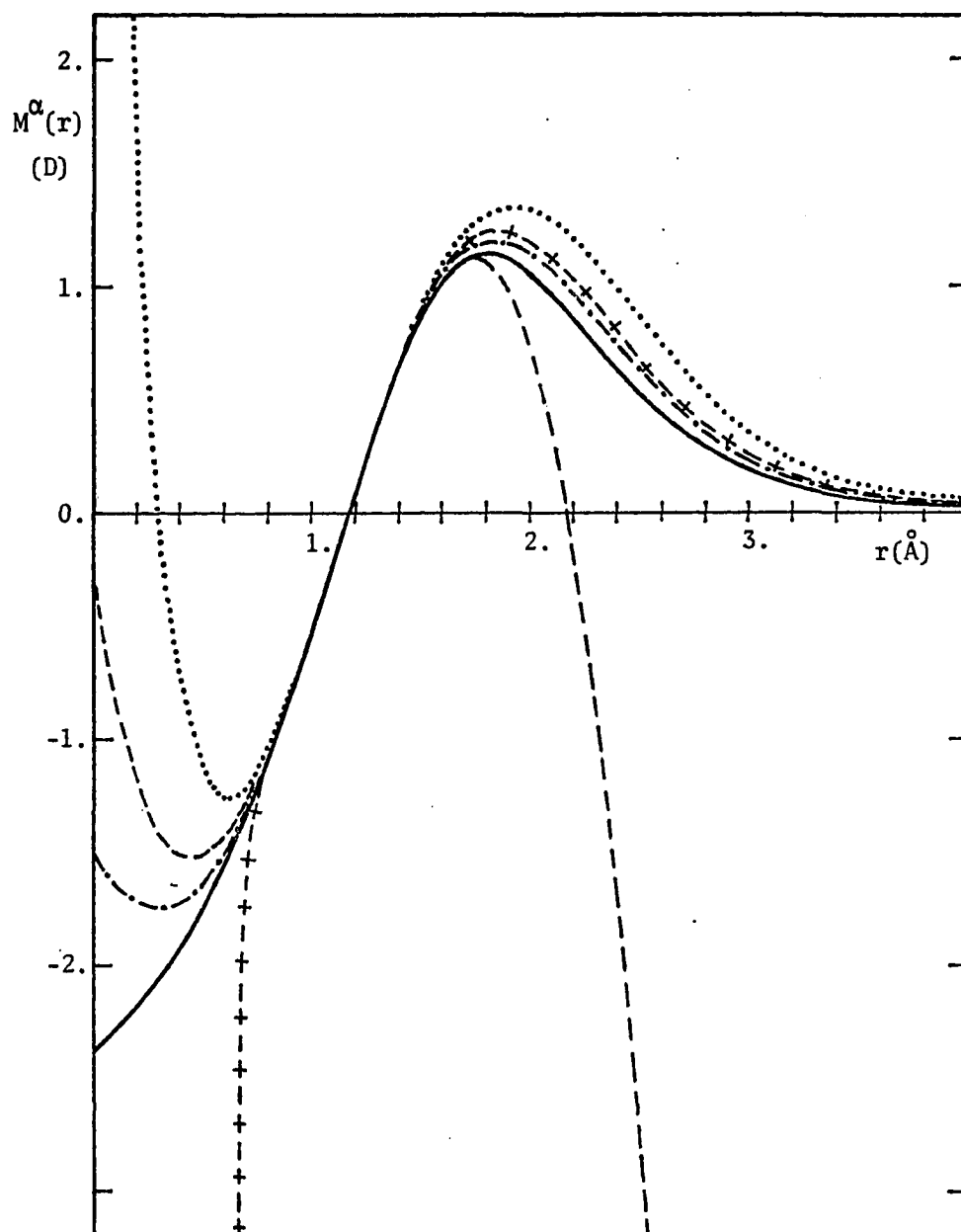


Fig. 5.6. CO dipole moment functions with correct large- r behavior obtained with minimization. Dash-crossed, solid, dash-dotted, and dotted curves represent $M^2(r)$, $M^3(r)$, $M^4(r)$, and $M^5(r)$ respectively. The dashed curve is the PMO cubic dipole moment function in u for CO.

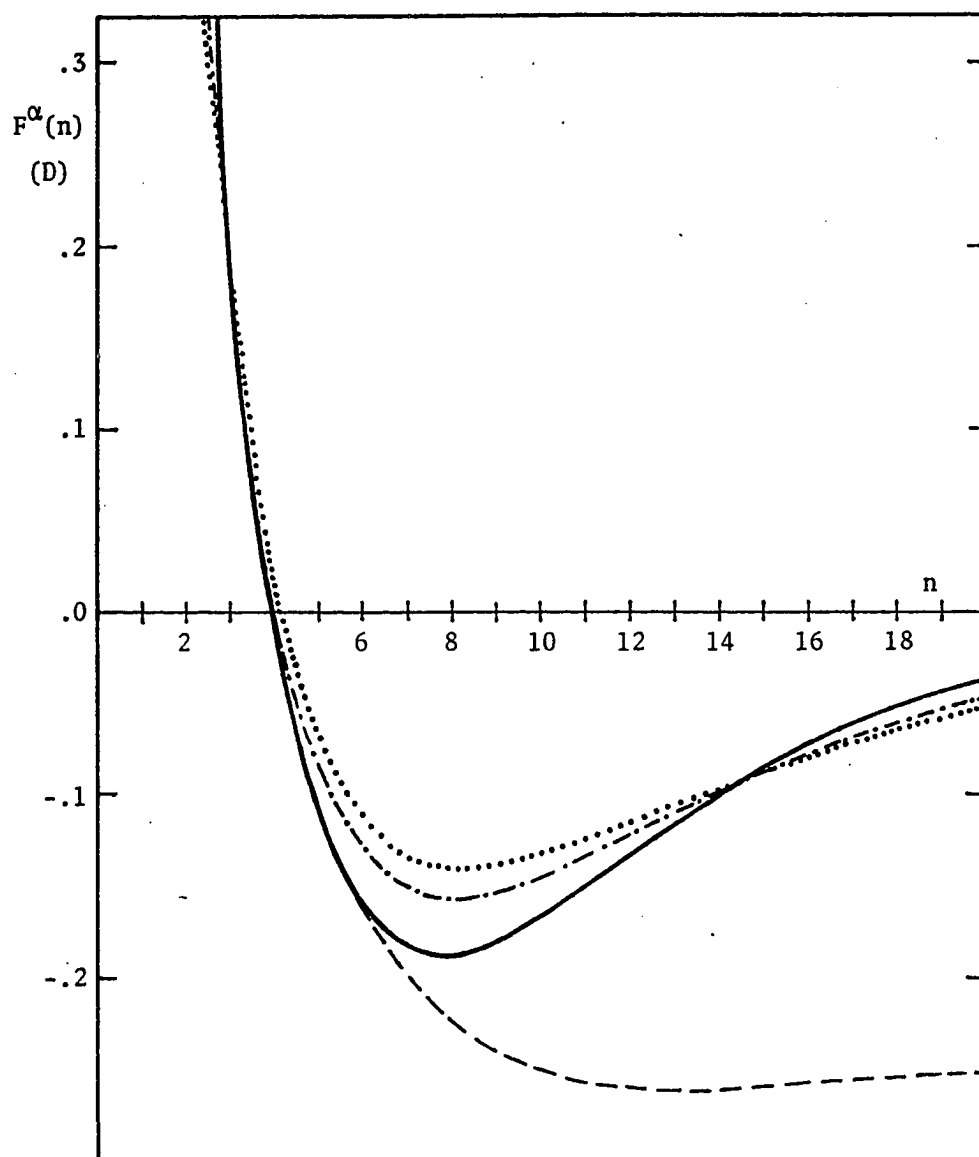


Fig. 5.7. Plots of various generating functions $F^\alpha(n)$ for CO obtained using $M_c y$ correction with minimization. Dash-crossed solid, dash-dotted, and dotted curves are $F^2(n)$, $F^3(n)$, $F^4(n)$, and $F^5(n)$ respectively. The dashed curve represents coefficients M_n^* of the y -series expansion of the PMO cubic dipole moment function in u for CO.

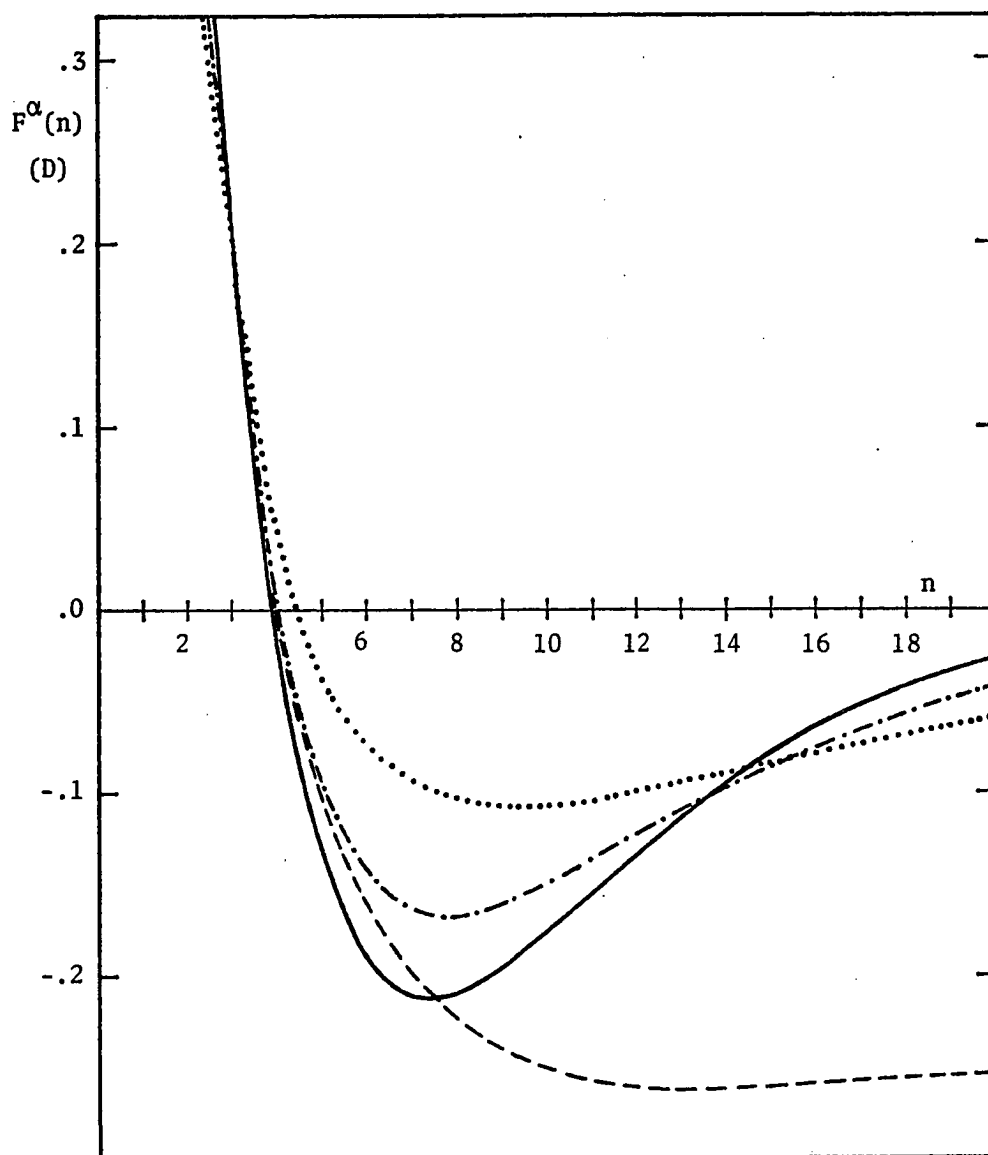


Fig. 5.8. Plots of various generating functions $F^\alpha(n)$ for CO obtained using $M_c y(1-y)$ correction with minimization. Dash-crossed, solid, dash-dotted, and dotted curves are $F^2(n)$, $F^3(n)$, $F^4(n)$, and $F^5(n)$ respectively. The dashed curve represents coefficients M_n^* of the y -series expansion of the PMO cubic dipole moment function in u for CO.

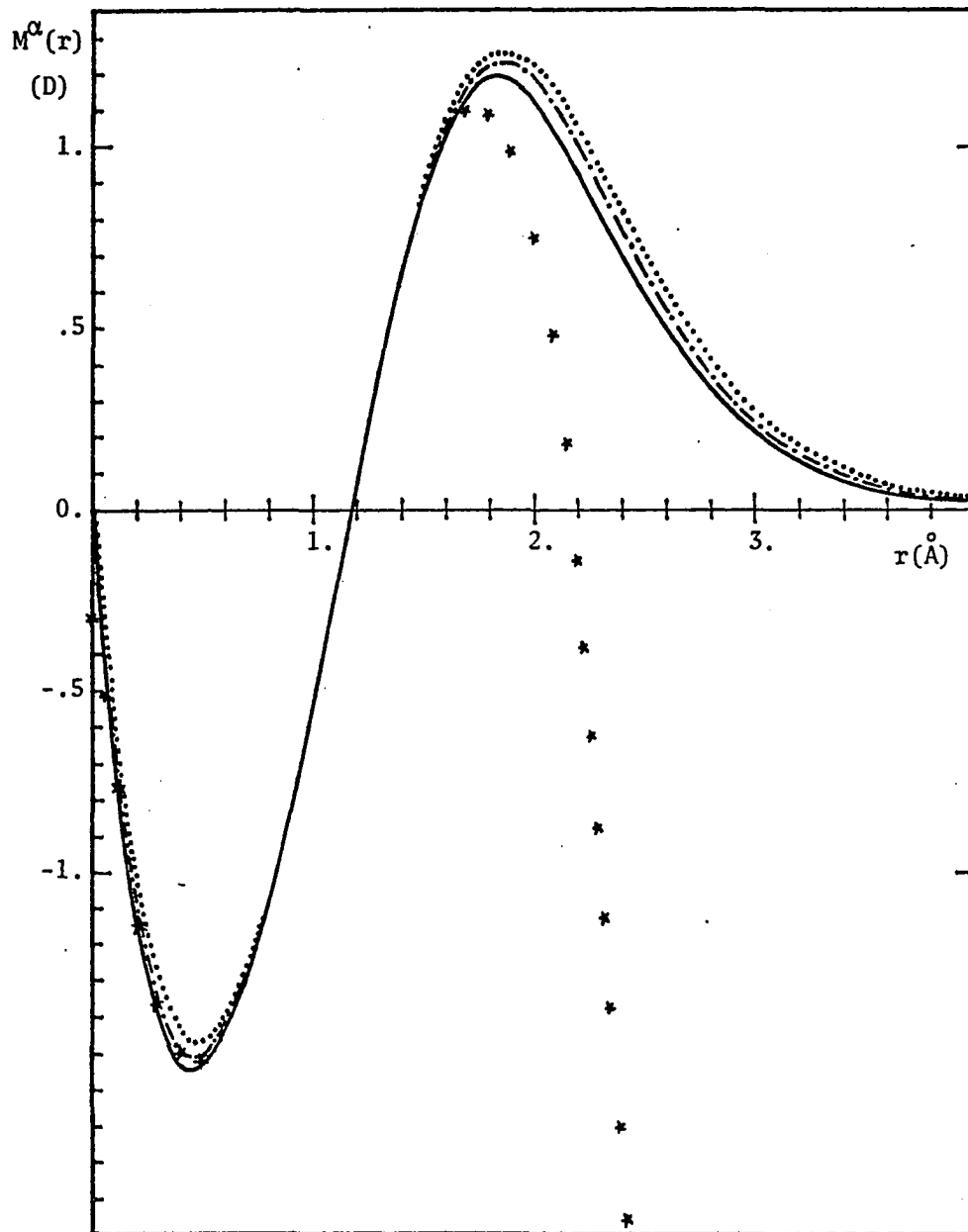


Fig. 5.9. Graphs of various CO dipole moment functions with correct large- r and small- r behaviors obtained using M_c correction with minimization. Solid, dash-dotted, dotted, and starred curves represent $M^3(r)$, $M^4(r)$, $M^5(r)$, and the PMO cubic dipole moment function in u.

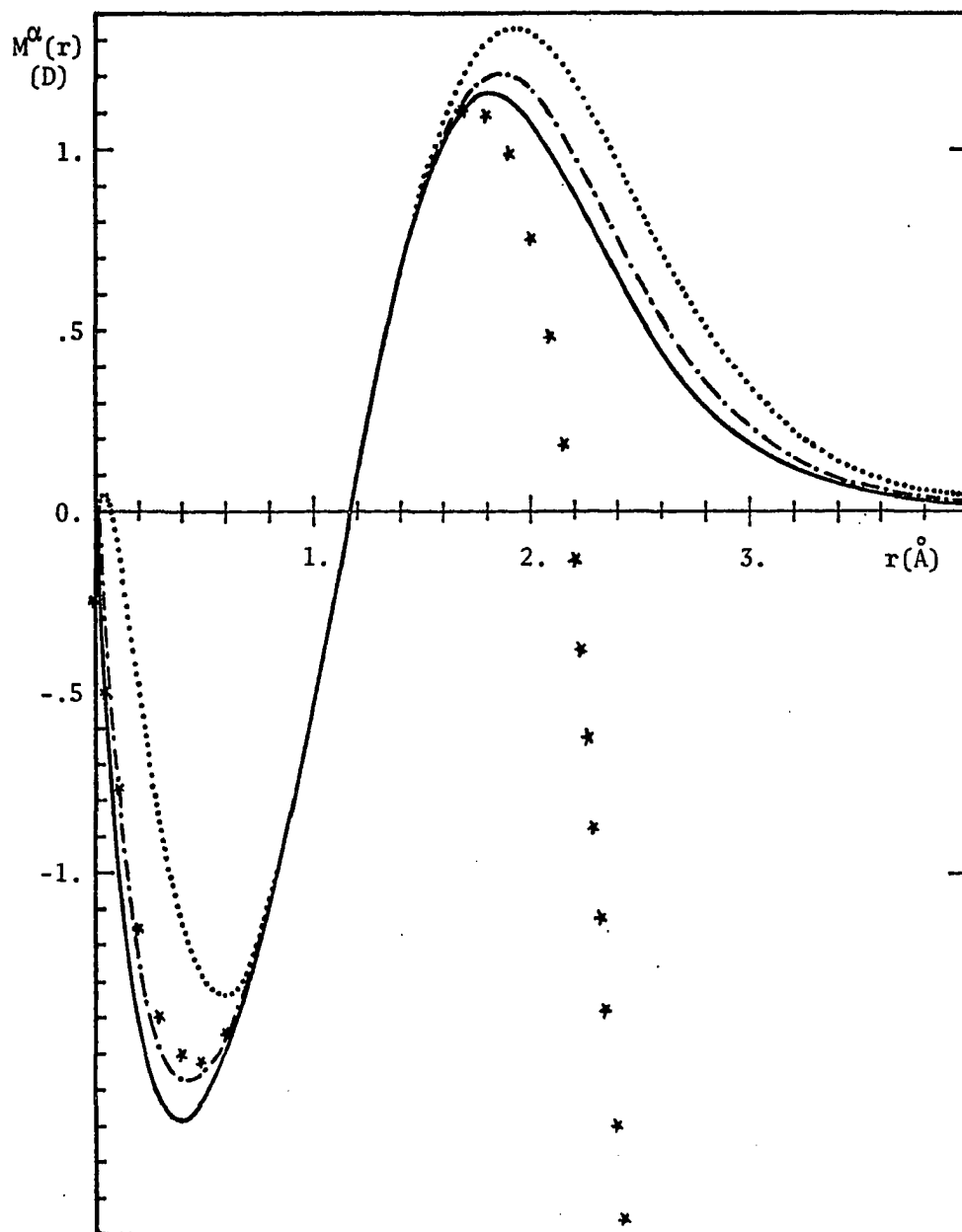


Fig. 5.10. Graphs of various CO dipole moment functions with correct large- r and small- r behaviors obtained using $M_c y(1-y)$ correction with minimization. Solid, dash-dotted, dotted, and starred curves represent $M^3(r)$, $M^4(r)$, $M^5(r)$, and the PMO cubic dipole moment function in u.

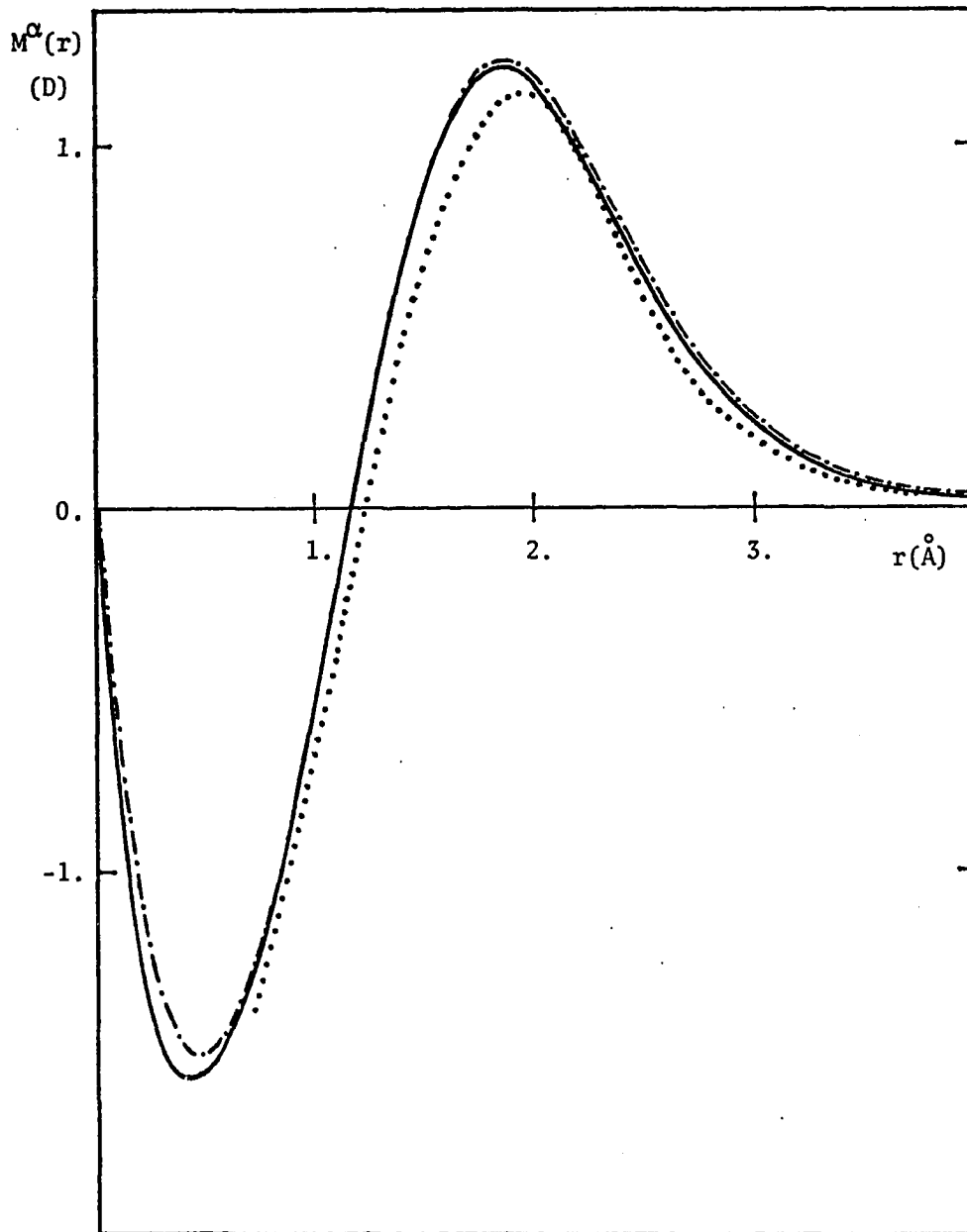


Fig. 5.11. Solid curve (—): function $M^4(r)$, using $M_c y(1-y)$ correction with minimization. Dash-dotted curve (-.-): function $M^4(y)$, using $M_c y$ correction with minimization. Dotted curve (...): result obtained by Kirby-Docken and Liu⁽²⁾.

CHAPTER VI

CALCULATIONS OF ROTATIONLESS VIBRATIONAL TRANSITION MOMENTS

The various CO dipole moment functions obtained in Chapters IV and V can now be used to predict hot-band transition moments. In this computation, we use the series forms of the dipole moment, instead of its closed and reduced forms given by Eqs. (5.14A) - (5.14E), because matrix elements of fairly large powers of y can be evaluated very easily. Using the PMO eigenfunctions obtained by matrix diagonalization as linear combinations of pure Morse wavefunctions (Chapter IV),

$$|v^{\text{PMO}}\rangle = \sum_{i=1}^M C_{v,i} |i\rangle$$

where M , taken to be 48, is the size of the truncated Morse basis. We express the matrix element of a dipole moment function $M(y)$ (written as a power series in y) as a linear combination of pure Morse matrix elements of powers of y :

$$\langle v | M(y) | v' \rangle = \mu_v^{v+\Delta v} = M_0 \delta_{v,v'} + \sum_{n=1}^L \sum_{i,j=0}^M C_{v,i} C_{v',j} \langle i | y^n | j \rangle M_n,$$

where $\Delta v = v' - v$ and L is the number of terms retained in the y -series and is chosen to be 20, which is sufficiently large to give nearly correct large- r behavior and not too excessive dipole moment values at very small r .

Numerical results obtained for μ_0^0 , μ_1^3 , μ_2^4 , μ_3^5 and μ_4^6 are listed in Table 6.1A; values for $v = 5, 10, 15, 20$ and $\Delta v = 0, 1, 2, 3, 4$ are given respectively in Table 6.1B, 6.1C, 6.1D, and 6.1E. In each column of a Table are displayed values of a given transition moment obtained by different groups of calculations, defined as follows:

Group a: including cubic dipole moment functions in u , z , and y respectively;

Group b: including y -series expansion $M^2(y)$ whose reduced form (5.14b) has correct large- r behavior and is determined without minimization, and y -series expansions $M^3(y)$, $M^4(y)$, and $M^5(y)$ whose closed forms have correct behavior at both large r and small r and are determined using the $M_c y$ correction without minimization;

Group c: including y -series expansions $M^3(y)$, $M^4(y)$, and $M^5(y)$ obtained using the $M_c y(1-y)$ correction without minimization.

Group d: representing $M^2(y)$ obtained using minimization, and $M^3(y)$, $M^4(y)$, and $M^5(y)$ obtained using minimization and $M_c y$ correction;

Group e: representing $M^3(y)$, $M^4(y)$, and $M^5(y)$ obtained using minimization and $M_c y(1-y)$ correction;

Group f: experimental value by Roux⁽⁵³⁾ or value calculated by Bouanich⁽¹⁰⁾ who used the dipole moment as a quartic power series in u and applied the perturbation method to an eight power Dunham potential.

We see that, except for the cubic dipole function in z , results obtained using all other functions are generally in excellent agreement with each other and with results experimentally deduced by

Roux or calculated by Bouanich, for $v \leq 20$ and $\Delta v \leq 4$. The discrepancy between the values of transition moments arising from different calculations become larger as v and Δv increase. The difference between values obtained from various y -series expansions is quite negligible for $v \leq 20$ and $\Delta v \leq 4$, because their large- r behaviors are nearly the same. However, the difference between these values and those given from the cubic expressions are appreciable for the same ranges of v and Δv , showing that the large- r behavior of the dipole moment is of importance. Therefore, to obtain more reliable calculated transition moments, the correct large- r behavior of the dipole moment should be taken into account. This may be further justified by the fact that the cubic dipole moment function in z , which has very bad large- r behavior [see Fig. (4.1)], gives nearly correct transition moments only for $v \leq 4$ and $\Delta v \leq 4$ and therefore is useless for the analysis of transitions at higher levels. Also, since the large- r behaviors of $M^2(y)$ and $M^4(y)$ are closer to each other than to those of $M^3(y)$ and $M^5(y)$, they give transition moments in better agreement with each other than with other values. For the same reason, dipole moment functions with correct small- r behavior determined by the $M_c y$ correction yield results agreeing with each other better than those arising from functions corrected by the $M_c y(1-y)$ term.

On the other hand, the wrong small- r behavior of the y -series expansion does not produce a serious effect on the calculated transition moments for $v \leq 20$ and $\Delta v \leq 15$, since increasing the number of terms of the truncated y -series from 20 to 40 does not cause an appreciable change in the results. This may be explained by the fact that

the Morse wavefunctions vanish as r tends to zero much faster than as r tends to infinity.

Finally, since the matrix diagonalization, which is equivalent to the infinite-order perturbation method, provides highly accurate PMO eigenfunctions, we believe that transition moments calculated using these eigenfunctions and cubic dipole moment functions in u and y should be better than those obtained by Bouanich using the Dunham potential and the finite-order perturbation method.

TABLE 6.1A. Comparison of purely vibrational matrix elements of various dipole moment functions for CO ($X^1\Sigma^+$): (a) PMO cubic functions in u, z, and y, (b) expansions in powers of y with reduced forms having correct large-r and/or small-r behavior, obtained using $M_c y$ correction without minimization, (c) using $M_c y(1-y)$ correction without minimization, (d) using $M_c y$ with minimization, (e) using $M_c y(1-y)$ with minimization, and (f) functions by Bouanich⁽¹⁰⁾ or experimental dipole matrix elements⁽⁵³⁾.

| | Function | μ_0^0 | μ_1^3 | μ_2^4 | μ_3^5 | μ_4^6 |
|---|--------------|-----------|-----------|-----------|-----------|-----------|
| a | cubic in u | -.10986 | -.11215-1 | -.16083-1 | -.21051-1 | -.26136-1 |
| | cubic in z | -.10987 | -.11172-1 | -.15927-1 | -.20679-1 | -.25400-1 |
| | cubic in y | -.10986 | -.11213-1 | -.16069-1 | -.21013-1 | -.26054-1 |
| b | $M^2(r)$ | -.10987 | -.11213-1 | -.16076-1 | -.21035-1 | -.26107-1 |
| | $M^3(r)$ | -.10986 | -.11218-1 | -.16089-1 | -.21062-1 | -.26152-1 |
| | $M^4(r)$ | -.10987 | -.11213-1 | -.16075-1 | -.21033-1 | -.26102-1 |
| | $M^5(r)$ | -.10987 | -.11209-1 | -.16064-1 | -.21011-1 | -.26066-1 |
| c | $M^3(r)$ | -.10986 | -.11225-1 | -.16110-1 | -.21103-1 | -.26221-1 |
| | $M^4(r)$ | -.10986 | -.11216-1 | -.16084-1 | -.21051-1 | -.26133-1 |
| | $M^5(r)$ | -.10987 | -.11200-1 | -.16036-1 | -.20956-1 | -.25974-1 |
| d | $M^2(r)$ | -.10987 | -.11224-1 | -.16091-1 | -.21055-1 | -.26131-1 |
| | $M^3(r)$ | -.10987 | -.11228-1 | -.16103-1 | -.21081-1 | -.26176-1 |
| | $M^4(r)$ | -.10987 | -.11223-1 | -.16090-1 | -.21052-1 | -.26127-1 |
| | $M^5(r)$ | -.10987 | -.11220-1 | -.16079-1 | -.21031-1 | -.26091-1 |
| e | $M^3(r)$ | -.10987 | -.11234-1 | -.16123-1 | -.21120-1 | -.26242-1 |
| | $M^4(r)$ | -.10987 | -.11226-1 | -.16098-1 | -.21070-1 | -.26156-1 |
| | $M^5(r)$ | -.10990 | -.11211-1 | -.16053-1 | -.20978-1 | -.26002-1 |
| f | Experimental | -.1098 | -.114 -1 | -.164 -1 | -.214 -1 | * |

TABLE 6.1B (continued)

| | Function ↓ | μ_5^5 | μ_5^6 | μ_5^7 | μ_5^8 | μ_5^9 |
|---|---------------|-----------|-----------|------------|------------|------------|
| a | cubic in u | .13840 -1 | -.25236 | -.31345 -1 | -.33944 -2 | -.36077 -3 |
| | cubic in z | .14981 -1 | -.25363 | -.30043 -1 | -.41317 -2 | -.29968 -4 |
| | cubic in y | .13978 -1 | -.25260 | -.31194 -1 | -.35554 -2 | -.36375 -3 |
| b | $M^2(r)$ | .13884 -1 | -.25241 | -.31295 -1 | -.34204 -2 | -.35043 -3 |
| | $M^3(r)$ | .13812 -1 | -.25235 | -.31366 -1 | -.34010 -2 | -.36477 -3 |
| | $M^4(r)$ | .13891 -1 | -.25241 | -.31289 -1 | -.34196 -2 | -.34850 -3 |
| | $M^5(r)$ | .13947 -1 | -.25245 | -.31234 -1 | -.34297 -2 | -.33625 -3 |
| c | $M^3(r)$ | .13705 -1 | -.25227 | -.31470 -1 | -.33849 -2 | -.38793 -3 |
| | $M^4(r)$ | .13843 -1 | -.25238 | -.31335 -1 | -.34126 -2 | -.35906 -3 |
| | $M^5(r)$ | .14090 -1 | -.25255 | -.31095 -1 | -.34509 -2 | -.30432 -3 |
| d | $M^2(r)$ | .13826 -1 | -.25237 | -.31324 -1 | -.34218 -2 | -.34942 -3 |
| | $M^3(r)$ | .13755 -1 | -.25231 | -.31395 -1 | -.34022 -2 | -.36400 -3 |
| | $M^4(r)$ | .13831 -1 | -.25238 | -.31319 -1 | -.34209 -2 | -.34763 -3 |
| | $M^5(r)$ | .13888 -1 | -.25242 | -.31264 -1 | -.34310 -2 | -.33530 -3 |
| e | $M^3(r)$ | .13655 -1 | -.25224 | -.31495 -1 | -.33861 -2 | -.38710 -3 |
| | $M^4(r)$ | .13786 -1 | -.25234 | -.31364 -1 | -.34139 -2 | -.35814 -3 |
| | $M^5(r)$ | .14023 -1 | -.25251 | -.31128 -1 | -.34524 -2 | -.30316 -3 |
| f | Bouanich | .139 -1 | -.252 | -.3135 -1 | -.333 -1 | -.314 -3 |

TABLE 6.1C (continued)

| | Function | μ_{10}^{10} | μ_{10}^{11} | μ_{10}^{12} | μ_{10}^{13} | μ_{10}^{14} |
|---|------------|-----------------|-----------------|-----------------|-----------------|-----------------|
| a | cubic in u | .13671 | -.33524 | -.59332 -1 | -.86930 -2 | -.12764 -2 |
| | cubic in z | .14959 | -.34835 | -.49318 -1 | -.13469 -1 | -.76609 -5 |
| | cubic in y | .13830 | -.33714 | -.58270 -1 | -.93480 -2 | -.13594 -2 |
| b | $M^2(r)$ | .13715 | -.33567 | -.59017 -1 | -.88258 -2 | -.21528 -2 |
| | $M^3(r)$ | .13667 | -.33527 | -.59322 -1 | -.87578 -2 | -.12692 -2 |
| | $M^4(r)$ | .13718 | -.33569 | -.56000 -1 | -.88209 -2 | -.12491 -2 |
| | $M^5(r)$ | .13753 | -.33596 | -.58781 -1 | -.88519 -2 | -.12326 -2 |
| c | $M^3(r)$ | .13603 | -.3479 | -.59713 -1 | -.87154 -2 | -.12997 -2 |
| | $M^4(r)$ | .13689 | -.33547 | -.59176 -1 | -.88015 -2 | -.12638 -2 |
| | $M^5(r)$ | .13838 | -.33661 | -.58247 -1 | -.89137 -2 | -.11864 -2 |
| d | $M^2(r)$ | .13700 | -.33557 | -.59070 -1 | -.88321 -2 | -.12509 -2 |
| | $M^3(r)$ | .13652 | -.33517 | -.59377 -1 | -.87638 -2 | -.12677 -2 |
| | $M^4(r)$ | .13702 | -.33558 | -.59055 -1 | -.88271 -2 | -.12472 -2 |
| | $M^5(r)$ | .13737 | -.33586 | -.58838 -1 | -.88582 -2 | -.12308 -2 |
| e | $M^3(r)$ | .13590 | -.33470 | -.59760 -1 | -.87213 -2 | -.12981 -2 |
| | $M^4(r)$ | .13675 | -.33538 | -.59228 -1 | -.88077 -2 | -.12620 -2 |
| | $M^5(r)$ | .13821 | -.33649 | -.58309 -1 | -.89206 -2 | -.11843 -2 |
| f | Bouanich | .137 | -.335 | -.5935 -1 | -.861 -2 | -.115 -2 |

TABLE 6.1D (continued)

| | Function | μ_{15}^{15} | μ_{15}^{16} | μ_{15}^{17} | μ_{15}^{18} | μ_{15}^{19} |
|---|------------|-----------------|-----------------|-----------------|-----------------|-----------------|
| | ↓ | | | | | |
| a | cubic in u | .25611 | -.39169 | -.90618 -1 | -.16518 -1 | -.30723 -2 |
| | cubic in z | .32006 | -.45356 | -.48599 -1 | -.34090 -1 | -.33391 -3 |
| | cubic in y | .26265 | -.39834 | -.87165 -1 | -.17942 -1 | -.34110 -2 |
| b | $M^2(r)$ | .25795 | -.39341 | -.89538 -1 | -.16887 -1 | -.30510 -2 |
| | $M^3(r)$ | .25642 | -.39214 | -.90288 -1 | -.16775 -1 | -.30396 -2 |
| | $M^4(r)$ | .25801 | -.39344 | -.89511 -1 | -.16873 -1 | -.30450 -2 |
| | $M^5(r)$ | .25905 | -.39426 | -.89014 -1 | -.16912 -1 | -.30411 -2 |
| c | $M^3(r)$ | .25460 | -.39074 | -.91136 -1 | -.16746 -1 | -.30483 -2 |
| | $M^4(r)$ | .25719 | -.39281 | -.89901 -1 | -.16856 -1 | -.30513 -2 |
| | $M^5(r)$ | .26157 | -.39620 | -.87811 -1 | -.16980 -1 | -.30172 -2 |
| d | $M^2(r)$ | .25766 | -.39321 | -.89614 -1 | -.16903 -1 | -.30494 -2 |
| | $M^3(r)$ | .25613 | -.39194 | -.90366 -1 | -.16791 -1 | -.30382 -2 |
| | $M^4(r)$ | .25771 | -.39323 | -.89593 -1 | -.16889 -1 | -.30436 -2 |
| | $M^5(r)$ | .25875 | -.39405 | -.89096 -1 | -.16928 -1 | -.30396 -2 |
| e | $M^3(r)$ | .25435 | -.39057 | -.91201 -1 | -.16761 -1 | -.30472 -2 |
| | $M^4(r)$ | .25691 | -.39261 | -.89976 -1 | -.16872 -1 | -.30499 -2 |
| | $M^5(r)$ | .26123 | -.39597 | -.87901 -1 | -.16997 -1 | -.30154 -2 |
| f | Bouanich | * | * | * | * | * |

(*) Bouanich did not list values for these hot bands.

TABLE 6.1E (continued)

| | Function | μ_{20}^{20} | μ_{20}^{21} | μ_{20}^{22} | μ_{20}^{23} | μ_{20}^{24} |
|---|------------|-----------------|-----------------|-----------------|-----------------|-----------------|
| | ↓ | | | | | |
| a | cubic in u | .36833 | -.42733 | -.12517 | -.27194 -1 | -.60994 -2 |
| | cubic in z | .59848 | -.64272 | -.10866 | -.78321 -1 | -.15015 -2 |
| | cubic in y | .38655 | -.44420 | -.11713 | -.29425 -1 | -.69517 -2 |
| b | $M^2(r)$ | .37386 | -.43228 | -.12238 | -.27959 -1 | -.61329 -2 |
| | $M^3(r)$ | .37030 | -.42941 | -.12378 | -.27876 -1 | -.60581 -2 |
| | $M^4(r)$ | .37396 | -.43232 | -.12236 | -.27932 -1 | -.61226 -2 |
| | $M^5(r)$ | .37627 | -.43411 | -.21248 | -.27928 -1 | -.61473 -2 |
| c | $M^3(r)$ | .36642 | -.42649 | -.12517 | -.27966 -1 | -.60250 -2 |
| | $M^4(r)$ | .37217 | -.43097 | -.12302 | -.27960 -1 | -.61103 -2 |
| | $M^5(r)$ | .38180 | -.43834 | -.11939 | -.27886 -1 | -.61793 -2 |
| d | $M^2(r)$ | .37339 | -.43197 | -.12247 | -.27990 -1 | -.61341 -2 |
| | $M^3(r)$ | .36982 | -.42909 | -.12387 | -.27908 -1 | -.60592 -2 |
| | $M^4(r)$ | .37346 | -.43198 | -.12246 | -.27964 -1 | -.61237 -2 |
| | $M^5(r)$ | .37577 | -.43377 | -.12159 | -.27960 -1 | -.61485 -2 |
| e | $M^3(r)$ | .36602 | -.42622 | -.12525 | -.27995 -1 | -.60265 -2 |
| | $M^4(r)$ | .37171 | -.43066 | -.12311 | -.27991 -1 | -.61117 -2 |
| | $M^5(r)$ | .38125 | -.43796 | -.11950 | -.27919 -1 | -.61803 -2 |
| f | Bouanich | .369 | -.427 | -.125 | -.273 -1 | -.567 -2 |

CHAPTER VII

CONCLUSION

We have demonstrated in this work that the factorization method provides a powerful technique for evaluating Morse matrix elements of the variables u , y , and z , and some of their powers, which are required for the determination of cubic dipole moment functions in u , y , and z . Our work also shows that the factorization combined with the matrix technique (matrix multiplication and matrix diagonalization) perhaps forms the most elegant and efficient approach for finding accurate PMO eigenfunctions as well as for determining various dipole moment functions in series form for a diatomic molecule such as CO, which fulfills the condition of having a sufficiently large number of bound states.

For many practical applications, the PMO cubic dipole moment functions in u and y are adequate. If information on the dipole moment over a small range of r about r_e is all one needs, then one could use the cubic polynomial in z , for it is the most convenient, although it has very bad behavior at large r .

An important aspect of our work is that an infinite series expansion in powers of y can be determined for the CO dipole moment from a few items of intensity data by assuming that its coefficients M_n other than M_0 are a certain function of the index n in such a way

that their infinite sum including M_0 vanishes. In this manner, the dipole moment function as an expansion in powers of y has the correct general asymptotic behavior as r goes to infinity. Five choices for the functional form of M_n are proposed, of which four are applicable to CO. Except the form containing the term in $1/n^2$, these generating functions have the interesting feature that they produce infinite series reducible to simple closed forms which can then be adjusted further to produce reasonably good behavior at small r .

Excellent agreement between our results for dipole moment functions or calculated transition moments and results from other sources illustrates the accuracy, convenience, and efficiency of our method, at least for CO.

Since the correct large- r behavior and the small- r behavior of the dipole moment function plays a critical role in the prediction of accurate transition moments at high vibrational levels and for large Δv , we suggest that the closed forms $M^3(y)$, $M^4(y)$, and $M^5(y)$ should be employed directly in the calculation of transition moments. For this purpose, exact Morse matrix elements of $(1-By)^{-1}$, $(1-By)^{-2}$, and $\ln(1-By)$ need to be evaluated. Matrix elements of inverse powers of $(1-By)$ may be easily computed numerically using matrix inversion and multiplication. Although we feel that it is possible to find from the factorization method a certain way to obtain exact matrix elements of $\ln(1-By)$, this task seems to be much more difficult than the evaluation of matrix elements of some powers of y as done in Appendix B.

APPENDIX A

POWER OF A POWER SERIES

Suppose that y is a function of x and expressed as a series (finite or infinite) in powers of x ,

$$y(x) = \sum_{n=0}^{\infty} A_n x^n, \quad (\text{A.1})$$

Raising y to a power p , we get y^p which is also a power series in x but with different coefficients:

$$z(x) = y^p = \left[\sum_{n=0}^{\infty} A_n x^n \right]^p = \sum_{n=0}^{\infty} B_n^p x^n \quad (\text{A.2})$$

where the superscript in B_m^p refers to the power p in y^p .

Taking the logarithmic derivatives of both sides in Eq.

(A.2) one obtains

$$\frac{1}{y^p} \frac{d(y^p)}{dx} = \frac{1}{z} \frac{dz}{dx},$$

or

$$py'z = yz'.$$

Hence,

$$p \left[\sum_{k=1}^{\infty} k A_k x^{k-1} \right] \left[\sum_{m=0}^{\infty} B_m^p x^m \right] = \left[\sum_{k=0}^{\infty} A_k x^k \right] \left[\sum_{m=1}^{\infty} m B_m^p x^{m-1} \right],$$

or

$$\sum_{k=0}^{\infty} \sum_{m=0}^{\infty} (pk - m) A_k B_m^p x^{k+m-1} = 0 \quad (\text{A.3})$$

Letting $n = k + m$ and changing the order of summation in Eq. (A.3), we get

$$\sum_{n=0}^{\infty} \left\{ \sum_{m=0}^n [p(n-m) - m] A_{n-m} B_m^P \right\} x^{n-1} = 0. \quad (\text{A.4})$$

We see that the coefficients of all powers of x in the above equation must be identically zero giving

$$\sum_{m=0}^n [p(n-m) - m] A_{n-m} B_m^P = 0 \quad (\text{A.5})$$

from which we obtain the recursion relation:

$$B_n^P = \frac{1}{nA_0} \sum_{m=0}^{n-1} [p(n-m) - m] A_{n-m} B_m^P : n > 0. \quad (\text{A.6})$$

Noting that in the expansion of $(A_0 + A_1x + A_2x^2 + \dots)^P$ the zero-order term in x is $(A_0)^P$, we find

$$B_0^P = (A_0)^P. \quad (\text{A.7})$$

Thus, starting with the coefficient B_0^P , the recursion relation (A.6) permits one to calculate all other coefficients B_n^P very easily in terms of coefficients A_k .

Particular Case $A_0 = 0$:

Of course, B_0^P also vanishes. In this case, Eq. (A.5) reduces to

$$\sum_{m=1}^n [p(n-m) - m] A_{n-m} B_m^P = 0 \quad (\text{A.8})$$

which can be rearranged to give the recursion relation:

$$B_n^P = \frac{1}{(n-p)A_1} \sum_{m=p}^{n-1} [p(n-m+1) - m] A_{n-m+1} B_m^P : n > p. \quad (\text{A.9})$$

Since in the expansion of $(A_1x + A_2x^2 + \dots)^P$, the lowest-order term is $(A_1)^P x^P$, we have

$$B_p^P = (A_1)^P, \quad (\text{A.10})$$

and

$$B_n^P = 0 \quad \text{for } n < p,$$

that is,

$$\left[\sum_{n=1}^{\infty} A_n x^n \right]^P = \sum_{n=p}^{\infty} B_n x^n.$$

This explains why the index m runs from p in Eq. (A.9).

APPENDIX B
EXACT MATRIX ELEMENTS OF y^2 AND y^3

We shall use the following notation for various matrix elements

$$F_{m,m'}^{S,S'} = \langle R_m^S | f(x) | R_{m'}^{S'} \rangle = \int_{-\infty}^{\infty} R_m^S f(x) R_{m'}^{S'} dx, \quad (\text{B.1a})$$

$$J_{m,m'}^{S,S'} = \langle R_m^S | e^{px} | R_{m'}^{S'} \rangle = \int_{-\infty}^{\infty} R_m^S e^{px} R_{m'}^{S'} dx, \quad (\text{B.1b})$$

$$J_{m,m'}^{S,S'} = J_{m,m'}^{S,S'} = \langle R_m^S | e^x | R_{m'}^{S'} \rangle,$$

where R_m^S is the eigensolution of the class II differential equation (3.3), p is a positive integer, and $f(x)$ is an arbitrary continuous function satisfying the condition: $f(x) R_m^S(x) \rightarrow 0$ as $x \rightarrow \pm\infty$.

We use the convention $m \geq n'$ (or $v \leq v'$) if not otherwise specified. We shall first derive a general recurrence relation for the matrix element (B.1a) of any function $f(x)$.

Using the mutually adjoint properties of the s -raising and lowering operators in Eq. (3.6a), we integrate by parts and write:

$$\begin{aligned} F_{m,m'}^{S,S'} &= \int_{-\infty}^{\infty} R_m^S f(x) \mathcal{H}_{m'}^-(s') R_{m'}^{S'-1} dx \\ &= \int_{-\infty}^{\infty} \mathcal{H}_{m'}^+(s') R_m^S f(x) R_{m'}^{S'-1} dx \\ &= (B_{m'}^{S'})^{-1} \int_{-\infty}^{\infty} \left(e^x - s' + \frac{d}{dx} \right) R_m^S f(x) R_{m'}^{S'-1} dx, \end{aligned} \quad (\text{B.2a})$$

$$\begin{aligned}
F_{m,m'}^{s,s'} &= (B_m^s \bar{B}_{m'}^{s'}) \int_{-\infty}^{\infty} \mathcal{H}_s^{+(m)} R_m^s f(x) R_{m'}^{s'-1} dx \\
&+ (s - s') \bar{B}_{m'}^{s'} \int_{-\infty}^{\infty} R_m^s f(x) R_{m'}^{s'-1} dx \\
&+ \bar{B}_{m'}^{s'} \int_{-\infty}^{\infty} R_m^s f'(x) R_{m'}^{s'-1} dx
\end{aligned}$$

which then can be written in the recurrence form:

$$F_{m,m'}^{s,s'} = (B_m^s \bar{B}_{m'}^{s'}) F_{m,m'}^{s-1,s'-1} + (s-s') F_{m,m'}^{s,s'-1} + \bar{B}_{m'}^{s'} F_{m,m'}^{s,s'-1} \quad (\text{B.2b})$$

where

$$f'(x) = \frac{df(x)}{dx} \quad \text{and} \quad \bar{B}_m^s = (B_m^s)^{-1} = [(s-m)(s+m)]^{-\frac{1}{2}}.$$

In particular, for $f(x) = e^{px}$ we have $f'(x) = pe^{px}$ and Eq.

(B.2a) gives

$$JP_{m,m'}^{s,s'} = (B_m^s \bar{B}_{m'}^{s'}) JP_{m,m'}^{s-1,s'-1} + (p+s-s') \bar{B}_{m'}^{s'} JP_{m,m'}^{s,s'-1}. \quad (\text{B.3})$$

Writing $s' = s - n$ where n is an integer, Eq. (B.3) becomes

$$JP_{m,m'}^{s,s-n} = (B_m^s \bar{B}_{m'}^{s-n}) JP_{m,m'}^{s-1,s-n-1} + (p+n) \bar{B}_{m'}^{s-n} JP_{m,m'}^{s,s-n-1}. \quad (\text{B.4a})$$

Interchanging s and $s' = s - n$ in the above equation yields a similar recurrence equation:

$$JP_{m,m'}^{s-n,s} = (B_m^{s-n} \bar{B}_{m'}^s) JP_{m,m'}^{s-n-1,s-1} + (p-n) \bar{B}_{m'}^s JP_{m,m'}^{s-n,s-1}. \quad (\text{B.4b})$$

Interchanging m and m' in Eq. (B.4a), we get another recurrence relation alternative to Eq. (B.4b):

$$JP_{m,m'}^{s-n,s} = (B_{m'}^s \bar{B}_m^{s-n}) JP_{m,m'}^{s-n-1,s-1} + (p+n) \bar{B}_m^{s-n} JP_{m,m'}^{s-n-1,s}. \quad (\text{B.4c})$$

Again, if we interchange s and $s' = s - n$ in the above equation, we obtain a recurrence relation alternative to Eq. (B.4a):

$$JP_{m,m'}^{s,s-n} = (\bar{B}_{m'}^{s-n} \bar{B}_m^s) JP_{m,m'}^{s-1,s-n-1} + (p-n) \bar{B}_m^s JP_{m,m'}^{s-1,s-n}. \quad (\text{B.4d})$$

Next, using the above recurrence relations, we shall evaluate several "intermediate" integrals that arise in deriving exact expressions for matrix elements of y^2 and y^3 .

$$\underline{1. \text{ Integral } \langle R_m^m | e^{px} | R_{m'}^{m+p} \rangle}$$

$$m \geq m', \quad p > 0$$

Putting $s = m$, $s' = m+p$, and $f(x) = e^{px}$ in Eq. (B.2a), we have

$$\begin{aligned} JP_{m,m'}^{m,m+p} &= \int_{-\infty}^{\infty} R_m^m e^{px} \mathcal{L}_{m'}^{-(m+p)} R_{m'}^{m+p} dx, \\ &= \bar{B}_{m'}^{m+p} \int_{-\infty}^{\infty} \left\{ \frac{1}{2} e^x - (m+p) + \frac{d}{dx} \right\} (R_m^m e^{px}) R_{m'}^{m+p} dx \\ &= \bar{B}_{m'}^{m+p} \int_{-\infty}^{\infty} \left\{ \frac{1}{2} e^x - m + \frac{d}{dx} \right\} R_m^m (e^{px} R_{m'}^{m+p}) dx, \end{aligned}$$

which must vanish according to Eq. (3.5b):

$$JP_{m,m'}^{m,m+p} = 0. \quad (\text{B.5})$$

The above result can also be obtained by using Eq. (B.4a) where we let $s = m$, $n = -p$, and noting that

$$JP_{m,m'}^{m-1,s'} = 0 \quad (\text{B.6})$$

since there is no eigenfunction R_m^{m-1} .

$$\underline{2. \text{ Integral } \langle R_m^{s-p} | e^{pX} | R_{m'}^s \rangle}$$

$$m \geq m', \quad s-p > m$$

From Eq. (B.4b), we can write for $p = n$

$$J_{m,m'}^{s-p,s} = (\text{const}) J_{m,m'}^{s-p-1,s-1} .$$

Repeating application of this relation to its right-hand side over and over a total of $(s - p - m)$ times, one finally gets

$$J_{m,m'}^{s-p,s} = (\text{const}) J_{m,m'}^{m,m+p}$$

which certainly vanishes due to Eq. (B.5). Thus,

$$J_{m,m'}^{s-p,s} = 0, \quad m \geq m' . \quad (\text{B.7})$$

In particular, for $p = 1$, we have

$$J_{m,m'}^{s-1,s} = \langle R_m^{s-1} | e^X | R_{m'}^s \rangle = 0 . \quad (\text{B.8})$$

$$\underline{3. \text{ Integral } \langle R_m^{s-n} | e^{pX} | R_{m'}^s \rangle}$$

$$m \geq m', \quad n > p, \quad s - n > m$$

First, using Eq. (B.4b), we write for $n = p + 1$

$$J_{m,m'}^{s-p-1,s} = (B_m^{s-p-1} \bar{B}_{m'}^s) J_{m,m'}^{s-p-2,s-1} - \bar{B}_{m'}^s J_{m,m'}^{(s-1)-p,(s-1)} .$$

The second integral in the right-hand side vanishes according to Eq. (B.7). Thus, we have

$$J_{m,m'}^{s-p-1,s} = (\text{const}) J_{m,m'}^{s-p-2,s-1}$$

which, by induction, leads to

$$J_{m,m'}^{s-p-1,s} = (\text{const}) J_{m,m'}^{m,m+p+1} = 0$$

because of Eq. (B.5).

In similar fashion, we can show that

$$J_{m,m'}^{s-p-2,s} = 0 ;$$

and therefore, inductively we obtain

$$J_{m,m'}^{s-n,s} = 0 , \quad n > p , \quad s - n > m . \quad (\text{B.9})$$

In particular, for $p = 1$, the above equation gives

$$J_{m,m'}^{s-n,s} = \langle R_m^{s-n} | e^X | R_{m'}^s \rangle = 0 . \quad (\text{B.10})$$

4. Integral $\langle R_m^m | e^{pX} | R_{m'}^{m-n} \rangle$

$$m > m' , \quad n > 0 , \quad m - n > 0$$

Putting $s = m$ in Eq. (B.4a) and using Eq. (B.6), we obtain

$$J_{m,m'}^{m,m-n} = (n + p) \bar{B}_{m'}^{m-n} J_{m,m'}^{m,m-n-1} .$$

Applying this relation over and over $(m-n-1-m')$ times, we finally obtain

$$J_{m,m'}^{m,m-n} = \left[\frac{(n+p)(n+p+1)\dots(m-m'+p-1)}{B_{m'}^{m-n} B_{m'}^{m-n-1} \dots B_{m'}^{m'+1}} \right] J_{m,m'}^{m,m'} . \quad (\text{B.11a})$$

The factor in the square brackets of the above equation, denoted by C , can be written in the form

$$C = \frac{(m-m'+p-1)!}{(m+p-1)!} \left[\frac{\Gamma(2m'+1)}{(m-m'-m)! \Gamma(m+m'-n+1)} \right]^{\frac{1}{2}} . \quad (\text{B.11b})$$

The integral $J_{m,m'}^{m,m'}$ is given by Eq. (C.4) in Appendix C.

Therefore, Eq. (B.11a) can be expressed as

$$J_{m,m'}^{m,m-n} = \frac{(m-m'+p-1)!}{(n+p-1)!} \left[\frac{2m' \Gamma^2(m+m'+p)}{(m-m'-n)! \Gamma(m+m'-n+1) \Gamma(2m)} \right]^{\frac{1}{2}}. \quad (\text{B.12})$$

In particular, for $p = 1$, this equation becomes

$$J_{m,m'}^{m,m-n} = \frac{(m-m')!}{n!} \left[\frac{2m' \Gamma^2(m+m'+1)}{(m-m'-n)! \Gamma(m+m'-n+1) \Gamma(2m)} \right]^{\frac{1}{2}}. \quad (\text{B.13})$$

The following relation between Eq. (B.12) and Eq. (B.13) can be obtained:

$$J_{m,m'}^{m,m-n} = \prod_{i=1}^{p-1} \left[\frac{B_{m'}^{m+i}}{n+i} \right] J_{m,m'}^{m,m-n}. \quad (\text{B.14})$$

We also obtain the relation

$$J_{m,m'}^{m,m-n} = \frac{1}{n} (B_{m'}^m)^2 K_{m,m'}^{m,m-n} = \frac{(m-m')(m+m')}{n} K_{m,m'}^{m,m-n} \quad (\text{B.15})$$

where $K_{m,m'}^{m,m-n} = \langle R_m^m | R_{m'}^{m-n} \rangle$ is given by Eq. (C.7) or Eq. (C.9) in Appendix C.

For convenience, we write several particular cases of Eqs.

(B.12) and (B.13) for later use.

$$J_{m,m'}^{m,m-1} = (m-m')(m+m') \left[2m' \frac{(m-m'-1)! \Gamma(m+m')}{\Gamma(2m)} \right]^{\frac{1}{2}},$$

$$J_{m,m'}^{m,m-1} = (B_{m'}^m)^2 K_{m,m'}^{m,m-1}. \quad (\text{B.16a})$$

$$J_{m,m'}^{m,m-2} = \frac{1}{2} B_{m'}^{m-1} J_{m,m'}^{m,m-1}. \quad (\text{B.16b})$$

$$J_{m,m'}^{m,m-1} = \frac{1}{2} (B_{m'}^m B_{m'}^{m+1})^2 K_{m,m'}^{m,m-1}. \quad (\text{B.17a})$$

$$J_{m,m'}^{m,m-2} = \frac{1}{6} B_{m'}^{m-1} (B_{m'}^m B_{m'}^{m+1})^2 K_{m,m'}^{m,m-1}. \quad (\text{B.17b})$$

5. Integral $\langle R_m^s | e^x | R_{m'}^{s-1} \rangle$

$$m > m'$$

Letting $n = 1$ and $p = 1$ in Eq. (B.4d), one obtains

$$J_{m,m'}^{s,s-1} = (B_{m'}^{s-1} \bar{B}_m^s) J_{m,m'}^{s-1,s-2} \quad (B.18a)$$

Applying this relation consecutively, we obtain, after $(s-m)$ times,

$$J_{m,m'}^{s,s-1} = \left[\frac{B_{m'}^{s-1} B_{m'}^{s-2} \cdots B_{m'}^m}{B_m^s B_m^{s-1} \cdots B_m^{m+1}} \right] J_{m,m'}^{m,m-1} \quad (B.18b)$$

The coefficient in the square brackets can be written as

$$C = \left[\frac{(s-m'-1)! \Gamma(s+m') \Gamma(2m+1)}{(m-m'-1)! (s-m)! \Gamma(s+m+1) \Gamma(m+m')} \right]^2$$

Substituting this expression and that for $J_{m,m'}^{m,m-1}$ given by Eq. (B.16a) into Eq. (B.18b), we obtain after some simplification,

$$J_{m,m'}^{s,s-1} = \frac{(m-m')(m+m')}{[(s-m')(s+m')]^{\frac{1}{2}}} \left[4m'm \frac{(s-m') \Gamma(s+m'+1)}{(s-m)! \Gamma(s+m+1)} \right]^{\frac{1}{2}} \quad (B.19a)$$

which can be related to the off-diagonal matrix elements of e^x in Eq. (3.42) by

$$J_{m,m'}^{s,s-1} = (B_{m'}^m)^2 \bar{B}_m^s J_{m,m'}^{s,s} \quad (B.19b)$$

Changing s into $s + 1$ in the last equation, we have

$$J_{m,m'}^{s+1,s} = (B_{m'}^m)^2 \bar{B}_m^{s+1} J_{m,m'}^{s,s} \quad (B.19c)$$

6. Integral $\langle R_m^s | e^x | R_{m'}^{s-2} \rangle$

$$m > m'$$

Again Eq. (B.4d) gives, for $n = 2$ and $p = 1$,

$$J_{m,m'}^{s,s-2} = (B_{m'}^{s-2} \bar{B}_m^s) J_{m,m'}^{s-1,s-3} - \bar{B}_m^s J_{m,m'}^{s-1,s-2} \quad . \quad (\text{B.20a})$$

Applying this recurrence relation repeatedly to the first integral in the right-hand side of the above equation, we obtain after the k th time,

$$\begin{aligned} J_{m,m'}^{s,s-2} &= (B_{m'}^{s-2} B_{m'}^{s-3} \dots B_{m'}^{s-k-1}) (\bar{B}_m^s \bar{B}_m^{s-1} \dots \bar{B}_m^{s-k+1}) J_{m,m'}^{s-k,s-k-2} \\ &- (B_{m'}^{s-1} B_{m'}^{s-2} \dots B_{m'}^{s-k}) (\bar{B}_m^s \bar{B}_m^{s-1} \dots \bar{B}_m^{s-k+1}) J_{m,m'}^{s-k,s-k-1} \\ &- \bar{B}_m^s J_{m,m'}^{s-1,s-2} \quad . \quad (\text{B.20b}) \end{aligned}$$

Making use of Eq. (B.18a), we can reduce the second term in the above equation to

$$2^{\text{nd}} \text{ term} = \bar{B}_{m'}^{s-1} J_{m,m'}^{s,s-1} \quad .$$

Since this result is for a general value of k , we see that all terms after the first term in Eq. (B.20b) are equal to the second term. Therefore, we can write

$$J_{m,m'}^{s,s-2} = (\text{const}) J_{m,m'}^{s-k,s-k-2} - k \bar{B}_{m'}^{s-1} J_{m,m'}^{s,s-1}$$

which becomes for $k = s - m$

$$J_{m,m'}^{s,s-2} = C J_{m,m'}^{m,m-2} - (s - m) \bar{B}_{m'}^{s-1} J_{m,m'}^{s,s-1} \quad (\text{B.20c})$$

where the constant factor C is

$$C = \left[\frac{(s-m'-2)(s+m'-2) \cdot (s-m'-3)(s+m'-3) \dots (m-m'-1)(m+m'-1)}{(s-m)(s+m) \cdot (s-m-1)(s+m-1) \dots (2)(2m+2)(1)(2m+1)} \right]^{\frac{1}{2}}$$

and the integral $J_{m,m'}^{m,m-2}$ is given by Eq. (B.16b).

The first term in the right side of Eq. (B.20c) then can be written as

$$\text{First term} = \frac{1}{2}(B_{m'}^m B_{m'}^{m-1})^2 \bar{B}_{m'}^s \bar{B}_{m'}^{s-1} J_{m,m'}^{s,s},$$

while, using Eq. (B.19b), the second term can be expressed as

$$\text{Second term} = (s - m)(B_{m'}^m)^2 \bar{B}_{m'}^s \bar{B}_{m'}^{s-1} J_{m,m'}^{s,s}.$$

These expressions permit us to write Eq. (B.20c) as

$$J_{m,m'}^{s,s-2} = \left[\frac{\frac{1}{2}(B_{m'}^m B_{m'}^{m-1})^2 - (s-m)(B_{m'}^m)^2}{B_{m'}^s B_{m'}^{s-1}} \right] J_{m,m'}^{s,s}. \quad (\text{B.21a})$$

Replacing s by $s + 2$ in this equation, we have

$$J_{m,m'}^{s+2,s} = \left[\frac{\frac{1}{2}(B_{m'}^m B_{m'}^{m-1})^2 - (s-m+2)(B_{m'}^m)^2}{B_m^{s+2} B_m^{s+1}} \right] J_{m,m'}^{s,s}. \quad (\text{B.21b})$$

7. Matrix Elements of y^2

7a. Diagonal matrix elements of y^2

Diagonal matrix elements of e^{2x} have been obtained by Huffaker and Dwivedi⁽²⁰⁾ in the form

$$\langle m | e^{2x} | m \rangle = A^s \langle m | e^x | m \rangle = 4m(s + \frac{1}{2}), \quad (\text{B.22})$$

from which one can easily obtain those for e^{-2au} and y^2 :

$$\langle v | e^{-2au} | v \rangle = \langle v | e^{-au} | v \rangle = \frac{s - v}{s + \frac{1}{2}}, \quad (\text{B.23})$$

and

$$\langle v | y^2 | v \rangle = \langle v | y | v \rangle = \frac{v + \frac{1}{2}}{s + \frac{1}{2}}. \quad (\text{B.24})$$

7b. Non-Diagonal matrix elements of y^2

The recursion relation (3.8a) permits us to write

$$e^{2x} R_{m'}^s = A^s e^x R_{m'}^s + B_{m'}^s e^x R_{m'}^{s-1} + B_{m'}^{s+1} e^x R_{m'}^{s+1}$$

from which we obtain

$$J_{m,m'}^{s,s} = A^s J_{m,m'}^{s,s} + B_{m'}^s J_{m,m'}^{s,s-1} + B_{m'}^{s+1} J_{m,m'}^{s,s+1} \quad (B.25)$$

The last integral in the above equation vanishes in view of Eq. (B.10) while the integral $J_{m,m'}^{s,s-1}$ is given by Eq. (B.19a or b).

Hence, we can write Eq. (B.25) as

$$J_{m,m'}^{s,s} = [A^s + (B_{m'}^m)^2] J_{m,m'}^{s,s}, \quad (B.26)$$

or

$$\langle m | e^{2x} | m' \rangle = [2s + 1 + (m-m')(m+m')] \langle m | e^x | m' \rangle$$

from which we obtain off-diagonal matrix elements of e^{-2au} and y^2 :

$$\langle v | e^{-2au} | v' \rangle = [1 + \frac{(v'-v)(2s-v'-v)}{2s+1}] \langle v | e^{-au} | v' \rangle \quad (B.27)$$

and

$$\langle v | y^2 | v' \rangle = [1 - \frac{(v'-v)(2s-v'-v)}{2s+1}] \langle v | y | v' \rangle \quad (B.28)$$

where the off-diagonal matrix elements of e^{-au} and y are given by Eqs. (3.43) and (3.44).

8. Matrix Elements of y^3

Using the recursion relation (3.8a) again, one can write

$$\begin{aligned} e^{3x} R_{m'}^s &= A^s e^{2x} R_{m'}^s + B_{m'}^s e^{2x} R_{m'}^{s-1} + B_{m'}^{s+1} R_{m'}^{s+1} \\ &= A^s e^{2x} R_{m'}^s + B_{m'}^s e^x [A^{s-1} R_{m'}^{s-1} + B_{m'}^{s-1} R_{m'}^{s-2} + B_{m'}^s R_{m'}^s] \end{aligned}$$

$$\begin{aligned}
&= A^s e^{2x} R_{m'}^s + B_{m'}^s e^x [A^{s-1} R_{m'}^{s-1} + B_{m'}^{s-1} R_{m'}^{s-2} + B_{m'}^s R_{m'}^s] \\
&\quad + B_{m'}^{s+1} e^x [A^{s+1} R_{m'}^{s+1} + B_{m'}^{s+1} R_{m'}^s + B_{m'}^{s+2} R_{m'}^{s+2}] ,
\end{aligned}$$

which then gives, after some rearrangement,

$$\begin{aligned}
J_{m,m'}^{s,s} &= A^s J_{m,m'}^{s,s} + [(B_{m'}^s)^2 + (B_{m'}^{s+1})^2] J_{m,m'}^{s,s} \\
&\quad + (B_{m'}^s B_{m'}^{s-1}) J_{m,m'}^{s,s-2} + (A^{s-1} B_{m'}^s) J_{m,m'}^{s,s-1} \\
&\quad + (A^{s+1} B_{m'}^{s+1}) J_{m,m'}^{s,s+1} + (B_{m'}^{s+1} B_{m'}^{s+2}) J_{m,m'}^{s,s+2} , \quad (B.29)
\end{aligned}$$

where $m \geq m'$.

8a. Diagonal matrix elements of y^3

For $m = m'$, the last four integrals in Eq. (B.29) vanish according to Eq. (B.10), yielding

$$J_{m,m}^{s,s} = [(A^s)^2 + (B_m^s)^2 + (B_m^{s+1})^2] J_{m,m}^{s,s} , \quad (B.30)$$

where we have used Eq. (B.22). The above equation can be written more explicitly as

$$J_{m,m}^{s,s} = \frac{1}{2} [1 + 3(2s+1)^2 - 4m^2] J_{m,m}^{s,s} ,$$

from which we can obtain diagonal matrix elements of e^{-3au} and y^3 :

$$\langle v | e^{-3au} | v \rangle = \left[\frac{1 + 3(2s+1)^2 - 4(s-v)^2}{2(2s+1)^2} \right] \langle v | e^{-au} | v \rangle , \quad (B.31)$$

and

$$\langle v | y^3 | v \rangle = 1 + \left[\frac{1 + 3(2s+1)^2 - 4(s-v)^2}{2(2s+1)^2} \right] \langle v | y | v \rangle . \quad (B.32)$$

8b. Non-Diagonal matrix elements of y^3

For $m > m'$, the last two integrals in Eq. (B.29) vanishes because of Eq. (B.10), giving

$$J_{m,m'}^{S,S} = A^S J_{m,m'}^{2,S,S} + [(B_{m'}^S)^2 + (B_{m'}^{S+1})^2] J_{m,m'}^{S,S} \\ + (B_{m'}^S B_{m'}^{S-1}) J_{m,m'}^{S,S-2} + (A^{S-1} B_{m'}^S) J_{m,m'}^{S,S-1} .$$

Replacing the first and the last two integrals in the right hand side of the above equation by their expressions given by Eqs. (B.26a), (B.21a), and (B.19b) respectively, we obtain

$$J_{m,m'}^{S,S} = [(A^S)^2 + (B_{m'}^S)^2 + (B_{m'}^{S+1})^2 + (A^S + A^{S-1} - s + m)(B_{m'}^m)^2 \\ + \frac{1}{2}(B_{m'}^m B_{m'}^{m-1})^2] J_{m,m'}^{S,S} , \quad (B.33)$$

or

$$J_{m,m'}^{S,S} = \frac{1}{2} \left\{ 1 + 3(2s+1)^2 - 4m'^2 + (m-m')(m+m') \right. \\ \left. \times [8s - 2(s-m) + (m-m'-1)(m+m'-1)] \right\} J_{m,m'}^{S,S} .$$

From this equation, we can find the expressions for off-diagonal matrix elements of e^{-3au} and y^3 :

$$\langle v | e^{-3au} | v' \rangle = \frac{1}{2} \left\{ 1 + 3(2s+1)^2 - 4(s-v)^2 + (v'-v)(2s-v'-v) \right. \\ \left. \times [2 + 3(2s+1) + (v'-v)(2s-v'-v)] \right\} \langle v | e^{-au} | v' \rangle \quad (B.34)$$

and

$$\langle v | y^3 | v' \rangle = \left\{ 1 + 3(2s+1)^2 - 4(s-v)^2 \right. \\ \left. + (v'-v)(2s-v'-v) [(v'-v)(2s-v'-v) - 6s - 1] \right\} \frac{\langle v | y | v' \rangle}{2(2s+1)^2} . \quad (B.35)$$

Note that, although we have fixed m' to be smaller than m , the expressions for non-diagonal matrix elements of e^{-pau} and e^{px} where $p = 1, 2, 3$, will reduce to those for diagonal matrix elements if we put $m' = m$.

Matrix elements of y^2 and y^3 computed using exact formulas or matrix multiplication for $0 \leq v \leq 9$ and $0 \leq v' \leq 9$ are listed in Tables B.1 and B.2. Also are given matrix elements of u^2 and u^3 obtained by matrix technique for $0 \leq v \leq 9$ and $0 \leq v' \leq 9$ in Tables B.3 and B.4.

TABLE B.1. Morse matrix elements of y^2 for $0 \leq v \leq 9$ and $0 \leq v' \leq 9$.

The last negative digit means power of 10.

| $v' \backslash v$ | 0 | 1 | 2 | 3 | 4 |
|-------------------|-------------|-------------|-------------|-------------|-------------|
| 0 | .647508 -2 | -.103190 -2 | .871435 -2 | .243659 -2 | .589255 -3 |
| 1 | -.103190 -2 | -.194252 -1 | -.288980 -2 | .145884 -1 | -.475793 -2 |
| 2 | .871435 -2 | -.288980 -2 | .323754 -1 | -.525558 -2 | .199223 -1 |
| 3 | .243659 -2 | .145884 -1 | -.525558 -2 | .453256 -1 | -.800895 -2 |
| 4 | .589255 -3 | .475793 -2 | .199223 -1 | -.800895 -2 | .582757 -1 |
| 5 | .141917 -3 | .129348 -2 | .734105 -2 | .248124 -1 | -.110769 -1 |
| 6 | .351989 -4 | .342730 -3 | .219838 -2 | .101251 -1 | .292876 -1 |
| 7 | .907982 -5 | .921726 -4 | .631926 -3 | .329366 -2 | .130553 -1 |
| 8 | .244200 -5 | .255115 -4 | .182394 -3 | .101662 -2 | .456642 -2 |
| 9 | .684575 -6 | .730331 -5 | .537431 -4 | .312462 -3 | .150171 -2 |

| $v' \backslash v$ | 5 | 6 | 7 | 8 | 9 |
|-------------------|-------------|-------------|-------------|-------------|-------------|
| 0 | .141917 -3 | .351989 -4 | .907982 -5 | .244200 -5 | .684575 -6 |
| 1 | .129348 -2 | .342730 -3 | .921726 -4 | .255115 -4 | .730331 -5 |
| 2 | .734105 -2 | .219838 -2 | .631926 -3 | .182394 -3 | .537431 -4 |
| 3 | .248124 -1 | .101251 -1 | .329366 -2 | .101662 -2 | .312412 -3 |
| 4 | -.110768 -1 | .292876 -1 | .130553 -1 | .456642 -2 | .150171 -2 |
| 5 | .712259 -1 | -.144076 -1 | .333622 -1 | .160861 -1 | .600322 -2 |
| 6 | -.144076 -1 | .841761 -1 | -.179613 -1 | .370462 -1 | .191789 -1 |
| 7 | .333622 -1 | -.179613 -1 | .971262 -1 | -.217057 -1 | .403474 -1 |
| 8 | .160861 -1 | .370462 -1 | -.217057 -1 | .110076 +0 | -.256135 -1 |
| 9 | .600322 -2 | .191789 -1 | .403474 -1 | -.256135 -1 | .123027 +0 |

TABLE B.2. Morse matrix elements of y^3 for $0 \leq v \leq 9$ and $0 \leq v' \leq 9$.

| $v \backslash v'$ | 0 | 1 | 2 | 3 | 4 |
|-------------------|-------------|-------------|-------------|-------------|-------------|
| 0 | .419267 -4 | -.154785 -2 | -.456158 -5 | -.115582 -2 | -.557575 -3 |
| 1 | -.154785 -2 | .541789 -3 | -.433469 -2 | -.235435 -4 | -.219751 -2 |
| 2 | -.456158 -5 | -.433469 -2 | .153500 -2 | -.788337 -2 | -.661351 -4 |
| 3 | -.115582 -2 | -.235435 -4 | -.788337 -2 | .301504 -2 | -.120134 -1 |
| 4 | -.557575 -3 | -.219751 -2 | -.661351 -4 | -.120134 -1 | .479540 -2 |
| 5 | -.200493 -3 | -.119641 -2 | -.330027 -2 | -.141306 -3 | -.166153 -1 |
| 6 | -.659359 -4 | -.474288 -3 | -.198686 -2 | -.442950 -2 | -.257743 -3 |
| 7 | -.211330 -4 | -.169338 -3 | -.856278 -3 | -.290741 -2 | -.555662 -2 |
| 8 | -.677740 -5 | -.582806 -4 | -.328524 -3 | -.134834 -2 | -.393537 -2 |
| 9 | -.220217 -5 | -.199057 -4 | -.120468 -3 | -.551572 -3 | -.194866 -2 |

| $v \backslash v'$ | 5 | 6 | 7 | 8 | 9 |
|-------------------|-------------|-------------|-------------|-------------|-------------|
| 0 | -.200493 -3 | -.659359 -4 | -.211330 -4 | -.677740 -5 | -.220217 -5 |
| 1 | -.119641 -2 | -.474289 -3 | -.169338 -3 | -.582806 -4 | -.119057 -4 |
| 2 | -.330027 -2 | -.198686 -2 | -.856278 -3 | -.328524 -3 | -.120468 -3 |
| 3 | -.141306 -3 | -.442950 -2 | -.290741 -2 | -.134834 -2 | -.551572 -3 |
| 4 | -.166153 -1 | -.257743 -3 | -.555662 -2 | -.393537 -2 | -.194866 -2 |
| 5 | .740955 -2 | -.216113 -1 | -.423844 -3 | -.665977 -2 | -.504878 -2 |
| 6 | -.216113 -1 | .103110 -1 | -2.69419 -1 | -.647700 -3 | -.772244 -2 |
| 7 | -.423844 -3 | -.269419 -1 | .136732 -1 | -.325585 -1 | -.937089 -3 |
| 8 | -.665977 -2 | -.647700 -3 | -.325585 -1 | .174897 -1 | -.384203 -1 |
| 9 | -.504878 -2 | -.772244 -2 | -.937089 -3 | -.384203 -1 | .217539 -1 |

TABLE B.3. Morse matrix elements of u^2 for $0 \leq v \leq 9$ and $0 \leq v' \leq 9$.

| $v' \backslash v$ | 0 | 1 | 2 | 3 | 4 |
|-------------------|-------------|-------------|-------------|-------------|-------------|
| 0 | .116094 -2 | -.461129 -3 | .158102 -2 | .223231 -3 | .333595 -4 |
| 1 | -.461129 -3 | .360007 -2 | -.131785 -2 | .271254 -2 | .446259 -3 |
| 2 | .158102 -2 | -.130457 -2 | .621876 -2 | -.244713 -2 | .379811 -2 |
| 3 | .223231 -3 | .271254 -2 | -.244713 -2 | .902465 -2 | -.380886 -2 |
| 4 | .333595 -4 | .446259 -3 | .379811 -2 | -.380886 -2 | .120258 -1 |
| 5 | .554126 -5 | .749597 -4 | .705137 -3 | .485238 -2 | -.538208 -2 |
| 6 | .101604 -5 | .137000 -4 | .130457 -3 | .996354 -3 | .587810 -2 |
| 7 | .203277 -6 | .272426 -5 | .258685 -4 | .200209 -3 | .131663 -2 |
| 8 | .439190 -7 | .584914 -6 | .552156 -5 | .426332 -4 | .284430 -3 |
| 9 | .101604 -7 | .134542 -6 | .126242 -5 | .969173 -5 | .645363 -4 |
| $v' \backslash v$ | 5 | 6 | 7 | 8 | 9 |
| 0 | .554126 -5 | .101604 -5 | .203277 -6 | .439190 -7 | .101604 -7 |
| 1 | .749597 -4 | .137000 -4 | .272426 -5 | .584914 -6 | .134542 -6 |
| 2 | .705137 -3 | .130457 -3 | .258685 -4 | .552156 -5 | .126231 -5 |
| 3 | .485238 -2 | .996354 -3 | .200209 -3 | .426332 -4 | .969173 -5 |
| 4 | -.538208 -2 | .587810 -2 | .131663 -2 | .284430 -3 | .645363 -4 |
| 5 | .152306 -1 | -.715432 -2 | .687536 -2 | .166322 -2 | .383294 -3 |
| 6 | -.715432 -2 | .186481 -1 | -.911780 -2 | .784337 -2 | .203384 -2 |
| 7 | .687536 -2 | -.911780 -2 | .222876 -1 | -.112677 -1 | .878090 -2 |
| 8 | .166322 -2 | .784337 -2 | -.112677 -1 | .261590 -1 | -.136011 -1 |
| 9 | .383294 -3 | .203384 -2 | .878090 -2 | -.136011 -1 | .302729 -1 |

TABLE B.4. Morse matrix elements of u^3 for $0 \leq v \leq 9$ and $0 \leq v' \leq 9$.

| $v' \backslash v$ | 0 | 1 | 2 | 3 | 4 |
|-------------------|-------------|-------------|-------------|-------------|-------------|
| 0 | .172140 -4 | -.121415 -3 | .392909 -4 | -.875307 -4 | -.218416 -4 |
| 1 | -.121415 -3 | .113808 -3 | -.360803 -3 | .113888 -3 | -.168956 -3 |
| 2 | .392909 -4 | -.360803 -3 | .314325 -3 | -.697097 -3 | .226368 -3 |
| 3 | -.875307 -4 | .113888 -3 | -.697097 -3 | .627310 -3 | -.112828 -2 |
| 4 | -.218416 -4 | -.168956 -3 | .226368 -3 | -.112828 -2 | .160192 -2 |
| 5 | -.467993 -5 | -.481572 -4 | -.257257 -3 | .377145 -3 | -.165664 -2 |
| 6 | -.100819 -5 | -.114103 -4 | -.821780 -4 | -.349496 -3 | .566583 -3 |
| 7 | -.226173 -6 | -.267231 -5 | -.221375 -4 | -.123565 -3 | -.442940 -3 |
| 8 | -.533105 -7 | -.644292 -6 | -.535262 -5 | -.344848 -4 | -.171851 -3 |
| 9 | -.132175 -7 | -.161836 -6 | -.137619 -5 | -.928153 -5 | -.514067 -4 |
| $v' \backslash v$ | 5 | 6 | 7 | 8 | 9 |
| 0 | -.467993 -5 | -.100819 -5 | -.226173 -6 | -.533105 -7 | -.132175 -7 |
| 1 | -.481572 -4 | -.114103 -4 | -.267231 -5 | -.644292 -6 | -.161836 -6 |
| 2 | -.257257 -3 | -.821780 -4 | -.212374 -4 | -.535262 -5 | -.137619 -5 |
| 3 | .377145 -3 | -.349496 -3 | -.123565 -3 | -.344848 -4 | -.928153 -5 |
| 4 | -.165664 -2 | .566583 -3 | -.442940 -3 | -.171851 -3 | -.514067 -4 |
| 5 | .162797 -3 | -.228647 -2 | .795008 -3 | -.535155 -3 | -.226512 -3 |
| 6 | -.228647 -2 | .233599 -2 | -.302325 -2 | .106270 -2 | -.623925 -3 |
| 7 | .795008 -3 | -.302325 -2 | .319725 -2 | -.387341 -2 | .136990 -2 |
| 8 | -.535155 -3 | .106270 -2 | -.387341 -2 | .422387 -2 | -.484408 -2 |
| 9 | -.226512 -3 | -.623925 -3 | .136990 -2 | -.484408 -2 | .542887 -2 |

APPENDIX C

EXPRESSIONS OF SOME INTEGRALS OBTAINED BY IH

We list below some important results obtained by IH⁽²²⁾ by the factorization method in connection with their evaluation of non-diagonal matrix elements of the variable x for a Morse oscillator. We also make some extensions of their results. Like IH, we assume that $m > m'$.

First we have

$$\int_{-\infty}^{\infty} R_{m'}^s R_m^{s-1} dx = 0 . \quad (C.1)$$

Using the same technique, this integral can be generalized into

$$\int_{-\infty}^{\infty} R_{m'}^s R_m^{s-n} dx = 0 \quad (C.2)$$

where n is an integer such that $s - n \geq m$.

Next, we have

$$\int_{-\infty}^{\infty} R_m^m R_{m'}^{m'} dx = \frac{\Gamma(m+m')}{[\Gamma(2m)\Gamma(2m')]^{\frac{1}{2}}} . \quad (C.3)$$

It is easy to show that

$$\int_{-\infty}^{\infty} R_m^m e^{px} R_{m'}^{m'} dx = \frac{\Gamma(m+m'+p)}{[\Gamma(2m)\Gamma(2m')]^{\frac{1}{2}}} \quad (C.4)$$

which obviously reduces to Eq. (C.3) for $p = 0$.

We will show that

$$\int_{-\infty}^{\infty} R_m^m x R_{m'}^m dx = \frac{\Gamma(m+m')}{[\Gamma(2m)\Gamma(2m')]^{\frac{1}{2}}} \psi(m+m') \quad (C.5)$$

where $\psi(m+m')$ is the digamma function defined by Eq. (3.31a).

Using the expression (3.5a) of R_m^m , we write the above integral as

$$\begin{aligned} X_{m,m'}^{m,m'} &= [\Gamma(2m)\Gamma(2m')]^{-\frac{1}{2}} \int_{-\infty}^{\infty} [x \cdot \exp(m+m')x - \frac{1}{2}e^x] dx, \\ &= (\text{constant}) \frac{d}{d(m+m')} \int_{-\infty}^{\infty} [\exp(m+m')x - \frac{1}{2}e^x] dx, \\ &= \frac{\Gamma(m+m')}{[\Gamma(2m)\Gamma(2m')]^{\frac{1}{2}}} \left[\frac{1}{\Gamma(m+m')} \frac{d\Gamma(m+m')}{d(m+m')} \right] \end{aligned}$$

which will take the form of Eq. (C.5) if the notation of the digamma function is put in.

A more general form of the integral (C.5) is

$$\int_{-\infty}^{\infty} R_m^m x^p R_{m'}^m dx = [\Gamma(2m)\Gamma(2m')]^{-\frac{1}{2}} \frac{d^p \Gamma(m+m')}{d(m+m')^p}. \quad (C.6)$$

Another important integral is

$$\int_{-\infty}^{\infty} R_m^m R_{m'}^{m-n} dx = \frac{(m-m'-1)!}{(n-1)!} \left[\frac{2m'\Gamma^2(m+m')}{(m-m'-n)! \Gamma(m+m'+1-n) \Gamma(2m)} \right]^{\frac{1}{2}}. \quad (C.7)$$

In particular, for $n = 1$, Eq. (C.7) gives

$$\int_{-\infty}^{\infty} R_m^m R_{m'}^{m-1} dx = \left[2m' \frac{(m-m'-1)! \Gamma(m+m')}{\Gamma(2m)} \right]^{\frac{1}{2}}; \quad (C.8a)$$

and for $n = 2$,

$$\int_{-\infty}^{\infty} R_m^m R_{m'}^{m-2} dx = [(m-m'-1)(m+m'-1)]^{\frac{1}{2}} \int_{-\infty}^{\infty} R_m^m R_{m'}^{m-1} dx. \quad (C.8b)$$

Finally, the integral (C.7) can be conveniently expressed in terms of the integral (C.8a) and the B-coefficients by

$$\langle R_m^m | R_{m'}^{m-n} \rangle = \frac{1}{(n-1)!} \underbrace{[B_{m'}^{m-1} B_{m'}^{m-2} \dots B_{m'}^{m-n+1}]}_{(n-1) \text{ factors}} \langle R_m^m | R_{m'}^{m-1} \rangle$$

or

$$\langle R_m^m | R_{m'}^{m-n} \rangle = \prod_{i=1}^{n-1} \left(\frac{B_{m'}^{m-i}}{i} \right) \langle R_m^m | R_{m'}^{m-1} \rangle ,$$

where

$$B_m^s = [(s-m)(s+m)]^{\frac{1}{2}} .$$

REFERENCES

1. G. C. Lie, J. Chem. Phys. 60, 2991 (1973).
2. K. Kirby-Docken and B. Liu, J. Chem. Phys. 66, 4309 (1976).
3. G. Herzberg, Spectra of Diatomic Molecules (Van Nostrand, New York, 1950), 2nd ed.
4. B. L. Crawford, Jr., and H. L. Dinsmore, J. Chem. Phys. 18, 983 (1950).
5. J. I. Steinfeld, Molecules and Radiation (Harper & Row, New York, 1974).
6. R. C. Herman and K. E. Shuler, J. Chem. Phys. 22, 481 (1954).
7. R. Herman and R. F. Wallis, J. Chem. Phys. 23, 637 (1955).
8. L. A. Young and W. J. Eachus, J. Chem. Phys. 44, 4195 (1966).
9. R. A. Toth, R. H. Hunt, and E. K. Plyler, J. Mol. Spectrosc. 32, 85 (1969).
10. J. P. Bouanich, J. Quant. Spectrosc. Radiat. Transfer 16, 1119 (1976).
11. J. K. Cashion, J. Chem. Phys. 41, 3988 (1964).
12. H. J. Babrov, A. L. Shabott, and B. S. Rao, J. Chem. Phys. 42, 4124 (1965).
13. R. L. Spellicy, R. E. Meredith, and F. G. Smith, J. Chem. Phys. 57, 5119 (1972).

14. P. Bernage and P. Niay, *J. Quant. Spectrosc. Radiat. Transfer* 18, 315 (1977).
15. J. Trischka and H. Salwen, *J. Chem. Phys.* 31, 218 (1959).
16. R. Herman and R. J. Rubin, *J. Chem. Phys.* 32, 1393 (1960).
17. K. Cashion, *J. Mol. Spectrosc.* 10, 182 (1963).
18. B. Chakraborty, Y. K. Pan, and T. Y. Chang, *J. Chem. Phys.* 55, 5147 (1971).
19. R. C. M. Learner, *Proc. Roy. Soc. (London) A* 269, 311 (1962).
20. J. N. Huffaker and P. H. Dwivedi, *J. Math. Phys.* 16, 862 (1975).
21. (a) J. N. Huffaker, *J. Chem. Phys.* 64, 3175 (1976);
(b) 64, 4564 (1976);
(c) P. H. Dwivedi and J. N. Huffaker, *ibid.* 66, 1726 (1977);
(d) J. N. Huffaker, *ibid.* 72, 2601 (1980);
(e) 74, 1217 (1981).
22. L. Infeld and T. E. Hull, *Rev. Mod. Phys.* 23, 21 (1951).
23. R. S. Mulliken, *J. Chem. Phys.* 2, 400 (1934).
24. W. M. Huo, *J. Chem. Phys.* 43, 624 (1965).
25. M. F. Weisbach and C. Chackerian, Jr., *J. Chem. Phys.* 59, 4272 (1973).
26. J. N. Huffaker, *J. Chem. Phys.* 70, 2720 (1979).
27. P. M. Morse, *Phys. Rev.* 34, 57 (1929).
28. J. L. Dunham, *Phys. Rev.* 34, 438 (1929).
29. J. E. Rosenthal, *Proc. Nat. Acad., Wash.* 21, 281 (1935).
30. H. S. Heaps and G. Herzberg, *Z. Physik* 133, 48 (1952).
31. R. Herman and R. J. Rubin, *Astrophys. J.* 121, 533 (1955).
32. R. Herman, R. W. Rothery and R. J. Rubin, *J. Mol. Spectrosc.* 2, 360 (1958); 9, 170 (1962).

33. E. B. Wilson, Jr., and A. J. Well, *J. Chem. Phys.* 14, 578 (1946).
34. S. S. Penner and D. Weber, *J. Chem. Phys.* 19, 807 (1951); 817 (1951).
35. R. L. Armstrong and H. L. Welsh, *Can. J. Phys.* 43, 547 (1965).
36. J. C. Breeze and C. C. Ferriso, *J. Chem. Phys.* 43, 3253 (1965).
37. F. Roux, C. Effantin, and J. D'Incan, *J. Quant. Spectrosc. Radiat. Transfer* 12, 97 (1972).
38. W. S. Benedict, R. Herman, G. E. Moore and S. Silverman, *Astrophys. J.* 135, 277 (1962).
39. P. E. Burch and D. Williams, *Appl. Opt.* 1, 587 (1962).
40. B. Schurin and R. E. Ellis, *J. Chem. Phys.* 45, 2528 (1966).
41. D. E. Burch and D. A. Gryvnak, *J. Chem. Phys.* 47, 4930 (1967).
42. C. L. Korb, R. H. Hunt and E. K. Plyler, *J. Chem. Phys.* 48, 4252 (1968).
43. G. M. Hoover and D. Williams, *J. Opt. Soc. Am.* 59, 28 (1969).
44. J. N. Huffaker, *J. Mol. Spectrosc.* 71, 160 (1978).
45. J. N. Huffaker (private communication).
46. C. A. Burrus, *J. Chem. Phys.* 56, 5409 (1972).
47. M. Mizushima, Advances in Molecular Spectroscopy (A. Mangini, Macmillan, New York, 1962), Vol. 3, p. 1167.
48. J. S. Muentzer, *J. Chem. Phys.* 56, 5409 (1972).
49. J. S. Muentzer, *J. Chem. Phys.* 48, 4544 (1968).
50. J. S. Muentzer, *J. Mol. Spectrosc.* 55, 490 (1975).
51. F. P. Billingsley and M. Krauss, *J. Chem. Phys.* 60, 4130 (1974).
52. E. R. Hansen, A Table of Series and Products (Prentice-Hall, Englewood Cliffs, N.J., 1975).
53. F. Roux, Thèse, Lyon (1973).